We are IntechOpen,
the world's leading publisher of
Open Access books
Built by scientists, for scientists

6,900
Open access books available

186,000
International authors and editors

200M
Downloads

Our authors are among the

154
Countries delivered to

TOP 1%
most cited scientists

12.2%
Contributors from top 500 universities

CLARIVATE ANALYTICS

BOOK
CITATION
INDEX

INDEXED

WEB OF SCIENCE™

Selection of our books indexed in the Book Citation Index
in Web of Science™ Core Collection (BKCI)

Interested in publishing with us?
Contact book.department@intechopen.com

Numbers displayed above are based on latest data collected.
For more information visit www.intechopen.com

Signal Processing by Generalized Receiver in DS-CDMA Wireless Communications Systems

Vyacheslav Tuzlukov

Additional information is available at the end of the chapter

1. Introduction

The additive and multiplicative noise exists forever in any wireless communication system. Quality and integrity of any wireless communication systems are defined and limited by statistical characteristics of the noise and interference, which are caused by an electromagnetic field of the environment.

The main characteristics of any wireless communication system are deteriorated as a result of the effect of the additive and multiplicative noise. The effect of addition of noise and interference to the signal generates an appearance of false information in the case of the additive noise. For this reason, the parameters of the received signal, which is an additive mixture of the signal, noise, and interference, differ from the parameters of the transmitted signal. Stochastic distortions of parameters in the transmitted signal, attributable to unforeseen changes in instantaneous values of the signal phase and amplitude as a function of time, can be considered as multiplicative noise. Under stimulus of the multiplicative noise, false information is a consequence of changed parameters of transmitted signals, for example, the parameters of transmitted signals are corrupted by the noise and interference. Thus, the impact of the additive noise and interference may be lowered by an increase in the signal-to-noise ratio (SNR). However, in the case of the multiplicative noise and interference, an increase in SNR does not produce any positive effects.

The main functional characteristics of any wireless communication systems are defined by an application area and are often specific for distinctive types of these systems. In the majority of cases, the main performance of any wireless communication systems are defined by some initial characteristics describing a quality of signal processing in the presence of noise: the precision of signal parameter measurement, the definition of resolution intervals of the signal parameters, and the probability of error.

The main idea is to use the **generalized approach to signal processing** (GASP) in noise in wireless communication systems [1-3]. The generalized approach is based on a seemingly abstract idea: the introduction of an additional noise source that does not carry any information about the signal and signal parameters in order to improve the qualitative performance of wireless communication systems. In other words, we compare statistical data defining the statistical parameters of the probability distribution densities (pdfs) of the observed input stochastic samples from two independent frequency time regions – a "yes" signal is possible in the first region and it is known a priori that a "no" signal is obtained in the second region. The proposed GASP allows us to formulate a decision-making rule based on the determination of **the jointly sufficient statistics of the mean and variance** of the likelihood function (or functional). Classical and modern signal processing theories allow us to define **only the mean** of the likelihood function (or functional). Additional information about the statistical characteristics of the likelihood function (or functional) leads us to better quality signal detection and definition of signal parameters in compared with the optimal signal processing algorithms of classical or modern theories.

Thus, for any wireless communication systems, we have to consider two problems – analysis and synthesis [8]. The first problem (analysis) – the problem to study a stimulus of the additive and multiplicative noise on the main principles and performance under the use of GASP – is an analysis of impact of the additive and multiplicative noise on the main characteristics of wireless communication systems, the receivers in which are constructed on the basis of GASP. This problem is very important in practice. This analysis allows us to define limitations on the use of wireless communication systems and to quantify the additive and multiplicative noise impact relative to other sources of interference present in these systems. If we are able to conclude that the presence of the additive and multiplicative noise is the main factor or one of the main factors limiting the performance of any wireless communication systems, then the second problem – the definition of structure and main parameters and characteristics of the generalized detector or receiver (GD or GR) under a dual stimulus of the additive and multiplicative noise – the problem of synthesis – arises.

GASP allows us to extend the well-known boundaries of the potential noise immunity set by classical and modern signal processing theories. Employment of wireless communication systems, the receivers of which are constructed on the basis of GASP, allows us to obtain high detection of signals and high accuracy of signal parameter definition with noise components present compared with that systems, the receivers of which are constructed on the basis of classical and modern signal processing theories. The optimal and asymptotic optimal signal processing algorithms of classical and modern theories, for signals with amplitude-frequency-phase structure characteristics that can be known and unknown a priori, are components of the signal processing algorithms that are designed on the basis of GASP.

In the proposed chapter, we would like to present and discuss the following aspects of GASP implemented in the direct-sequence code-division multiple access (DS-CDMA) wireless communication systems:

• The main theoretical statements and brief description;

• Signal processing in DS-CDMA wireless communication systems with optimal combining and partial cancellation;

• Signal processing in DS-CDMA wireless communication systems with frequency-selective channels;

• Signal processing in DS-CDMA downlink wireless communication systems with fading channels;

• Summary and discussion.

2. Main functioning principles under employment of GASP in DS-CDMA wireless communication systems

2.1. GR flowchart

The receiver in wireless communication system has an antenna array with the number of elements equal to M and each antenna array element receives N samples during the sensing time. The signal detection problem can be modeled as the conventional binary hypothesis test:

$$\begin{cases} \mathcal{H}_0 \Rightarrow z_i[k] = w_i[k], & i = 1,\ldots,M;\ k = 0,\ldots,N-1, \\ \mathcal{H}_1 \Rightarrow z_i[k] = h_i[k]\,s[k] + w_i[k], & i = 1,\ldots,M;\ k = 0,\ldots,N-1, \end{cases} \tag{1}$$

where $z_i[k]$ is the discrete-time received signal at the receiver input; $w_i[k]$ is the discrete-time circularly symmetric complex Gaussian noise with zero mean and variance σ^2, i.e. $w_i[k] \sim \mathcal{CN}(0,\sigma^2)$; $h_i[k]$ is the discrete-time channel coefficients obeying the circularly symmetric complex Gaussian distribution with zero mean and variance equal to σ_h^2, i.e., $h_i[k] \sim \mathcal{CN}(0,\sigma_h^2)$; and $s[k]$ is the discrete-time signal, i.e., the signal to be detected. We consider the same initial conditions with respect to $s[k]$ as in [4,5]. Throughout this chapter, the signal $s[k]$, the channel coefficients $h_i[k]$, and the noise $w_i[k]$ are independent between each other.

We define the $NM \times 1$ signal vector $\mathbf{Z}$ that collects all the observed signal samples during the sensing time:

$$\mathbf{Z} = \left[z_1[0], \ldots, z_M[0], \ldots, z_1[N-1], \ldots, z_M[N-1] \right]^T , \tag{2}$$

where T denotes a transpose. The data distribution in the complex matrix $\mathbf{Z}$ can be expressed as:

$$\mathbf{Z} \sim \begin{cases} \mathcal{GN}(0, \sigma^2 \mathbf{I}) , & \Rightarrow \mathcal{H}_0 \\ \mathcal{GN}(0, E_s \sigma_h^2 \mathbf{I} + \sigma^2 \mathbf{I}), & \Rightarrow \mathcal{H}_1 \end{cases}, \tag{3}$$

where E_s is the average signal energy at the receiver input, and $\mathbf{I}$ is the $MN \times MN$ identity matrix. We consider a situation when the signaling scheme is unknown (the receiver has a total freedom of choosing the signaling strategy) excepting a known power within the limits of the frequency band of interest. Thus, the receiver should be able to detect a presence of any possible signals satisfying the power and bandwidth constraints for robust detection of the signal $s[k]$ incoming at the receiver input in wireless communication systems.

The generalized receiver (GR) has been constructed based on the generalized approach to signal processing (GASP) in noise and discussed in numerous journal and conference papers and some monographs, namely, in [1–21]. GR is considered as a linear combination of the correlation detector that is optimal in the Neyman-Pearson criterion sense under detection of signals with known parameters and the energy detector that is optimal in the Neyman-Pearson criterion sense under detection of signals with unknown parameters. The main functioning principle of GR is a matching between the model signal generated by the local oscillator in GR and the information signal incoming at the GR input by whole range of parameters. In this case, the noise component of the GR correlation detector caused by interaction between the model signal generated by the local oscillator in GR and the input noise and the random component of the GR energy detector caused by interaction between the energy of incoming information signal and the input noise are cancelled in the statistical sense. This GR feature allows us to obtain the better detection performance in comparison with other classical receivers.

The specific feature of GASP is introduction of additional noise source that does not carry any information about the signal with the purpose to improve a qualitative signal detection performance. This additional noise can be considered as the reference noise without any information about the signal to be detected. The jointly sufficient statistics of the mean and variance of the likelihood function is obtained in the case of GASP implementation, while the classical and modern signal processing theories can deliver only a sufficient statistics of the mean or variance of the likelihood function (no the jointly sufficient statistics of the mean and variance of the likelihood function). Thus, the implementation of GASP allows us to obtain more information about the input process or received information signal. Owing to this fact, an implementation of the receivers constructed based on GASP basis allows us to

improve the signal detection performance of wireless communication system in comparison with employment of other conventional receivers.
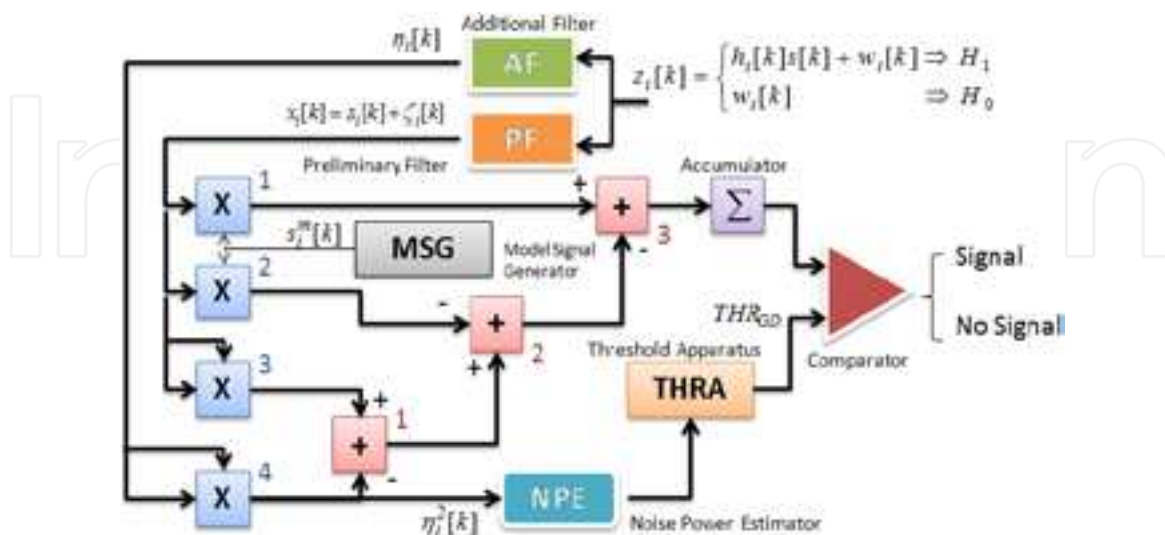
Figure 1. GR flowchart.

The GR flowchart is presented in Fig. 1. As we can see from Fig. 1, the GR consists of three channels:

- the correlation channel – the preliminary filter PF, multipliers 1 and 2, model signal generator MSG;

- the autocorrelation channel – the preliminary filter PF, the additional filter AF, multipliers 3 and 4, summator 1;

- the compensation channel – the summators 2 and 3 and accumulator 1.

As follows from Fig. 1, under the hypothesis $\mathcal{H}_1$ (a "yes" signal), the GR correlation channel generates the signal component $s_{\text{mod}_i}[k]s_i[k]$ caused by interaction between the model signal (the reference signal at the GR MSG output) and the incoming information signal and the noise component $s_{\text{mod}_i}[k]\xi_i[k]$ caused by interaction between the model signal $s_{\text{mod}_i}[k]$ and the noise $\xi_i[k]$ (the PF output). Under the hypothesis $\mathcal{H}_1$, the GR autocorrelation channel generates the information signal energy $s_i^2[k]$ and the random component $s_i[k]\xi_i[k]$ caused by interaction between the information signal $s_i[k]$ and the noise $\xi_i[k]$. The main purpose of the GR compensation channel is to cancel in the statistical sense the GR correlation channel noise component $s_{\text{mod}_i}[k]\xi_i[k]$ and the GR autocorrelation channel random component $s_i[k]\xi_i[k]$ between each other based on the same nature of the noise $\xi_i[k]$.

For description of the GR flowchart we consider the discrete-time processes without loss of any generality. Evidently, the cancelation between the GR correlation channel noise component $s_{\mathrm{mod}_i}[k]\xi_i[k]$ and the GR autocorrelation channel random component $s_i[k]\xi_i[k]$ is possible only based on the same nature of the noise $\xi_i[k]$ satisfying the condition of equality between the signal model $s_{\mathrm{mod}_i}[k]$ and incoming signal $s_i[k]$ over the whole range of parameters. The condition $s_{\mathrm{mod}_i}[k] = s_i[k]$ is the **GR main functioning condition**. To satisfy this condition, we are able to define the incoming signal parameters. Naturally, in practice, signal parameters are random. How we can satisfy the GR main functioning condition and define the signal parameters in practice if there is no a priori information about the signal and there is an uncertainty in signal parameters, i.e. information signal parameters are stohastic, is discussed in detail in [1,3,21].

Under the hypothesis $\mathcal{H}_0$ (a "no" information signal), satisfying the GR main functioning condition $s_{\mathrm{mod}_i}[k] = s_i[k]$, we obtain only the background noise $\eta_i^2[k] - \xi_i^2[k]$ at the GR output. Additionally, the practical implementation of the GR decision statistics requires an estimation of the noise variance σ_w^2 using the reference noise $\eta_i[k]$ at the AF output. AF is the reference noise source and the PF bandwidth is matched with the bandwidth of the information signal $s_i[k]$ to be detected. The threshold apparatus (THRA) device defines the GR threshold. PF and AF can be considered as the linear systems, for example, as the bandpass filters, with the impulse responses $h_{PF}[m]$ and $h_{AF}[m]$, respectively. For simplicity of analysis, we assume that these filters have the same amplitude-frequency characteristics or impulse responses by shape. Moreover, the AF central frequency is detuned with respect to the PF central frequency on such a value that the information signal cannot pass through the AF. Thus, the information signal and noise can be appeared at the PF output and the only noise is appeared at the AF output. If a value of detuning between the AF and PF central frequencies is more than $4 \text{ or } 5\Delta f_s$, where Δf_s is the signal bandwidth, the processes at the AF and PF outputs can be considered as the uncorrelated and independent processes and, in practice, under this condition, the coefficient of correlation between PF and AF output processes is not more than 0.05 that was confirmed experimentally in [22,23].

The processes at the AF and PF outputs present the input stochastic samples from two independent frequency-time regions. If the noise $w[k]$ at the PF and AF inputs is Gaussian, the noise at the PF and AF outputs is Gaussian, too, owing to the fact that PF and AF are the linear systems and we believe that these linear systems do not change the statistical parameters of the input process. Thus, the AF can be considered as a reference noise generator with a priori knowledge a "no" signal (the reference noise sample). A detailed discussion of the AF and PF can be found in [6,7]. The noise at the PF and AF outputs can be presented in the following form:

$$\begin{cases} w_{PF}[k] = \xi[k] = \displaystyle\sum_{m=-\infty}^{\infty} h_{PF}[m]w[k-m] \ , \\[4mm] w_{AF}[k] = \eta[k] = \displaystyle\sum_{m=-\infty}^{\infty} h_{AF}[m]w[k-m] \ . \end{cases} \tag{4}$$

Under the hypothesis $\mathcal{H}_1$, the signal at the PF output can be defined as $x_i[k] = s_i[k] + \xi_i[k]$ (see Fig. 1), where $\xi_i[k]$ is the observed noise at the PF output and $s_i[k] = h_i[k] \times s[k]$; $h_i[k]$ are the channel coefficients indicated here only in a general case. Under the hypothesis $\mathcal{H}_0$ and for all i and k, the process $x_i[k] = \xi_i[k]$ at the PF output is subjected to the complex Gaussian distribution and can be considered as the independent and identically distributed (i.i.d.) process. The process at the AF output is the reference noise $\eta_i[k]$ with the same statistical parameters as the noise $\xi_i[k]$ in the ideal case (we make this assumption for simplicity). In practice, the statistical parameters of the noise $\xi_i[k]$ and $\eta_i[k]$ are different.

The decision statistics at the GR output presented in [1,3] is extended to the case of antenna array employment when an adoption of multiple antennas and antenna arrays is effective to mitigate the negative attenuation and fading effects [4,5]. The GR decision statistics can be presented in the following form:

$$T_{GR}(\boldsymbol{X}) = \sum_{k=0}^{N-1}\sum_{i=1}^{M} 2x_i[k]s_{\mathrm{mod}_i}[k] - \sum_{k=0}^{N-1}\sum_{i=1}^{M} x_i^2[k] + \sum_{k=0}^{N-1}\sum_{i=1}^{M} \eta_i^2[k] \underset{\mathcal{H}_0}{\overset{\mathcal{H}_1}{\gtrless}} THR_{GR}, \tag{5}$$

where $\boldsymbol{X} = [x_1[0],\ldots,x_M[0],\ldots,x_1[N-1],\ldots,x_M[N-1]]^T$ is the vector of random process at the PF output, and THR_{GR} is the GR detection threshold. We can rewrite (5) using the vector form:

$$T_{GR}(X) = 2\mathbf{S}_{\mathrm{mod}}\mathbf{X} - \mathbf{X}^2 + \boldsymbol{\eta}^2 \underset{\mathcal{H}_0}{\overset{\mathcal{H}_1}{\gtrless}} THR_{GR}, \tag{6}$$

where $\mathbf{X} = [\mathbf{x}(0),\ldots,\mathbf{x}(N-1)]$ is the $M \times 1$ vector of the random process at the PF output with elements defined as $\mathbf{x}[k] = [x_1[k],\ldots,x_M[k]]^T$; $\mathbf{S}_{\mathrm{mod}} = [\mathbf{s}_{\mathrm{mod}}(0),\ldots,\mathbf{s}_{\mathrm{mod}}(N-1)]$ is the $M \times 1$ vector of the process at the MSG output with the elements defined as $\mathbf{s}_{\mathrm{mod}}[k] = [s_{\mathrm{mod}_1}[k],\ldots,s_{\mathrm{mod}_M}[k]]^T$; $\boldsymbol{\eta} = [\boldsymbol{\eta}(0),\ldots,\boldsymbol{\eta}(N-1)]$ is the $M \times 1$ vector of the random process at the AF output with the elements defined as $\boldsymbol{\eta}[k] = [\eta_1[k],\ldots,\eta_M[k]]^T$ and THR_{GR} is the GR detection threshold.

According to GASP and GR structure shown in Fig. 1, the GR test statistics takes the following form under the hypotheses $\mathcal{H}_1$ and $\mathcal{H}_0$, respectively:

$$T_{GR}(\mathbf{X}) = \begin{cases} \displaystyle\sum_{k=0}^{N-1}\sum_{i=1}^{M} s_i^2[k] + \sum_{k=0}^{N-1}\sum_{i=1}^{M} \eta_i^2[k] - \sum_{k=0}^{N-1}\sum_{i=1}^{M} \xi_i^2[k] \;\Rightarrow \mathcal{H}_1\;, \\[2em] \displaystyle\sum_{k=0}^{N-1}\sum_{i=1}^{M} \eta_i^2[k] - \sum_{k=0}^{N-1}\sum_{i=1}^{M} \xi_i^2[k] \qquad\qquad \Rightarrow \mathcal{H}_0\;. \end{cases} \qquad (7)$$

The term $\sum_{k=0}^{N-1}\sum_{i=1}^{M} s_i^2[k] = E_s$ is the average signal energy and the term $\sum_{k=0}^{N-1}\sum_{i=1}^{M}\eta_i^2[k] - \sum_{k=0}^{N-1}\sum_{i=1}^{M}\xi_i^2[k]$ presents the background noise at the GR output that is a difference between the noise power at the PF and AF outputs. It is important to mention that the main GR functioning condition is the equality between parameters of the model signal $s_{\mathrm{mod}_i}[k]$ and the signal $s_i[k]$, i.e. $s_{\mathrm{mod}_i}[k] = s_i[k]$ over all range of parameters and, in particular, by amplitude. How we can satisfy this condition in practice is discussed in detail in [1] and [3, Chapter 7, pp 611-621] when there is no a priori information about the signal $s_i[k]$. This condition is essential for complete compensation in the statistical sense between the noise component of the correlation channel $2s_{\mathrm{mod}_i}[k]\xi_i[k]$, the GR correlation channel, caused by interaction between the model signal $s_{\mathrm{mod}_i}[k]$ and noise $\xi_i[k]$, and the random component of the GR autocorrelation channel $2s_i[k]\xi_i[k]$, the GR ED, caused by interaction between the signal $s_i[k]$ and noise $\xi_i[k]$ [1] and [6, Chapter 3]. The complete matching between the model signal $s_{\mathrm{mod}_i}[k]$ and the incoming signal $s_i[k]$, especially by amplitude, is a very hard problem in practice and only in the ideal case the complete matching is possible. How the GR detection performance can be deteriorated under mismatching between the model signal $s_{\mathrm{mod}_i}[k]$ and the incoming signal $s_i[k]$ is discussed in [24]. Additionally, a practical implementation of the GR decision statistics requires an estimation of the noise variance σ_w^2 using the reference noise $\eta_i[k]$ at the AF output.

The mean $m_{\mathcal{H}_0}^{GR}$ and the variance $Var_{\mathcal{H}_0}^{GR}$ of the test statistics $T_{GR}(\mathbf{X})$ under the hypothesis $\mathcal{H}_0$ are given in the following form [6, Chapter 3]:

$$\begin{cases} m_{\mathcal{H}_0}^{GR} = \mathrm{E}\big[T_{GR}(\mathbf{X})|\mathcal{H}_0\big] = 0\;, \\[1.5em] Var_{\mathcal{H}_0}^{GR} = Var\big[T_{GR}(\mathbf{X})|\mathcal{H}_0\big] = 4NM\sigma^4\;. \end{cases} \qquad (8)$$

2.2. MGF of the GR partial test statistics $T_{GR}(\mathbf{X}_k)$

To complete consideration of the GR main functioning principles the moment generating function (MGF) definition of the GR partial test statistics $T_{GR}(\mathbf{X}_k)$ under the main GR functioning condition $s_{\mathrm{mod}_i}[k] = s_i[k]$ and the hypothesis $\mathcal{H}_1$ given by

$$T_{GR}(\mathbf{X}_k) = \sum_{i=1}^{M} s_i^2[k] + \sum_{i=1}^{M} \eta_i^2[k] - \sum_{i=1}^{M} \xi_i^2[k] \qquad (9)$$

is required. We say that the random variable x has a chi-square distribution with υ degree of freedom if its probability density function (pdf) is determined as

$$p(x) = cx^{0.5\upsilon - 1} \exp(-0.5x) , \qquad (10)$$

where c is a constant given by [25]

$$c = \frac{1}{2^{0.5\upsilon} \Gamma(0.5\upsilon)} , \qquad (11)$$

$\Gamma(\cdot)$ is the gamma function. The MGF general form for the chi-square distributed random variable x is given by [25]

$$\mathcal{M}_x(l) = \mathrm{E}[\exp(lx)] = \int_{-\infty}^{\infty} \exp(lx) p(x) dx = c \int_0^{\infty} \exp(lx) x^{0.5\upsilon - 1} \exp(-0.5x) \, dx , \qquad (12)$$

where $\mathrm{E}[\cdot]$ is the mathematical expectation. At $\upsilon = 1$, the constant

$$c = \frac{1}{2^{0.5} \Gamma(0.5\upsilon)} = \frac{1}{\sqrt{2\pi}} . \qquad (13)$$

Assume that $z_{1i}[k] = \xi_i^2[k]$ and $z_{2i}[k] = \eta_i^2[k]$. The pdfs for the random variables z_{1i} and z_{2i} are defined by the chi-square χ^2 distribution law with one degree of freedom [3]:

$$p(z_{1i}) = \frac{1}{\sqrt{2\pi z_{1i}} \ \sigma_w} \exp\left\{ -\frac{z_{1i}}{2\sigma_w^2} \right\} , \ z_{1i} > 0 , \qquad (14)$$

$$p(z_{2i}) = \frac{1}{\sqrt{2\pi z_{2i}} \ \sigma_w} \exp\left\{ -\frac{z_{2i}}{2\sigma_w^2} \right\} , \ z_{2i} > 0 . \qquad (15)$$

Introduce a new random variable $z_i = z_{1i} - z_{2i}$. The MGF of the random variable z_i is given using the following formula:

$$\begin{aligned} \mathcal{M}_{z_i}(l) &= \mathrm{E}[\exp(lz_i)] = \mathrm{E}\{\exp[l(z_{1i} - z_{2i})]\} = \mathrm{E}[\exp(lz_{1i})\exp(-lz_{2i})] \\ &= \mathrm{E}[\exp(lz_{1i})]\mathrm{E}[\exp(-lz_{2i})] = \mathcal{M}_{z_{1i}}(l)\mathcal{M}_{z_{2i}}(-l). \end{aligned} \qquad (16)$$

The MGF of the random variable z_1 is defined in the following form:

$$\mathcal{M}_{z_{1i}}(l) = \frac{1}{\sqrt{2\pi}\,\sigma_w} \int_0^\infty \exp(l z_{1i}) z_{1i}^{-0.5} \exp\left\{-\frac{z_{1i}}{2\sigma_w^2}\right\} dz_{1i} = \frac{1}{\sqrt{2\pi}\,\sigma_w} \int_0^\infty z_{1i}^{-0.5} \exp\left\{-\left(\frac{1}{2\sigma_w^2}-l\right)z_{1i}\right\} dz_{1i}. \quad (17)$$

Introducing the variable $g_i = (0.5\sigma_w^{-2} - l)z_{1i}$, we can obtain:

$$\mathcal{M}_{z_{1i}}(l) = \frac{2\sigma_w^2}{\sqrt{2\pi}\sigma_w} \int_0^\infty \left[2\sigma_w^2(1-2\sigma_w^2 l)^{-1}\right]^{-\frac{1}{2}} g_i^{-0.5} \exp(-g_i)(1-2\sigma_w^2 l)^{-1} dg_i$$

$$= \frac{1}{\sqrt{2\pi}\sigma_w}\left[2\sigma_w^2(1-2\sigma_w^2 l)^{-1}\right]^{-\frac{1}{2}} \int_0^\infty g_i^{-0.5}\exp(-g_i)dg_i = \left[\pi(1-2\sigma_w^2 l)\right]^{-\frac{1}{2}} \int_0^\infty g_i^{-0.5}\exp(-g_i)dg_i. \quad (18)$$

Based on the definition of the gamma function [26]

$$\Gamma(x) = \int_0^\infty l^{x-1}\exp(-l)dl \ , \quad (19)$$

we obtain that

$$\int_0^\infty g_i^{-0.5}\exp(-g_i)dg_i = \Gamma(0.5) = \sqrt{\pi}. \quad (20)$$

Finally, the MGF of the random variable z_{1i} is defined as

$$\mathcal{M}_{z_{1i}}(l) = \sqrt{\pi}\left[\pi(1-2\sigma_w^2 l)\right]^{-\frac{1}{2}} = (1-2\sigma_w^2 l)^{-\frac{1}{2}}. \quad (21)$$

The mean and the variance of the random variables z_{1i} can be determined in the following form:

$$\mathrm{E}[z_{1i}] = \frac{\partial \mathcal{M}_{z_{1i}}(l)}{\partial l}\bigg|_{l=0} = \sigma_w^2 \ , \quad (22)$$

$$Var[z_{1i}] = \mathrm{E}[z_{1i}^2] - \mathrm{E}[z_{1i}]^2 = \frac{\partial^2 \mathcal{M}_{z_{1i}}(l)}{\partial^2 l}\bigg|_{l=0} - \mathrm{E}[z_{1i}]^2 = 3\sigma_w^4 - \sigma_w^4 = 2\sigma_w^4 \ . \quad (23)$$

By the analogous way, we can find that the MGF of the random variable z_{2_i} takes the following form:

$$\mathcal{M}_{z_{2_i}}(-l) = (1 + 2\sigma_w^2 l)^{-0.5} . \tag{24}$$

Since $\{s_i[k]\}_{i=1}^M$ are spatially correlated for i-th antenna array elements, and according to [28], the MGF of $\sum_{i=1}^M s_i^2[k]$ is defined as

$$\mathcal{M}_{\sum_{i=1}^M s_i^2[k]}(l) = \prod_{i=1}^M (1 - E_s \sigma_h^2 \beta_i l)^{-1}, \tag{25}$$

where β_i is the eigenvalue of the i-th spatial channel of the correlation matrix $\mathbf{C}$ given by (2). Based on (21), (24), and (25), the MGF of the GD partial decision statistics $T_{GR}(\mathbf{X}_k)$ is determined in the following form:

$$\mathcal{M}_{T_{GR}(\mathbf{X}_k)}(l) == \prod_{i=1}^M [1 - E_s \sigma_h^2 \beta_i l]^{-1} \prod_{i=1}^M \mathcal{M}_{z_{1_i}}(l) \prod_{i=1}^M \mathcal{M}_{z_{2_i}}(-l) = \prod_{i=1}^M [1 - E_s \sigma_h^2 \beta_i l]^{-1} \prod_{i=1}^M (1 - 2\sigma_w^2 l)^{-0.5} \prod_{i=1}^M (1 + 2\sigma_w^2 l)^{-0.5}$$

$$= \prod_{i=1}^M [1 - E_s \sigma_h^2 \beta_i l]^{-1} (1 - 2\sigma_w^2 l)^{-0.5M} (1 + 2\sigma_w^2 l)^{-0.5M} = (1 - 4\sigma_w^4 l^2)^{-0.5M} \prod_{i=1}^M [1 - E_s \sigma_h^2 \beta_i l]^{-1} . \tag{26}$$

Based on (26) and taking into consideration results discussed in [27], the mean and the variance of the test statistics $T_{GR}(\mathbf{X})$ under the hypothesis $\mathcal{H}_1$ take the following form, respectively:

$$m_{\mathcal{H}_1}^{GR} = \mathrm{E}[T_{GR}(\mathbf{X}_k)|\mathcal{H}_1] = NM(E_s \sigma_h^2 + 2\sigma_w^2) , \tag{27}$$

$$Var_{\mathcal{H}_1}^{GR} = Var[T_{GR}(\mathbf{X}_k)|\mathcal{H}_1] = N\left[\sum_{i=1}^M E_s^2 \sigma_h^4 \beta_i^2 + 4M\sigma_w^4\right]. \tag{28}$$

3. Signal processing with optimal combining and partial cancellation

3.1. Brief review

In this section, we investigate the generalized receiver (GR) under the quadrature subbranch hybrid selection/maximal-ratio combining (HS/MRC) for 1-D modulations in multipath fading channel and compare its symbol error rate (SER) performance with that of the traditional HS/MRC scheme discussed in [29,30]. It is well known that the HS/MRC receiver selects the L strongest signals from N available diversity branches and coherently combines

them. In traditional HS/MRC scheme, the strongest L signals are selected according to signal-envelope amplitude [29–35]. However, some receiver implementations recover directly the in-phase and quadrature components of the received branch signals. Furthermore, the optimal maximum likelihood estimation (MLE) of the phase of a diversity branch signal is implemented by first estimating the in-phase and quadrature branch signal components and obtaining the signal phase as a derived quantity [36,37]. Other channel-estimation procedures also operate by first estimating the in-phase and quadrature branch signal components [38–41]. Thus, rather than N available signals, there are $2N$ available quadrature branch signal components for combining. In general, the largest $2L$ of these $2N$ quadrature branch signal components will not be the same as the $2L$ quadrature branch signal components of the L branch signals having the largest signal envelopes.

In this section, we investigate how much improvement in performance can be achieved employing the GR with modified HS/MRC, namely, with the quadrature subbranch HS/MRC and HS/MRC schemes, instead of the conventional HS/MRC combining scheme for 1-D signal modulations in multipath fading channel. At GR discussed in [42], the N diversity branches are split into $2N$ in-phase and quadrature subbranches. Then the GR with HS/MRC scheme is applied to these $2N$ subbranches. Obtained results show the better performance is achieved by this quadrature subbranch HS/MRC scheme in comparison with the traditional HS/MRC scheme for the same value of average signal-to-noise ratio (SNR) per diversity branch.

Another problem discussed is the problem of partial cancellation factor (PCF) in DS-CDMA wireless communication system with multipath fading channel. It is well known that the multiple access interference (MAI) can be efficiently estimated by the partial parallel interference cancellation (PPIC) procedure and then partially be cancelled out of the received signal on a stage-by-stage basis for DS-CDMA wireless communication system [43]. To ensure a high-quality performance, PCF for each PPIC stage needs to be chosen appropriately, where the PCF should be increased as the reliability of the MAI estimates improves. There are some papers on the selection of the PCF for a receiver based on the PPIC. In [44–46], formulas for the optimal PCF were derived through straightforward analysis based on soft decisions. In contrast, it is very difficult to obtain the optimal PCF for a receiver based on PPIC with hard decisions owing to their nonlinear character. One common approach to solve the nonlinear problem is to select an arbitrary PCF for the first stage and then increase the value for each successive stage, since the MAI estimates may become more reliable in later stages [43, 47, 48]. This approach is simple, but it might not provide satisfactory performance.

In this section, we use the Price's theorem [49, 50] to derive a range of the optimal PCF for the first stage in PPIC of DS-CDMA wireless communication system with multipath fading channel employing GR based on GASP [1–3], where the lower and upper boundary values of the PCF can be explicitly calculated from the processing gain and the number of users of DS-CDMA wireless communication system in the case of periodic code scenario. Computer

simulation shows that, using the average of these two boundary values as the PCF for the first stage, we are able to reach the bit error rate (BER) performance that is very close to the potentially achieved one [51] and surpasses the BER performance of the real PCF for DS-CDMA wireless communication systems discussed, for example, in [43].

With this result, a reasonable PCF can quickly be determined without using any time-consuming Monte Carlo simulations. It is worth mentioning that the two-stage GR considered in [52] based on the PPIC using the proposed PCF at the first stage achieves the BER performance comparable to that of the three-stage GR based on the PPIC using an arbitrary PCF at the first stage. In other words, at the same BER performance, the proposed approach for selecting the PCF can reduce the GR complexity based on the PPIC. The PCF selection approach is derived for multipath fading channel cases discussed in [42, 53].

In this section, we describe the multipath fading channel model and provide system models for selection/maximal ratio combining and synchronous DS-CDMA wireless communication systems; carry out the performance analysis obtaining a symbol error rate expression in the closed-form and define a marginal moment generating function of SNR per symbol of a single quadrature branch; determine the lower and upper PCF bounds based on the processing gain N and the number of users K under multipath fading channel model in DS-CDMA wireless communication systems employing GR; discuss simulation results; and make some conclusions.

3.2. System model

3.2.1. Multipath fading channel model

Let the transfer function for user k's channel be

$$W_k(Z) = \sum_{i=1}^{M} \alpha_{k,i} Z^{-\tau_{k,i}}. \tag{29}$$

As we can see from (29), the number of paths is M and the channel power and delay for i-th channel path are $\alpha_{k,i}$ and $\tau_{k,i}$, respectively.

We use two vectors to represent these parameters:

$$\boldsymbol{\tau}_k = [\tau_{k,1}, \tau_{k,2}, \ldots, \tau_{k,L}]^T \tag{30}$$

and

$$\boldsymbol{\alpha}_k = [\alpha_{k,1}, \alpha_{k,2}, \ldots, \alpha_{k,L}]^T. \tag{31}$$

Let

$$\tau_{k,1} \leq \tau_{k,2} \leq \cdots \leq \tau_{k,L} \tag{32}$$

and the channel power is normalized

$$\sum_{i=1}^{L} \alpha_{k,i}^2 = 1. \tag{33}$$

Without loss of generality, we may assume that $\tau_{k,1} = 0$ for each user and L is the maximum possible number of paths. When a user's path number, say M_1, is less than M, we can let all the elements in $\tau_{k,i}$ and $\alpha_{k,i}$ be zero if the following condition is satisfied

$$M_1 + 1 \leq i \leq M. \tag{34}$$

We may also assume that the maximum delay is much smaller than the processing gain N [46]. Before our formulation, we first define a $(2N-1) \times L$ composite signature matrix $\mathbf{A}_k$ in the following form

$$A_k = [\tilde{\mathbf{a}}_{k,1}, \tilde{\mathbf{a}}_{k,2}, \ldots, \tilde{\mathbf{a}}_{k,L}] \tag{35}$$

where $\tilde{\mathbf{a}}_{k,i}$ is a vector containing i-th delayed spreading code for user k. It is defined as

$$\tilde{\mathbf{a}}_{k,i} = [\overbrace{0,\ldots,0}^{\tau_{k,i}}, a_k^T, \overbrace{0,\ldots,0}^{N-\tau_{k,i}-1},]^T. \tag{36}$$

Since a multipath fading channel is involved, the current received bit signal will be interfered by previous bit signal. As mentioned above, the maximum path delay is much smaller than the processing gain. The interference will not be severe and for simplicity, we may ignore this effect. Let us denote the channel gain for multipath fading as

$$\mathbf{h}_k = \boldsymbol{\alpha}_k \mathbf{A}_k. \tag{37}$$

3.2.2. Selection/maximal-ratio combining

We assume that there are N diversity branches experiencing slow and flat Rayleigh fading, and all of the fading processes are independent and identically distributed (i.i.d.). During analysis, we consider only the hypothesis H_1 "a yes" signal in the input stochastic process. Then the equivalent received baseband signal for the k-th diversity branch takes the following form:

$$x_k(t) = h_k(t)s(t - \tau_k) + w_k(t), \quad k = 1, \ldots, N, \tag{38}$$

where $s(t - \tau_k)$ is a 1-D baseband transmitted signal that without loss of generality, is assumed to be real, $h_k(t)$ is the complex channel gain for the k-th branch subjected to Rayleigh fading, τ_k is the propagation delay along the k-th path of received signal, and $w_k(t)$ is the zero-mean complex AWGN with two-sided power spectral density $N_0/2$ with the dimension W/Hz. At GR front end, for each diversity branch, the received signal is split into its in-phase and quadrature signal components. Then, the conventional HS/MRC scheme is applied over all of these quadrature branches, as shown in Fig.2.
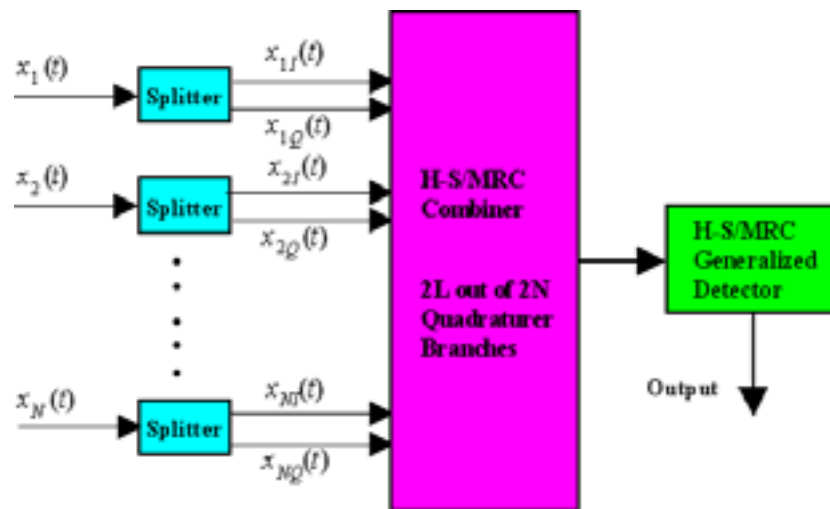
Figure 2. Block diagram receiver based on GR with quadrature subbranch HS/MRC and HS/MRC schemes.

We can present $h_k(t)$ given by (29)–(37) as i.i.d. complex Gaussian random variables assuming that each of the L branches experiences the slow and flat Rayleigh fading

$$h_k(t) = \alpha_k(t)\exp\{-j\phi_k(t)\} = \alpha_k \exp\{-j\phi_k\}, \tag{39}$$

where α_k is a Rayleigh random variable and φ_k is a random variable uniformly distributed within the limits of the interval $[0, 2\pi)$. Owing to the fact that the fade amplitudes are Rayleigh distributed, we can present $h_k(t)$ as

$$h_k(t) = h_{kI}(t) + jh_{kQ}(t) \tag{40}$$

and $w_k(t)$ as

$$w_k(t) = w_{kI}(t) + jw_{kQ}(t). \tag{41}$$

The in-phase signal component $x_{kI}(t)$ and quadrature signal component $x_{kQ}(t)$ of the received signal $x_k(t)$ are given by

$$x_{kI}(t) = h_k(t)a(t - \tau_k) + w_{kI}(t),\qquad(42)$$

$$x_{kQ}(t) = h_{kQ}(t)a(t - \tau_k) + w_{kQ}(t).\qquad(43)$$

Since $h_k(t), (k = 1, \ldots, K)$ are subjected to i.i.d. Rayleigh fading, we can assume that the in-phase $h_{kI}(t)$ and quadrature $h_{kQ}(t)$ channel gain components are independent zero-mean Gaussian random variables with the same variance [41]

$$\sigma_h^2 = 0.5E[\,|\,h_k^2(t)\,|\,],\qquad(44)$$

where $E[\cdot]$ is the mathematical expectation. Further, the in-phase $w_{kI}(t)$ and quadrature $w_{kQ}(t)$ noise components are also the independent zero-mean Gaussian random processes, each with two-sided power spectral density $0.5N_0$ with the dimension W/Hz [36]. Due to the independence of the in-phase $h_{kI}(t)$ and quadrature and quadrature $h_{kQ}(t)$ channel gain components and the in-phase $w_{kI}(t)$ and quadrature $w_{kQ}(t)$ noise components, the $2N$ quadrature branch received signal components conditioned on the transmitted signal are i.i.d.

We can reorganize the in-phase and quadrature components of the channel gains h_k and Gaussian noise $w_k(t)$ when $k = 1, \ldots, N$ as g_k and v_k, given, respectively by

$$g_k(t) = \begin{cases} h_{kI}(t), & k = 1, \ldots, N \\ h_{(k-N)Q}(t), & k = N+1, \ldots, 2N; \end{cases}\qquad(45)$$

$$v_k(t) = \begin{cases} w_{kI}(t), & k = 1, \ldots, N \\ w_{(k-N)Q}(t), & k = N+1, \ldots, 2N. \end{cases}\qquad(46)$$

The GR output with quadrature subbranch HS/MRC and HS/MRC schemes according to GASP [2, 3, 6–9] is given by:

$$Z_{QBHS/MRC}^{GR}(t) = s^2(t)\sum_{k=1}^{2N} b_k^2 g_k^2(t) + \sum_{k=1}^{2N} b_k^2 g_k^2(t)\left[v_{k_{AF}}^2(t) - v_{k_{PF}}^2(t)\right],\qquad(47)$$

where $v_{k_{AF}}^2(t) - v_{k_{PF}}^2(t)$ is the background noise forming at the GR output for the k-th branch; $b_k \in \{0,1\}$ and $2L$ of the b_k equal 1.

3.2.3. Synchronous DS-CDMA wireless communication system

Consider a synchronous DS-CDMA system employing the GR with K users, the processing gain N, the number of frame L, the chip duration T_c, the bit duration $T_b = \dfrac{NT_c}{R}$ with information bit encoding rate R. The signature waveform of the user k is given by

$$a_k(t) = \sum_{i=1}^{N} a_{ki} p_{T_c}(t - iT_c), \tag{48}$$

where $\{a_{k1}, a_{k2}, ..., a_{kN}\}$ is a random spreading code with each element taking value on $\pm 1/\sqrt{N}$ equiprobably, $p_{T_c}(t)$ is the unit amplitude rectangular pulse with duration T_c. The baseband signal transmitted by the user k is given by

$$s_k(t) = A_k(t) \sum_{i=1}^{L} b_{k,i} a_k(t - iT_b), \tag{49}$$

where $A_k(t)$ is the transmitted signal amplitude of the user k. The following form can present the received baseband signal:

$$x(t) = \sum_{k=1}^{K} h_k(t) s_k(t) + w(t) = \sum_{k=1}^{K} \sum_{i=1}^{L} S_k(t) b_{k,i} a_k(t - iT_b) + w(t) , \quad t \in [0, T_b] \tag{50}$$

where taking into account (29)–(37) and (39) and as it was shown in [13]

$$S_k(t) = h_k(t) A_k(t) = \alpha_k^2 A_k(t) \tag{51}$$

is the received signal amplitude envelope for the user k, $w(t)$ is the complex Gaussian noise with zero mean with

$$E[w_k(t)(w_j(t))^*] = \begin{cases} 2\alpha_k^2 \sigma_w^2 , & \text{if} \quad j = k \\ 2\alpha_k^2 \sigma_w^2 \rho_{kj} , & \text{if} \quad j \neq k \end{cases}, \tag{52}$$

ρ_{kj} is the coefficient of correlation. Using GR based on the multistage PPIC for DS-CDMA systems and assuming the user k is the desired user, we can express the corresponding GR output according to GASP and the main functioning condition of GR expressed by $s_{\text{mod}_i}[k] = s_i[k]$ as the first stage of the PPIC GR:

$$Z_k(t) = \int_0^{T_b} [2x_k(t)s_k^*(t-\tau_k) - x_k(t)x_k(t-\tau_k)]dt + \int_0^{T_b} \alpha_k^2[w_{k_{AF}}(t)w_{k_{AF}}(t-\tau_k) - w_{k_{PF}}(t)w_{k_{PF}}(t-\tau_k)]dt, \quad (53)$$

where $s_k^*(t)$ is the model of the signal transmitted by the user k ($s_{\mathrm{mod}_i}[k] = s_i[k]$); τ_k is the delay factor that can be neglected for simplicity of analysis. For this case, we have

$$Z_k = S_k(t)b_k + \sum_{j=1, j\neq k}^{K} S_j(t)b_j\rho_{kj} + \zeta_k(t) = S_k(t)b_k + I_k(t) + \zeta_k(t) = h_k(t)A_k(t)b_k + I_k(t) + \zeta_k(t), \quad (54)$$

where the first term in (54) is the desired signal;

$$\rho_{kj} = \int_0^{T_b} s_k(t)s_j(t)dt \quad (55)$$

is the coefficient of correlation between signature waveforms of the k-th and j-th users; the third term in (54)

$$\zeta_k(t) = \int_0^{T_b} \alpha_k^2[w_{k_{AF}}^2(t) - w_{k_{PF}}^2(t)]\,dt \quad (56)$$

is the total noise component at the GR output; and the second term in (54)

$$I_k = \sum_{j=1, j\neq k}^{K} S_j b_j \rho_{kj} = \sum_{j=1, j\neq k}^{K} h_j A_j b_j \rho_{kj} = \sum_{j=1, j\neq k}^{K} \alpha_j^2 A_j b_j \rho_{kj} \quad (57)$$

is the MAI. The conventional GR makes a decision based on Z_k. Thus, MAI is treated as another noise source. When the number of users is large, MAI will seriously degrade the system performance. GR with partial interference cancellation, being a multiuser detection scheme [31], is proposed to alleviate this problem.

Denoting the soft and hard decisions at the GR output for the user k by

$$\tilde{b}_k^{(0)} = Z_k \text{ and } \hat{b}_k^{(0)} = sgn(Z_k) \quad (58)$$

respectively, the output of the GR with the first PPIC stage with a partial cancellation factor equal to p_1 can be written by [43]

$$\tilde{b}_k^{(1)} = p_1(Z_k - \hat{I}_k) + (1 - p_1)\tilde{b}_k^{(0)} = Z_k - p_1\hat{I}_k, \tag{59}$$

where $\tilde{b}_k^{(1)}$ denotes the soft decision of user k at the GR output with the first stage of PPIC and

$$\hat{I}_k = \sum_{j=1,j\neq k}^{K} S_j \hat{b}_j^{(0)} \rho_{kj} = \sum_{j=1,j\neq k}^{K} h_j A_j \hat{b}_j^{(0)} \rho_{kj} = \sum_{j=1,j\neq k}^{K} \alpha_j^2 A_j \hat{b}_j^{(0)} \rho_{kj} \tag{60}$$

is the estimated MAI using a hard decision.

3.3. Performance analysis

3.3.1. Symbol error rate expression

Let q_k denote the instantaneous SNR per symbol of the k-th quadrature branch $(k = 1, \ldots, 2N)$ at the GR output under quadrature subbranch HS/MRC and HS/MRC schemes. In line with [3, 46] and (29)–(37) and (39), the instantaneous SNR q_k can be defined in the following form:

$$q_k = \frac{E_b \alpha_k^2}{2\sigma_w^2}, \tag{61}$$

where E_b is the average symbol energy of the transmitted signal $s(t)$.

Assume that we choose $2L (1 \leq L \leq N)$ quadrature branched out of the 2N branches. Then, the SNR per symbol at the GR output under quadrature subbranch HS/MRC and HS/MRC schemes may be presented as

$$q_{QBHS/MRC} = \sum_{k=1}^{2L} q_{(k)}, \tag{62}$$

where $q_{(k)}$ are the ordered instantaneous SNRs q_k and satisfy the following condition

$$q_{(1)} \geq q_{(2)} \geq \cdots \geq q_{(2N)}. \tag{63}$$

When $L = N$, we obtain the MRC, as expected. Using the MGF method discussed in [33, 41], SER of M-ary pulse amplitude modulation (PAM) system conditioned on $q_{QBHS/MRC}$ is given by

$$P_s(q_{QBHS/MRC}) = \frac{2(M-1)}{M\,\pi} \int\limits_{0}^{0.5\pi} \exp\left(-\frac{g_{M-PAM}}{\sin^2\theta} q_{QBHS/MRC}\right) d\theta, \tag{64}$$

where

$$g_{M-PAM} = \frac{3}{M^2 - 1}. \tag{65}$$

Averaging (64) over $q_{QBHS/MRC}$ the SER of M-ary PAM system is determined in the following form:

$$P_s = \frac{2(M-1)}{M\,\pi} \int\limits_{0}^{0.5\pi} \int\limits_{0}^{\infty} \exp\left(-\frac{g_{M-PAM}}{\sin^2\theta} q\right) f_{q_{QBHS/MRC}}(q)\,dq\,d\theta \;=\; \frac{2(M-1)}{M\,\pi} \int\limits_{0}^{0.5\pi} \varphi_{q_{QBHS/MRC}}\left(-\frac{g_{M-PAM}}{\sin^2\theta}\right) d\theta, \tag{66}$$

where

$$\varphi_q(s) = E_q\{\exp(sq)\} \tag{67}$$

is the MGF of random variable q, $E_q\{\cdot\}$ is the mathematical expectation of MGF with respect to SNR per symbol.

A finite-limit integral for the Gaussian Q-function, which is convenient for numerical integrations, is given by [54]

$$Q(x) = \begin{cases} \dfrac{1}{\pi} \displaystyle\int\limits_{0}^{0.5\pi} \exp\left\{-\dfrac{x^2}{2\sin^2\theta}\right\} d\theta\,, & x \geq 0 \\[4mm] 1 - \dfrac{1}{\pi} \displaystyle\int\limits_{0}^{0.5\pi} \exp\left\{-\dfrac{x^2}{2\sin^2\theta}\right\} d\theta\,. & x < 0 \end{cases} \tag{68}$$

The error function can be related to the Gaussian Q-function by

$$erf(x) = \frac{2}{\sqrt{\pi}} \int\limits_{0}^{x} \exp(-t^2)\,dt = 1 - 2Q(\sqrt{2}x). \tag{69}$$

The complementary error function is defined as $erfc(x) = 1 - erf(x)$ so that

$$Q(x) = \frac{1}{2} erfc\left(\frac{x}{\sqrt{2}}\right) \quad \text{or} \quad erfc(x) = 2Q(\sqrt{2}x), \tag{70}$$

which is convenient for computing values using MATLAB since **erfc** is a subprogram in MATLAB but the Gaussian Q-function is not (unless you have a *Communications Toolbox*). Note that the Gaussian Q-function is the tabulated function.

Now, let us compare (64) and (68) to obtain the closed form expression for the SER of M-ary PAM wireless communication system employing the GR with quadrature subbranch HS/MRC and HS/MRC schemes. We can easily see that taking into account (44), (45), (61), (62), and (65), the SER of M-ary PAM system employing the GR with quadrature subbranch HS/MRC and HS/MRC schemes can be defined in the following form

$$P_s(q_{QBHS/MRC}) = \frac{2M-1}{M} Q\left(\sqrt{\frac{6}{M^2-1} q_{QBHS/MRC}} \right). \tag{71}$$

Thus, we obtain the closed form expression for the SER of M-ary PAM system employing the GR with quadrature subbranch HS/MRC and HS/MRC schemes that agrees with (8.136) and (8.138) in [55]. If $M = 2$, the average BER performance of coherent binary phase-shift keying (BPSK) wireless communication system using the quadrature subbranch HS/MRC and HS/MRC schemes under GR implementation can be determined in the following form:

$$P_b = \frac{1}{\pi} \int_0^{0.5\pi} \varphi_{q_{QBHS/MRC}} \left(-\frac{1}{\sin^2\theta} \right) d\theta. \tag{72}$$

3.3.2. MGF of $q_{QBHS/MRC}$

Since all of the $2N$ quadrature branches are i.i.d., the MGF of $q_{QBHS/MRC}$ takes the following form [35]:

$$\varphi_{q_{QBHS/MRC}} = 2L \binom{2N}{2L} \int_0^\infty \exp(sq) f(q) [\varphi(s,q)]^{2L-1} [F(q)]^{2(N-L)} dq, \tag{73}$$

where $f(q)$ and $F(q)$ are, respectively, the probability density function (pdf) and the cumulative distribution function (cdf) of q, the SNR per symbol, for each quadrature branch, and

$$\varphi(s,q) = \int_q^\infty \exp(sx) f(x) dx \tag{74}$$

is the marginal moment generating function (MMGF) of SNR per symbol of a single quadrature branch.

Since g_k and g_{k+N} $(k = 1, \ldots, N)$ follow the zero-mean Gaussian distribution with the variance σ_h^2 given by (44), one can show that q_k and q_{k+N} follow the Gamma distribution with pdf given by [49]

$$f(q) = \begin{cases} \dfrac{1}{\sqrt{q}} \exp\left(-\dfrac{q}{\overline{q}}\right) \sqrt{\pi \overline{q}}, & q \geq 0 \\ 0, & q \leq 0, \end{cases} \tag{75}$$

where

$$\overline{q} = \frac{E_b \sigma_h^2}{\sigma_w^2} \tag{76}$$

is the average SNR per symbol for each diversity branch. The MMGF of SNR per symbol of a single quadrature branch can be determined in the following form:

$$\varphi(s, q) = \frac{1}{\sqrt{1 - s\overline{q}}} erfc \left(\sqrt{\frac{1 - s\overline{q}}{\overline{q}}} q \right). \tag{77}$$

Moreover, the cdf of q becomes

$$F(q) = 1 - \varphi(0, q) = 1 - erfc \left(\sqrt{\frac{q}{\overline{q}}} \right), \tag{78}$$

where $erfc(x)$ is the complimentary error function.

3.4. PCF determination

3.4.1. AWGN channel

In this section, we determine the PCF at the GR output with the first stage of PPIC. From [43], the linear minimum mean-square error (MMSE) solution of PCF for the first stage of PPIC is given by

$$p_{1,\text{opt}} = \frac{\sigma_{2,0}^2 - \rho_1 \sigma_{1,1} \sigma_{2,0}}{\sigma_{1,1}^2 + \sigma_{2,0}^2 - 2\rho_1 \sigma_{1,1} \sigma_{2,0}}, \tag{79}$$

where

$$\sigma_{1,1}^2 = E\{(I_k + \zeta_k - \hat{I}_k)^2\} \tag{80}$$

is the power of residual MAI plus the total noise component forming at the GR output at the first stage;

$$\sigma_{2,0}^2 = E\{(I_k + \zeta_k)^2\} \tag{81}$$

is the power of true MAI plus the total noise component forming at the GR output (also called the 0-th stage);

$$\rho_1 \sigma_{1,1} \sigma_{2,0} = E\{(I_k + \zeta_k - \hat{I}_k)(I_k + \zeta_k)\} \tag{82}$$

is a correlation between these two MAI terms. It can be rewritten as

$$
\begin{aligned}
p_{1,\text{opt}} &= \frac{E\{(I_k + \zeta_k)\hat{I}_k\}}{E\{\hat{I}_k^2\}} = \frac{1}{\dfrac{1}{N}\displaystyle\sum_{u \neq l}^{K} S_u^2 + \sum_{u \neq l}^{K}\sum_{v \neq l, u}^{K} S_u S_v E\{\rho_{ul}\rho_{vl}\hat{b}_u^{(0)}\hat{b}_v^{(0)}\}} \\
&\times \left\{ \frac{1}{N}\sum_{u \neq l}^{K} A_u^2(1 - 2P_{e,u}) + \sum_{u \neq l}^{K}\sum_{v \neq l, u}^{K} S_u S_v E\{\rho_{ul}\rho_{vl}\hat{b}_u^{(0)}\hat{b}_v^{(0)}\} + \sum_{v \neq l}^{K} S_v E\{\rho_{vl}\zeta_l\hat{b}_v^{(0)}\} \right\} \\
&= \frac{E\left\{\left[\displaystyle\sum_{j=1, j \neq k}^{K}\alpha_j^2 A_j b_j \rho_{kj} + \int_0^{T_b}\alpha_k^2[w_{k_{AF}}^2(t) - w_{k_{PF}}^2(t)]\,dt\right]\displaystyle\sum_{j=1, j \neq k}^{K}\alpha_j^2 A_j \hat{b}_j^{(0)}\rho_{kj}\right\}}{E\left\{\left[\displaystyle\sum_{j=1, j \neq k}^{K}\alpha_j^2 A_j \hat{b}_j^{(0)}\rho_{kj}\right]^2\right\}} \\
&= \frac{1}{\dfrac{1}{N}\displaystyle\sum_{i \neq k}^{K}\alpha_i^4 A_i^2 + \sum_{i \neq k}^{K}\sum_{j \neq k, i}^{K}\alpha_i^2 A_i \alpha_j^2 A_j E\{\rho_{ik}\rho_{jk}\hat{b}_i^{(0)}\hat{b}_j^{(0)}\}} \\
&\times \left\{\frac{1}{N}\sum_{i \neq k}^{K}\alpha_i^4 A_i^2(1 - 2P_{e,i}) + \sum_{i \neq k}^{K}\sum_{j \neq k, i}^{K}\alpha_i^2 A_i \alpha_j^2 A_j E\{\rho_{ik}\rho_{jk}\hat{b}_i^{(0)}\hat{b}_j^{(0)}\} + \sum_{j \neq k}^{K}\alpha_j^2 A_j E\{\rho_{jk}\hat{b}_j^{(0)}\int_0^{T_b}\alpha_k^2[w_{k_{AF}}^2(t) - w_{k_{PF}}^2(t)]\,dt\}\right\},
\end{aligned}
\tag{83}
$$

where $P_{e,i}$ is the BER of user i at the corresponding GR output;

$$E\{\hat{b}_i^{(0)}\hat{b}_i^{(0)}\} = 1 - 2P_{e,i} \quad \text{and} \quad E\{\rho_{ik}^2\} = N^{-1}. \tag{84}$$

The PCF $p_{1,\text{opt}}$ can be regarded as the normalized correlation between the true MAI plus the total noise component forming at the GR output and the estimated MAI. Assume that

$$\mathbf{b} = \{b_k\}_{k=1}^{K} \tag{85}$$

is the data set of all users;

$$\boldsymbol{\rho} = \{\rho_{ik}\}_{i,k=1}^{K} \tag{86}$$

is the correlation coefficient set of random sequences;

$$f_{\tilde{b}_i^{(0)}|\mathbf{b},\boldsymbol{\rho}}(\tilde{b}_i^{(0)} \mid \mathbf{b}, \boldsymbol{\rho}) = \mathcal{N}(E\{\tilde{b}_i^{(0)} \mid \mathbf{b}, \boldsymbol{\rho}\}, 4\alpha^4\sigma_w^4) \tag{87}$$

is the conditional normal pdf of $\tilde{b}_i^{(0)}$ given $\mathbf{b}$ and $\boldsymbol{\rho}$ and $f_{\tilde{b}_i^{(0)},\tilde{b}_j^{(0)}|\mathbf{b},\boldsymbol{\rho}}(\tilde{b}_i^{(0)}, \tilde{b}_j^{(0)} \mid \mathbf{b}, \boldsymbol{\rho})$ is the conditional joint normal pdf of $\tilde{b}_i^{(0)}$ and $\tilde{b}_j^{(0)}$ given $\mathbf{b}$ and $\boldsymbol{\rho}$. Following the derivations in [43], the expectation terms with hard decisions in (83) can be evaluated based on Price's theorem [49] as follows

$$E\{\rho_{ik}\rho_{jk}\hat{b}_i^{(0)}\hat{b}_j^{(0)}\} = E\{E\{E\{\rho_{ik}\rho_{jk}\hat{b}_i^{(0)}\hat{b}_j^{(0)} \mid \mathbf{b}, \boldsymbol{\rho}\} \mid \boldsymbol{\rho}\}\} = E\{E\{\rho_{ik}\rho_{jk}\hat{b}_i^{(0)}(2Q_j - 1) \mid \boldsymbol{\rho}\}\}; \tag{88}$$

$$E\{\rho_{jk}\zeta_k\hat{b}_j^{(0)}\} = E\{E\{E\{\rho_{jk}\zeta_k\hat{b}_j^{(0)} \mid \mathbf{b}, \boldsymbol{\rho}\} \mid \boldsymbol{\rho}\}\} = 4\alpha^4\sigma_w^4 E\{E\{\rho_{jk}^2 f_{\tilde{b}_j^{(0)}|\mathbf{b},\boldsymbol{\rho}}(0 \mid \mathbf{b}, \boldsymbol{\rho}) \mid \boldsymbol{\rho}\}\}; \tag{89}$$

$$E\{\rho_{ul}\rho_{vl}\hat{b}_u^{(0)}\hat{b}_v^{(0)}\} = E\{E\{E\{\rho_{ik}\rho_{jk}\hat{b}_i^{(0)}\hat{b}_j^{(0)} \mid \mathbf{b}, \boldsymbol{\rho}\} \mid \boldsymbol{\rho}\}\} = E\{E\{\rho_{ik}\rho_{jk}[16\rho_{ij}\alpha^4\sigma_w^4 f_{\tilde{b}_i^{(0)},\tilde{b}_j^{(0)}|\mathbf{b},\boldsymbol{\rho}}(0,0 \mid \mathbf{b}, \boldsymbol{\rho}) +$$
$$+ (2Q_i - 1)(2Q_j - 1)] \mid \boldsymbol{\rho}\}\}, \tag{90}$$

where

$$Q_k = Q\left(-\frac{M\{\tilde{b}_k^{(0)} \mid \mathbf{b}, \boldsymbol{\rho}\}}{2\alpha^2\sigma_w^2}\right) \tag{91}$$

and

$$Var\{\zeta_k\} = 4\alpha_k^4\sigma_w^4 \tag{92}$$

is the total background noise variance forming at the GR output taking into account multipath fading channel; σ_w^2 is the additive Gaussian noise variance forming at the PF and AF outputs of GR linear tract; the Gaussian Q- function is given by (68).

Although numerical integration in [43, 56] can be adopted for determining the optimal PCF $p_{1,\text{opt}}$ for the first stage based on (83)-(90), it requires huge computational complexity. To simplify this problem, we assume that the total background noise forming at the GR output can be considered as a constant factor and may be small enough such that the Q functions in (88) and (90) are all constants and (89) can be approximated to zero. That is

$$4\alpha_k^4\sigma_w^4 << \min_{\{\alpha_k A_k, \boldsymbol{\rho}\}}(E\{\tilde{b}_i^{(0)} \mid \mathbf{b}, \boldsymbol{\rho}\})^2 = 4\alpha_m^4 A_m^2 N^{-2}, \tag{93}$$

where [57]

$$\begin{cases} \alpha_m^2 A_m = \min \alpha_k^2 A_k \; ; \\ \displaystyle\sum_{k\neq m}^{K} \alpha_k^2 A_k b_k \rho_{kl} = -\alpha_m^2 A_m b_m \rho'_{mk} \; ; \\ \min \mid \rho_{mk} - \rho'_{mk} \mid = \dfrac{2}{N} \; . \end{cases} \tag{94}$$

With this, we can rewrite (88) and (90) as follows:

$$E\{E\{\rho_{ik}\rho_{jk}\hat{b}_i^{(0)}(2Q_j - 1) \mid \boldsymbol{\rho}\}\} = B_1 E\{\rho_{ik}\rho_{jk}\}E\{\hat{b}_i^{(0)} \mid \boldsymbol{\rho}\} = 0; \tag{95}$$

$$\begin{aligned} &E\{E\{\rho_{ik}\rho_{jk}[16\rho_{ik}\alpha^4\sigma_w^4 f_{\tilde{b}_i^{(0)},\tilde{b}_j^{(0)}\mid\mathbf{b},\boldsymbol{\rho}}(0,0\mid\mathbf{b},\boldsymbol{\rho}) + (2Q_i - 1)(2Q_j - 1)]\mid\boldsymbol{\rho}\}\} \\ &= E\{E\{16\alpha^4\sigma_w^4\rho_{ik}\rho_{jk}\rho_{ij}f_{\tilde{b}_i^{(0)},\tilde{b}_j^{(0)}\mid\mathbf{b},\boldsymbol{\rho}}(0,0\mid\mathbf{b},\boldsymbol{\rho})\mid\boldsymbol{\rho}\}\} + B_2 E\{E\{\rho_{ik}\rho_{jk}\mid\boldsymbol{\rho}\}\} \\ &= E\{E\{4\alpha^4\sigma_w^4\rho_{ik}\rho_{jk}\rho_{ij}f_{\tilde{b}_i^{(0)},\tilde{b}_j^{(0)}\mid\mathbf{b},\boldsymbol{\rho}}(0,0\mid\mathbf{b},\boldsymbol{\rho})\mid\boldsymbol{\rho}\}\}, \end{aligned} \tag{96}$$

where B_1 and B_2 are constants. According to assumptions made above, $f_{\tilde{b}_u^{(0)},\tilde{b}_v^{(0)}\mid\mathbf{b},\boldsymbol{\rho}}(0,0\mid\mathbf{b},\boldsymbol{\rho})$ can be expressed by

$$f_{\tilde{b}_i^{(0)},\tilde{b}_j^{(0)}\mid\mathbf{b},\boldsymbol{\rho}}(0,0\mid\mathbf{b},\boldsymbol{\rho}) = \frac{\exp(-0.5 m_b^T B_b^{-1} m_b)}{8\pi\alpha^4\sigma_w^4\sqrt{1-\rho_{ij}^2}}, \tag{97}$$

where

$$\mathbf{m}_b = [E\{\tilde{b}_i^{(0)} \mid \mathbf{b}, \boldsymbol{\rho}\}, E\{\tilde{b}_j^{(0)} \mid \mathbf{b}, \boldsymbol{\rho}\}]^T \tag{98}$$

and

$$\mathbf{B}_b = E\{(\tilde{\mathbf{b}} - \mathbf{m}_b)(\tilde{\mathbf{b}} - \mathbf{m}_b)^T\} \tag{99}$$

with

$$\tilde{\mathbf{b}} = [\tilde{b}_i^{(0)}, \tilde{b}_j^{(0)}]^T. \tag{100}$$

Since $\mathbf{B}_b^{-1}$ is a positive semi-definite matrix, i.e.

$$\mathbf{m}_b^T \mathbf{B}_b^{-1} \mathbf{m}_b \geq 0, \tag{101}$$

we can have

$$0 < f_{\tilde{b}_i^{(0)}, \tilde{b}_j^{(0)} | \mathbf{b}, \boldsymbol{\rho}}(0, 0 | \mathbf{b}, \boldsymbol{\rho}) \leq \max_{\substack{\rho_{ij} \\ \rho_{ij} \neq \pm 1}} \frac{1}{8\pi\alpha^4 \sigma_w^4 \sqrt{1 - \rho_{ij}^2}}. \tag{102}$$

With the above results,

$$\min_{\rho_{ij}, \rho_{ij} \neq \pm 1} \sqrt{1 - \rho_{ij}^2} = \frac{2\sqrt{N-1}}{N}. \tag{103}$$

where [57]

$$\rho_{ij} = 1 - 2N^{-1} \quad \text{or} \quad -1 + 2N^{-1} \tag{104}$$

and

$$E\{\rho_{ik}\rho_{jk}\rho_{ij}\} = \sum_{m=1}^{N} \sum_{p=1}^{N} \sum_{q=1}^{N} E\{c_{im}c_{km}c_{jp}c_{kp}c_{iq}c_{jq}\} = \sum_{m=1}^{N} N^{-3} = N^{-2}. \tag{105}$$

Thus, we can derive a range of $p_{1,\text{opt}}$ as follows

$$\frac{\sum\limits_{i \neq k}^{K} \alpha_i^4 A_i^2 (1 - 2P_{e,u})}{\sum\limits_{i \neq k}^{K} \alpha_i^4 A_i^2 + \frac{1}{\pi\sqrt{N-1}} \sum\limits_{i \neq k}^{K} \sum\limits_{j \neq l, i}^{K} \alpha_i^2 A_i \alpha_j^2 A_j} \leq p_{1,\text{opt}} < 1 - \frac{2\sum\limits_{i \neq k}^{K} \alpha_i^4 A_i^2 P_{e,u}}{\sum\limits_{i \neq k}^{K} \alpha_i^4 A_i^2}. \tag{106}$$

If the power control is perfect, i.e.

$$\alpha_i^2 A_i = \alpha_j^2 A_j = \alpha^2 A \quad \text{and} \quad P_{e,i} = P_e \tag{107}$$

and P_e is approximated by the BER of high SNR case, i.e., the $Q\left(\sqrt{\frac{N}{K-1}}\right)$ function [58, 59], (83) can be rewritten as

$$\frac{1 - 2Q\left(\sqrt{\frac{N}{K-1}}\right)}{1 + \frac{K-2}{\pi\sqrt{N-1}}} \leq p_{1,\text{opt}} < 1 - 2Q\left(\sqrt{\frac{N}{K-1}}\right). \tag{108}$$

It is interesting to see that the lower and upper boundary values can be explicitly calculated from the processing gain N and the number of users K.

3.4.2. Multipath channel

Based on representation in (37), we can obtain the received signal vector in the following form:

$$\mathbf{x}(t) = \sum_{k=1}^{K} A_k(t) b_k \mathbf{h}_k + \mathbf{w}(t). \tag{109}$$

Introduce the following notation for the correlation coefficient

$$\varpi_{jk} = \mathbf{h}_j^T \mathbf{h}_k \quad \text{and} \quad \varpi_k = \varpi_{kk}. \tag{110}$$

In commercial DS-CDMA wireless communication systems, the users' spreading codes are often modulated with another code having a very long period. As far as the received signal is concerned, the spreading code is not periodic. In other words, there will be many possible spreading codes for each user. If we use the result derived above, we then have to calculate the optimum PCFs for each possible code and the computational complexity will become very high. Since the period of the modulating code is usually very long, we can treat the code chips as independent random variables and approximate the correlation coefficient ϖ_{jk} given by (110) as a Gaussian random variable. In this case, the GR output for the first stage can be presented in the following form:

$$Z_k(t) = A_k(t) b_k \mathbf{h}_k^T \mathbf{h}_k + \sum_{j=1,j\neq k}^{K} A_j(t) b_j \mathbf{h}_j^T \mathbf{h}_k + \zeta_k(t) = A_k(t) b_k \varpi_k + \sum_{j=1,j\neq k}^{K} A_j(t) b_j \varpi_k + \zeta_k(t), \tag{111}$$

where the background noise $\zeta_k(t)$ forming at the GR output is given by (56).

Evaluating the GR output process given by (111), based on the well-known results, for example, discussed in [60], we can define the BER performance for the user k in the following form:

$$P_b^{(k)} = 0.5 P(Z_k \mid b_k = 1) + 0.5 P(Z_k \mid b_k = -1) = P(Z_k \mid b_k = 1). \tag{112}$$

In (112), we assume that the occurrence of probabilities for $b_k = 1$ and $b_k = -1$ are equal, and that the error probabilities for $b_k = 1$ and $b_k = -1$ are also equal. As we can see from (111), there are three terms. The first term corresponds to the desired user bit. If we let $b_k = 1$, it is a deterministic value. The third term in (111) given by (56) corresponds to the GR background noise interference which pdf is defined in [3, Chapter 3, pp. 250–263, 324–328]. The second term in (111) corresponds to the interference from other users and is subjected to the binomial distribution. Note that correlation coefficients in (111) are small and DS-CDMA wireless communication systems are usually operated in low *SNR* environments. The variance of the second term is then much smaller in comparison with the variance of the third term. Thus, we can assume that Z_k conditioned on $b_k = 1$ can be approximated by Gaussian distribution, as shown in [3, Chapter 3, pp. 250–263, 324–328] and [13]. Then the BER performance takes the following form

$$P(Z_k) = Q\left\{\sqrt{\frac{E_{\mathscr{L}}\left\{\mathcal{M}_k^{(l)}\right\}}{E_{\mathscr{L}}\left\{\mathcal{V}_k^{(l)}\right\}}}\right\}, \tag{113}$$

where $E_{\mathscr{L}}\{\cdot\}$ denotes the expectation operator over the spreading code set $\mathscr{L}$ and $\mathcal{M}_k^{(l)}$ and $\mathcal{V}_k^{(l)}$ are the expected squared mean and variance of Z_k, respectively, given the *l*-th possible code in $\mathscr{L}$. Letting

$$R_k = \sum_{j \neq k} q_j \qquad \text{and} \qquad \Lambda_k = \sum_{j \neq k} \varpi_{jk}^2, \tag{114}$$

where q_j is defined in (61), considering ϖ_{jk} as a Gaussian random variable, we obtain

$$E_{\mathscr{L}}[\mathcal{M}_k^{(l)}] = A_k^2 \{E_{\mathscr{L}}[\varpi_k^{(l)}] - p_k E_{\mathscr{L}}[\Lambda_k^{(l)}]\}^2 = A_k^2 \{1 - p_k E_{\mathscr{L}}[\Lambda_k^{(l)}]\}^2 \tag{115}$$

and the mathematical expectation of variance as

$$E_{\mathscr{L}}[\mathcal{V}_k^{(l)}] = 4\sigma_w^4 \{E_{\mathscr{L}}[\Omega_{1,k}^{(l)}]p_k^2 - 2E_{\mathscr{L}}[\Omega_{2,k}^{(l)}]p_k + E_{\mathscr{L}}[\Omega_{3,k}^{(l)}]\}. \tag{116}$$

Note that the expectations in (115) and (116) are operated on interfering user bits and noise using the correlation coefficient ϖ_{jk} given by (110). The coefficients of $E_{\mathscr{L}}[\mathcal{V}_k^{(l)}]$ are represented by

$$\Omega_{1,k}^{(l)} = R_k \left[\sum_{j \neq k} \varpi_{jk}\varpi_j + \sum_{j \neq k}\sum_{m \neq j,k} \varpi_{jm}\varpi_{mk}\right]^2 + \left[\sum_{j \neq k} \varpi_{jk}^2\varpi_j + \sum_{j \neq k}\sum_{m \neq j,k} \varpi_{jm}\varpi_{mk}\varpi_{jk}\right]; \tag{117}$$

$$\Omega_{2,k}^{(l)} = R_k \Big[\sum_{j \neq k} \varpi_{jk}^2 \varpi_j + \sum_{j \neq k} \sum_{m \neq j,k} \varpi_{jm} \varpi_{mk} \varpi_{jk} \Big] + \sum_{j \neq k} \varpi_{jk}^2; \tag{118}$$

$$\Omega_{3,k}^{(l)} = R_k \sum_{j \neq k} \varpi_{jk}^2 + \varpi_k. \tag{119}$$

The optimal PCF for the user k can be found as

$$p_{k,\text{opt}} = \arg\max_{p_k} \left\{ \frac{E_{\mathscr{X}}[\mathcal{M}_k^{(l)}]}{E_{\mathscr{X}}[\mathcal{V}_k^{(l)}]} \right\} = \left\{ p_{k,\text{opt}} : E_{\mathscr{X}}[\mathcal{V}_k^{(l)}] \frac{dE_{\mathscr{X}}[\mathcal{M}_k^{(l)}]}{dp_k} - E_{\mathscr{X}}[\mathcal{M}_k^{(l)}] \frac{dE_{\mathscr{X}}[\mathcal{V}_k^{(l)}]}{dp_k} = 0 \right\}. \tag{120}$$

Substituting (115)–(119) into (120) and simplifying the result, we obtain the following equation

$$p_{k,\text{opt}} = \frac{E_{\mathscr{X}}[\Omega_{2,k}^{(l)}] - E_{\mathscr{X}}[\Omega_{3,k}^{(l)}] E_{\mathscr{X}}[\Lambda_k^{(l)}]}{E_{\mathscr{X}}[\Omega_{1,k}^{(l)}] - E_{\mathscr{X}}[\Omega_{2,k}^{(l)}] E_{\mathscr{X}}[\Lambda_k^{(l)}]}. \tag{121}$$

Unlike that in AWGN channel, the result for the aperiodic code scenario is more difficult to obtain because there are more correlation terms in (114)–(120) to work with. Before evaluation of the expectation terms in (98), we define some function as follows:

$$\alpha_{jk}(m,n) = \alpha_{j,m} \alpha_{k,n}; \tag{122}$$

$$\tau_{jk}(m,n) = \tau_{j,m} - \tau_{k,n}; \tag{123}$$

$$\psi_{jk}(m,n) = \tilde{\mathbf{a}}_{j,m}^T \tilde{\mathbf{a}}_{k,n}. \tag{124}$$

Thus, (122)–(124) define some relative figures between the m-th channel path of the j-th user and the n-th channel path of the k-th user. The notation $\alpha_{jk}(m,n)$ denotes the path gain product, $\tau_{jk}(m,n)$ is the relative path delay, and $\psi_{jk}(m,n)$ is the code correlation with the relative delay $\tau_{jk}(m,n)$. Expanding (122)–(124), we have seven expectation terms to evaluate. For purpose of illustration, we show how to evaluate the first term, $E_{\mathscr{X}}[\varpi_{jk}^2]$ here. By definition, we have ϖ_{jk} as

$$\varpi_{jk} = \mathbf{h}_j^T \mathbf{h}_k = \left\{ \sum_{m=1}^{L} \tilde{\mathbf{a}}_{j,m} \alpha_{j,m} \right\}^T \left\{ \sum_{n=1}^{L} \tilde{\mathbf{a}}_{k,n} \alpha_{k,n} \right\} = \sum_{m=1}^{L} \sum_{n=1}^{L} \alpha_{j,m} \alpha_{k,n} \tilde{\mathbf{a}}_{j,m}^T \tilde{\mathbf{a}}_{k,n} = \sum_{m=1}^{L} \sum_{n=1}^{L} \alpha_{jk}(m,n) \psi_{jk}(m,n). \tag{125}$$

The expectation of ϖ_{jk} over all possible codes can be presented in the following form:

$$E_{\mathscr{L}}\{\varpi_{jk}^2\} = E\left\{\sum_{m_1=1}^{L}\sum_{n_1=1}^{L}\sum_{m_2=1}^{L}\sum_{n_2}^{L}\alpha_{jk}(m_1,n_1)\psi_{jk}(m_1,n_1)\alpha_{jk}(m_2,n_2)\psi_{jk}(m_2,n_2)\right\}$$
$$= \sum_{m_1=1}^{L}\sum_{n_1=1}^{L}\sum_{m_2=1}^{L}\sum_{n_2}^{L}\alpha_{jk}(m_1,n_1)\alpha_{jk}(m_2,n_2)E\{\psi_{jk}(m_1,n_1)\psi_{jk}(m_2,n_2)\}. \tag{126}$$

Introduce the following function

$$G_{jk}(m_1,n_1,m_2,n_2) = B^2 E[\psi_{jk}(m_1,n_1)\psi_{jk}(m_2,n_2)]. \tag{127}$$

The coefficient B^2 in (127) is only the normalization constant. Since the spreading codes are seen as random, only if $\tau_{jk}(m_1,n_1)$ is equal to $\tau_{jk}(m_2,n_2)$ will $G_{jk}(m_1,n_1,m_2,n_2)$ be nonzero. Consider a specific set of $\{m_1,n_1,m_2,n_2\}$ such that

$$\tau_{jk}(m_1,n_1) = \tau_{jk}(m_2,n_2) = \tau , \qquad \tau \geq 0. \tag{128}$$

In this case, we have

$$G_{jk}(m_1,n_1,m_2,n_2) = B^2 \sum_{v=0}^{N-\tau-1} E\{a_{j,v+\tau}^2 a_{k,v}^2\} = N-\tau. \tag{129}$$

At $\tau < 0$, we have the same result except that the sign of τ in (129) is plus. We can conclude that the function $G_{jk}(m_1,n_1,m_2,n_2)$ in (127) can be written in the following form:

$$G_{jk}(m_1,n_1,m_2,n_2) = \begin{cases} N-|\tau| , & \text{if} \quad \tau_{jk}(m_1,n_1) = \tau_{jk}(m_2,n_2) = \tau \\ 0 , & \text{otherwise} \end{cases}. \tag{130}$$

Using (126), (127), and (129), we can evaluate $E_{\mathscr{L}}[\varpi_{jk}^2]$ in (117)–(119). The formulations from the other six expectation terms can be obtained by mathematical transformation that is not difficult.

We now provide a simple example to show the multipath effect on the optimal PCFs. Introduce the following notations that are satisfied for all k:

$$\boldsymbol{\tau}_k = [0,T]^{\mathrm{T}} ; \quad \mathbf{a}_k = [\beta,\delta]^{\mathrm{T}} ; \quad \text{and} \quad \beta^2 + \delta^2 = 1. \tag{131}$$

Using (131) and taking into consideration that in the case of AWGN channel

$$E_{\mathscr{L}}[\Lambda_k^{(l)}] = \frac{K-1}{N}, \tag{132}$$

at given the l-th possible code in $\mathcal{K}$, we can write for the case of the multipath channel

$$E_{\mathcal{K}}[\Lambda_k^{(l)}] = \frac{K-1}{N} + \frac{2(N-T)\beta^2\delta^2(K-1)}{N^2};$$ (133)

$$E_{\mathcal{K}}[\Omega_{1,k}^{(l)}] = E_{\mathcal{K}}\left\{R_k^{(l)}\left\{\sum_{j=1,j\neq k}^{K}\rho_{jk}^{(l)} + \sum_{j=1,j\neq k}^{K}\sum_{m=1,m\neq j,k}^{K}\rho_{jm}^{(l)}\rho_{mk}^{(l)}\right\}^2 + \sum_{j=1,j\neq k}^{K}(\rho_{jk}^{(l)})^2 + \sum_{j=1,j\neq k}^{K}\sum_{m=1,m\neq j,k}^{K}\rho_{jm}^{(l)}\rho_{mk}^{(l)}\rho_{jk}^{(l)}\right\}$$
$$+2(N-T)\beta^2\delta^2\{R_kN^{-4}[N^2+10N+4(N-T)\beta^2\delta^2+2(K-2)(4N+3K+(N-T)\beta^2\delta^2+1]$$
$$+(K-1)N^{-3}(N+3K-2)\} + 4(N-2T)\beta^4\delta^4[R_kKN^{-4}+6K-12]+R_kN^{-4}(6N-10T)\beta^4\delta^4;$$ (134)

$$E_{\mathcal{K}}[\Omega_{2,k}^{(l)}] = E_{\mathcal{K}}\left\{R_k^{(l)}\left\{\sum_{j=1,j\neq k}^{K}(\rho_{jk}^{(l)})^2 + \sum_{j=1,j\neq k}^{K}\sum_{m=1,m\neq j,k}^{K}\rho_{jm}^{(l)}\rho_{mk}^{(l)}\rho_{jk}^{(l)}\right\} + \sum_{j=1,j\neq k}^{K}(\rho_{jk}^{(l)})^2\right\}$$
$$+2(N-T)\beta^2\delta^2[R_kN^{-3}(N+3K-2)+(k-1)N^{-2}];$$ (135)

$$E_{\mathcal{K}}[\Omega_{3,k}^{(l)}] = E_{\mathcal{K}}\left\{R_k\sum_{j=1,j\neq k}^{K}(\rho_{jk}^{(l)})^2 + 1\right\} + 2(N-T)\beta^2\delta^2R_kN^{-2}.$$ (136)

Note that the first terms in (133)–(136) correspond to the optimal PCFs in AWGN channel. Other terms are due to the multipath effect. It is evident to see that if $\delta = 0$ we have the case of AWGN channel.

3.5. Simulation results

3.5.1. Selection/maximal-ratio combining

In this section, we discuss some examples of GR performance with quadrature subbranch HS/MRC and HS/MRC schemes and compare with the conventional HS/MRC receiver. The average SER of coherent BPSK and 8-PAM signals under processing by the GR with the quadrature subbranch HS/MRC and HS/MRC schemes as a function of average SNR per symbol per diversity branch for various values of $2L$ and $2N = 8$ is presented in Fig.3. It is seen that the GR SER performance with quadrature subbranch HS/MRC and HS/MRC schemes at $(L,N) = (3,4)$ achieves virtually the same performance as the GR with traditional MRC, and that the performance at $(L,N) = (2,4)$ is typically less than 0.5 dB in SNR poorer than that of GR with traditional MRC in [42]. Additionally, a comparison with the traditional HS/MRC receiver in [29, 30] is made. Advantage of GR implementation in DS-CDMA wireless communication systems is evident.

The average SER of coherent BPSK and 8-PAM signals under processing by GR with quadrature subbranch HS/MRC and HS/MRC schemes as a function of average SNR per

symbol per diversity branch for various values of $2N$ at $2L = 4$ is shown in Fig.4. We note the substantial benefits of increasing the number of diversity branches N for fixed L. Comparison with the traditional HS/MRC receiver is made. Advantage of GR implementation in DS-CDMA wireless communication systems is evident.
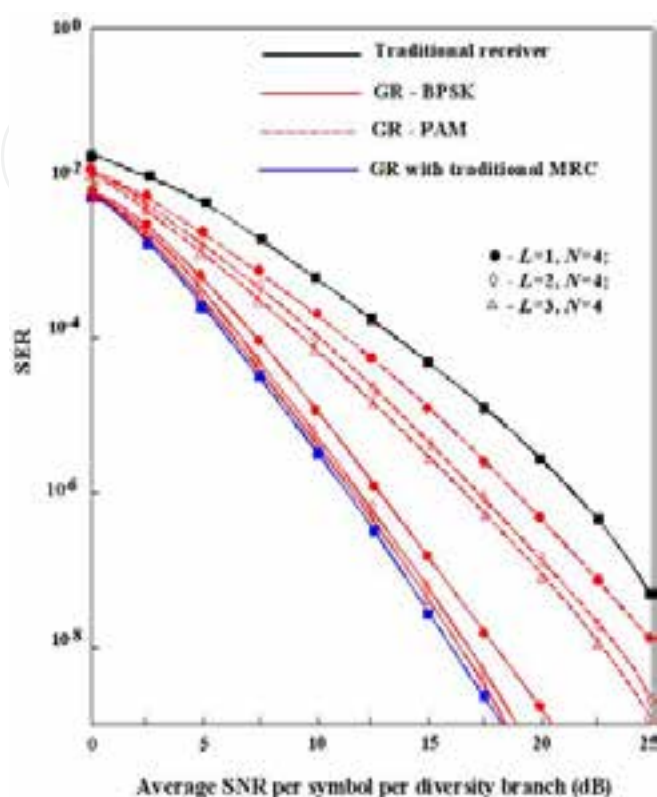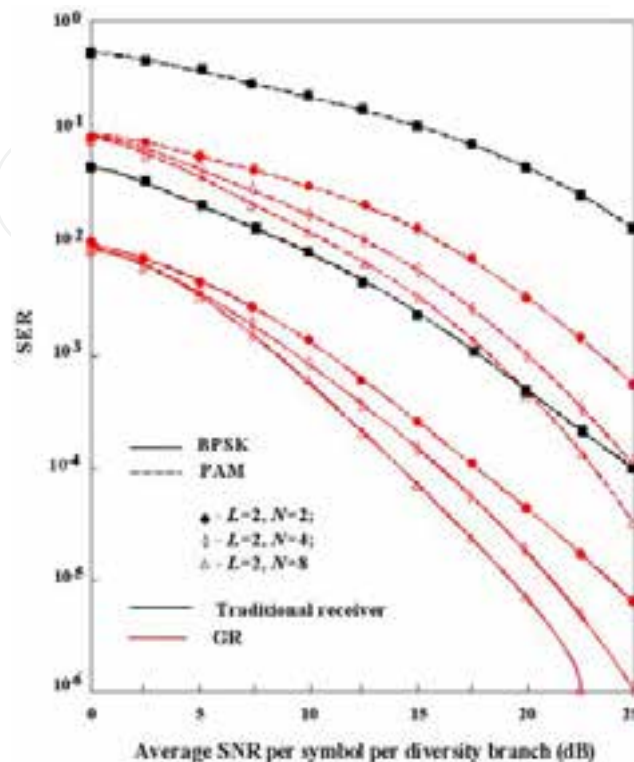

Figure 3. Average SER of coherent BPSK and 8-PAM for GR with quadrature subbranch HS/MRC and HS/MRC schemes versus the average SNR per symbol per diversity for various values of $2L$ with $2N = 8$.

Comparative analysis of average BER as a function of the average SNR per bit per diversity branch of coherent BPSK signals employing GR with quadrature subbranch HS/MRC and HS/MRC schemes and GR with traditional HS/MRC scheme for various values of L with $N = 8$ is presented in Fig. 5. To achieve the same value of average SNR per bit per diversity branch, we should choose $2L$ quadrature branches for the GR with quadrature subbranch HS/MRC, HS/MRC schemes, and L diversity branches for the GR with traditional HS/MRC scheme. Figure 5 demonstrates that the GR BER performance with quadrature subbranch HS/MRC and HS /MRC schemes is much better than that of the GR with traditional HS/MRC scheme, about 0.5 dB to 1.2 dB, when L is less than one half N. This difference decreases with increasing L. This is expected because when $L = N$ we obtain the same performance. Some discussion of increases in GR complexity and power consumption is in order. We first note that GR with quadrature subbranch HS/MRC and HS/MRC schemes requires the same number of antennas as GR with traditional HS/MRC scheme. On the other hand, the former requires twice as many comparators as the latter, to select the best signals for further processing. However, GR designs that process the quadrature signal components will require $2L$ receiver chains for either the GR with quadrature subbranch HS/MRC and HS/MRC

schemes or the GR with traditional HS/MRC scheme. Such receiver designs will use only a little additional power, as GR chains consume much more power than the comparators.

Figure 4. Average SER of coherent BPSK and 8-PAM for GR with quadrature subbranch HS/MRC and HS/MRC schemes versus the average SNR per symbol per diversity for various values of $2N$ with $2L = 4$.

On the other hand, GR designs that implement co-phasing of branch signals without splitting the branch signals into the quadrature components will require L receiver chains for GR with traditional HS/MRC scheme and $2L$ receiver chains for GR with quadrature subbranch HS/MRC and HS/MRC schemes, with corresponding hardware and power consumption increases.

3.5.2. Synchronous DS-CDMA wireless communication system

To demonstrate a usefulness of the optimal PCF range given by (108), we performed a number of simulations for asynchronous DS-CDMA wireless communication system with perfect power control. In simulations, the random spreading codes with length $N = 64$ were used for each user and the number of users was $K = 40$ [61]. Figure 6 shows the BER performance of single-stage hard-decision GR based on PPIC for different magnitudes of SNR and various values of PCF where the optimal PCF for the first stage lies between 0.3169 (lower boundary) and 0.7998 (upper boundary). It can be seen that, for all the SNR cases, the GR based on PPIC using the average of the lower and upper boundary values, i.e., 0.5584, as the PCF, has the close BER performance to that using the optimal PCF. Additionally,

comparison of GR implementation in DS-CDMA systems with the conventional detector discussed in [43] is presented.
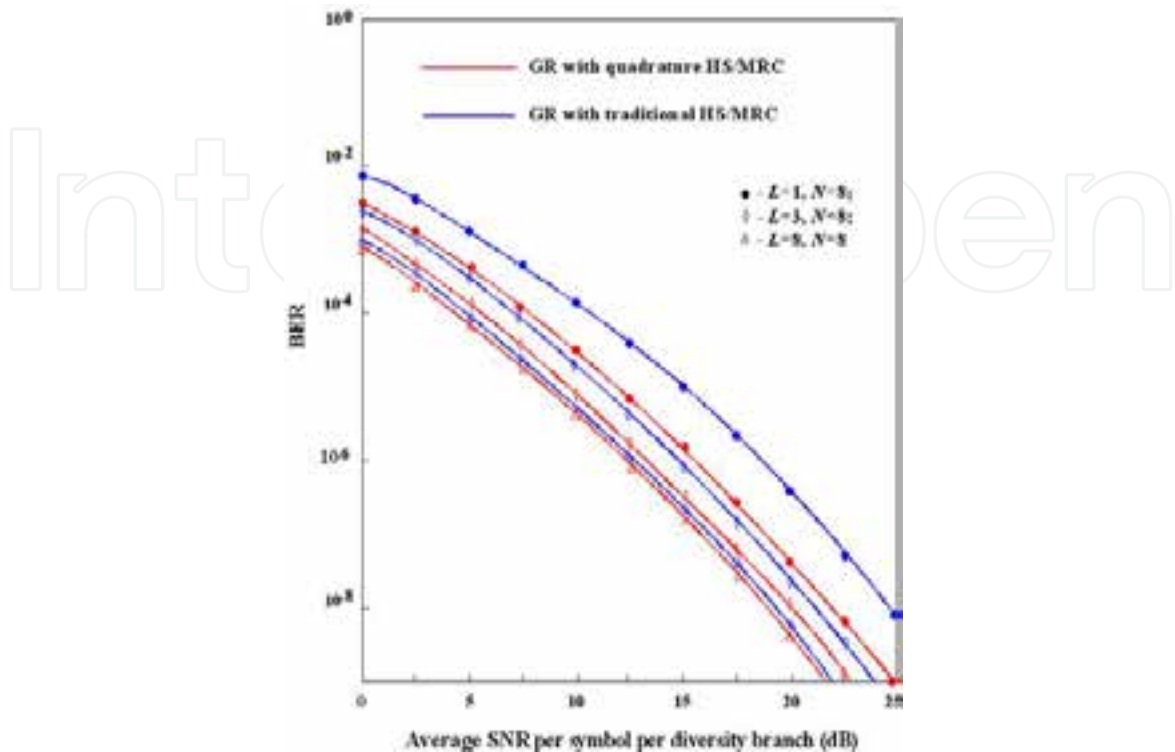

Figure 5. Comparison of the average BER of coherent BPSK and 8-PAM for GR with quadrature subbranch HS/MRC and HS/MRC schemes versus the average SNR per symbol per diversity for various values of $2L$ with $N = 8$.

These results demonstrate us a great superiority of the GR employment over the conventional detector in [43].
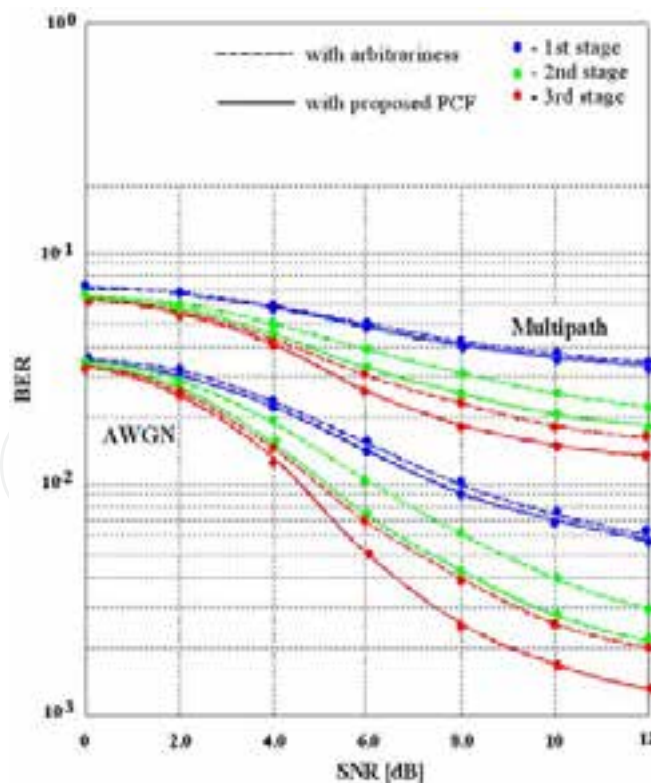
Figure 7 shows the BER performance at each stage for the three-stage GR based on the PPIC using different PCFs at the first stage, i.e., the average value and an arbitrary value. PCFs for these two three-stage cases are

$$(a_1, a_2, a_3) = (0.5584, 0.8, 0.9) \quad \text{and} \quad (0.7, 0.8, 0.9) \tag{137}$$

respectively. The results demonstrate that the BER performances of GR employed by DS-CDMA systems for the cases using the proposed PCF at the first stage outperform ones of GR implemented in DS-CDMA system using arbitrary PCF at the first stage. Furthermore, the GR BER performance at the second stage for the case using the proposed PCF at the first stage achieves the GR BER performance of the GR comparable to that of the three-stage GR based on PPIC using an arbitrary PCF at the first stage. Comparison between the AWCN and multipath channels is also presented in Fig.7. We see that in the case of multipath channel, the BER performance is deteriorated. This fact can be explained by the additional correlation terms in (133)–(136).
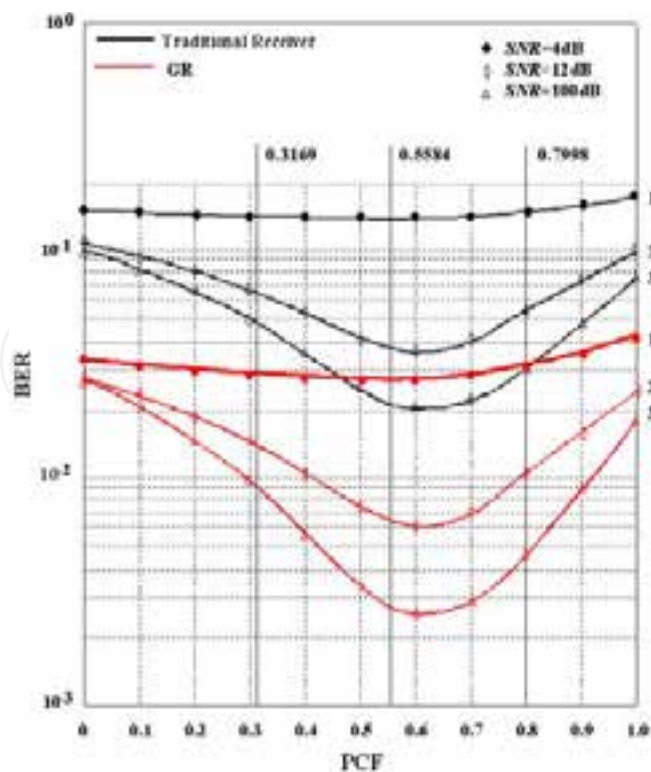
Figure 6. The BER performance of the single-state GR based on PPIC with hard decisions for different SNRs and PCFs.

Figure 7. The BER performance at each stage for three-stage GR based on the PPIC with hard decisions for different PCFs at the first stage, i.e., the average value and an arbitrary value: AWGN and multipath channels.

Figure 8 demonstrates the optimal PCF versus the number of users both for the synchronous AWGN and for the multipath channels. We carry out simulation for the AWGN channel under the following conditions: the Gold codes, *SNR*=12 dB, the spreading codes are the periodic and perfect power control. The multipath channel assumed is a two-ray channel with the transfer function

$$W_k(Z) = 0.762 + 0.648Z^{-2} \qquad (138)$$

for all users. In the case of multipath channel, we employ aperiodic codes, *SNR* =12 dB, and perfect power control.
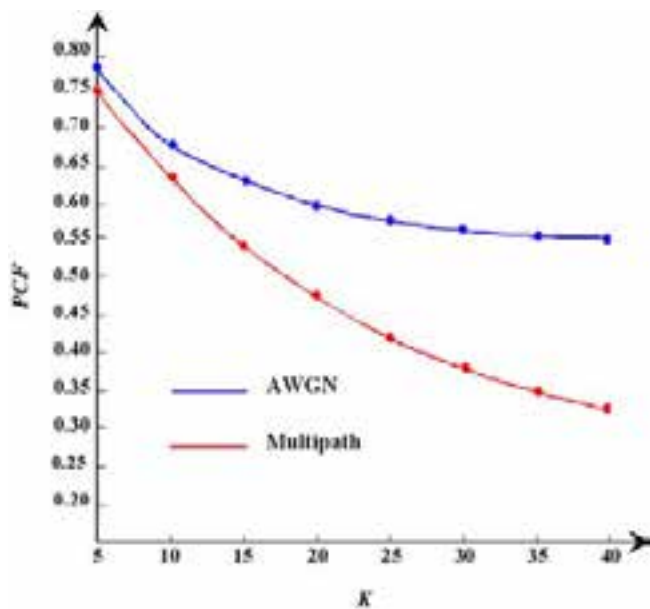

Figure 8. Optimal PCF versus the number of users: the AWGN and multipath channels.

3.6. Conclusions

The GR performance with quadrature subbranch HS/MRC and HS/MRC schemes for a 1-D signal modulation in Rayleigh fading was investigated. The SER of *M*-ary PAM, including coherent BPSK modulation, was derived. Results show the GR with quadrature subbranch HS/MRC and HS/MRC schemes performs substantially better the GR with traditional HS/MRC scheme, particularly, when *L* is smaller than one half *N*, and much better the traditional HS/MRC receiver. We have also derived the optimal PCF range for GR first stage based on the PPIC, which is employed by DS-CDMA system, with hard decisions in multipath fading channel. Computer simulation shows that the BER performance of the GR employed by DS-CDMA wireless communication system with multipath fading channel in the case of periodic code scenario and using the average of the lower and upper boundary values is close to that of the GR of the case using the real optimal PCF, whether the SNR is high or low. It has also been shown that GR employment in DS-CDMA system with multipath fading channel in the case of periodic code scenario allows us to observe a great

superiority over the conventional receiver discussed in [43]. The procedure discussed in [43] is also acceptable for GR employment by DS-CDMA systems. It has also been demonstrated that the two-stage GR based on PPIC using the proposed PCF at the first stage achieves such BER performance comparable to that of the three-stage GR based on PPIC using an arbitrary PCF at the first stage. This means that at the same BER performance, the number of stages (or complexity) required for the multistage GR based on PPIC could be reduced when the proposed PCF is used at the first stage. It can be shown that the proposed PCF selection approach is applicable to multipath fading cases at GR employment in DS-CDMA systems even if no perfect power control is assumed but this is a subject of future work. We have also compared the BER performance at the optimal PCF in the case of AWGN and multipath channels and presented a sensitivity of the BER performance to the values of PCF for both cases.

4. Signal processing with frequency-selective channels

4.1. Brief review

In this section, we consider and study the GR in DS-CDMA wireless communication system with frequency-selective channels. We discuss the linear equalization with the finite impulse response (FIR) beamforming filters and channel estimation and spatially correlation.

4.1.1. Linear equalization and FIR beamforming filters

The use of multiple antennas in wireless communication system attracts significant interest and attention of researchers. Transmit beamforming has received considerable attention because of its simplicity and ability to exploit the benefits of multiple transmit antenna [62]. Information about channel state at the transmitter is generally required for beamforming. At the present time, an impact of noisy and/or quantized information about channel state is a pivot of recent research owing to the fact that the perfect channel state information may not be available at the transmitter [63–65]. In [66], beamforming techniques for DS-CDMA wireless communication systems used a multicarrier approach to cope with frequency-selective fading were also proposed. We should note, however, that the multicarrier techniques are not used in single carrier systems. In this section, we investigate the transmit beamforming for single carrier transmission over frequency-selective fading channels with the perfect channel state information at the GR. A necessity of equalization at the GR is generated by the intersymbol interference (ISI) caused by the channel frequency selectivity. It must be emphasized that the optimum beamforming depends on the equalizer used. As it is well-known, the linear equalization possesses a low complexity. By this reason, we adopt the linear equalization. In comparison and in contrast to [67], we consider the more realistic case of FIR beamforming filters at the GR. Unlike the infinite impulse response case, a closed-form solution for the FIR beamforming filters at the GR does not seem to exist. Because of this, we need to calculate the optimum FIR beamforming filters. Numerical

results show that for typical Global System for Mobile Communications/Enhanced Data Rates for GSM Evolution (GSM/EDGE) channels the performance of short GR FIR beamforming filters can be closely approached with infinite impulse response beamforming at the GR and significant gains over single antenna transmission can be achieved.

4.1.2. Channel estimation and spatial correlation

Under consideration of channel estimation and correlation part, we investigate the minimum mean square error (MMSE) GR. It takes an error of maximum likelihood (ML) multiple-input multiple-output (MIMO) channel estimation and GR spatially correlation into consideration in the computation of MMSE GR and log-likelihood ratio (LLR) of each coded bit. Our GR analysis and investigation are based on the following statements:

- It is well-known [68–70] that the existing soft-output MMSE vertical Bell Lab Space Time (V-BLAST) detectors have been designed based on perfect channel estimation. Unfortunately, the estimated MIMO channel coefficient matrix is noisy and imperfect in practical application environment, [71,72]. Therefore, these soft-output MMSE V-BLAST detectors will suffer from performance degradation under practical channel estimation.

- The ML symbol detection scheme is investigated in [72]. It takes into consideration the channel estimation error under condition that the MIMO channel estimation is imperfect. MMSE based on V-BLAST symbol detection algorithm addressing the impact of the channel estimation error is discussed in [73]. However, the channel coding, decision error propagation compensation, and spatially channel correlation are not discussed and considered.

In the present section, we derive the MMSE GR for detecting each transmitted symbol and provide a method to compute the LLR of each coded bit. When compared with the detection scheme discussed in [73], our simulation results show that the MMSE GR can obtain sizable performance gain.

4.2. Problem statement and system model

We consider a MIMO DS-CDMA wireless communication system with N_T transmit and N_R receive antennas. The modulated symbols $b[k]$ are taken from a scalar symbol alphabet $\mathscr{F}$ such as quadriphase-shift keying (QPSK) or quadrature amplitude modulation (QAM), and have the following variance

$$\sigma_b^2 = E\{|b[k]|^2\} = 1, \tag{139}$$

where $E\{\}$ denotes the mathematical expectation. The coefficients of the FIR beamforming filters of length L_g at the transmit antenna n_t, $1 \le n_t \le N_T$ are denoted by $g_{n_t}[k]$, where $0 \le k \le L_g - 1$ and their energy is normalized to

$$\sum_{n_t=1}^{N_T}\sum_{k=0}^{L_g-1}|g_{n_t}[k]|^2=1.\tag{140}$$

The signal transmitted over antenna n_t at time k is given by

$$a_{n_t}[k]=g_{n_t}[k]\otimes b[k],\tag{141}$$

where $\otimes$ denotes a linear discrete-time convolution. The discrete-time received signal at the receive antenna n_r, $1\le n_r\le N_R$ can be modeled in the following manner

$$s_{n_r}[k]=\sum_{n_t=1}^{N_T}h_{n_t n_r}[k]\otimes a_{n_t}[k]+w_{n_r}[k],\tag{142}$$

where $w_{n_r}[k]$ denotes the spatially and temporally AWGN with zero mean and variance given by

$$\sigma_w^2=E\{|w_{n_r}[k]|^2\}=0.5N_0,\tag{143}$$

where $0.5N_0$ denotes the two-sided power spectral density of the underlying continuous in time passband noise process.

The notation $h_{n_t n_r}[k]$, where $0\le k\le L-1$, represents the overall channel impulse response between the transmit antenna n_t and the receive antenna n_r of length L. In our model, $h_{n_t n_r}[k]$ contains the combined effects of transmit pulse shaping, wireless channel, receive filtering, and sampling. We assume an existence of block fading model, i.e., the channel is constant for the duration of at least one data burst before it changes independently to a new realization. In general, $h_{n_t n_r}[k]$ are spatially and temporally correlated because of insufficient antenna spacing and transmit/receive filtering, respectively. Substituting (141) into (142), we obtain

$$s_{n_r}[k]=h_{n_r}^{eq}[k]\otimes b[k]+w_{n_r}[k],\tag{144}$$

where the equivalent channel impulse response $h_{n_r}^{eq}[k]$ corresponding to the receiving antenna n_r is defined as

$$h_{n_r}^{eq}[k]=\sum_{n_t=1}^{N_T}h_{n_t n_r}[k]\otimes g_{n_t}[k]\tag{145}$$

and has the length $L_{eq} = L + L_g - 1$. Equation (144) shows that the MIMO DS-CDMA wireless communication system with beamforming can be modeled as an equivalent single-input multiple-output (SIMO) system. Therefore, the GR can use the same equalization, channel estimation, and channel tracking techniques as for a single antenna transmission. We assume that the GR employs receive diversity zero forcing or MMSE linear equalization [74].

Let us rewrite the main statements and definitions mentioned above in the matrix form for our convenience in subsequent analysis of channel estimation. Thus, the received signal can be expressed in the following form:

$$\mathbf{s} = \mathbf{H}\mathbf{a} + \mathbf{w} = \sum_{k=1}^{N_T} \mathbf{h}_k a_k + \mathbf{w}, \tag{146}$$

where $\mathbf{s} = [s_1, s_2, \ldots, s_{N_R}]^T$ is the received signal vector; $\mathbf{H} = [\mathbf{h}_1, \mathbf{h}_2, \ldots, \mathbf{h}_{N_T}]^T$ is the $N_R \times N_T$ MIMO channel coefficient matrix with elements $h_{n_t n_r}[k]$ denoting the channel fading coefficient between the n_t-th transmit antenna and the n_r-th receive antenna.

We adopt the following GR spatially correlated MIMO channel model

$$\mathbf{H} = \sqrt{\mathbf{R_r}}\,\mathbf{H}_w \tag{147}$$

with $\mathbf{H}_w$ denoting an independent and identically distributed (i.i.d.) matrix with entries obeying the Gaussian law with zero mean and unit variance, and $\mathbf{R_r}$ is the $N_R \times N_R$ receive array correlation matrix determined by

$$\mathbf{R_r} = \sqrt{\mathbf{R_r}}\left(\sqrt{\mathbf{R_r}}\right)^H. \tag{148}$$

Then, we have

$$E\{\mathbf{H}\mathbf{H}^H\} = N_T \mathbf{R_r}. \tag{149}$$

The channel is considered to be flat fading with coherence time of $(N_P + N_D)$ MIMO vector symbols, where N_P symbol intervals are dedicated to pilot matrix $\mathbf{S}_p$ and the remaining N_D to data transmission, where $\mathbf{a} = [a_1, a_2, \ldots, a_{N_T}]^T$ is the transmitted complex signal vector whose element given by (141) is taken from the complex modulation constellation $\mathscr{F}$, because the modulated symbols $b[k]$ are taken from the scalar symbol alphabet $\mathscr{F}$, such as QPSK signal, by mapping the coefficient of FIR beamforming filters $g_{n_t}[k]$ like the coded bit vector

$$\mathbf{g}_{n_t} = \left[\mathbf{g}_{n_t}^1, \mathbf{g}_{n_t}^2, \ldots, \mathbf{g}_{n_t}^{\log_2 M}\right]^T \tag{150}$$

to one modulation symbol belonging to $\mathscr{F}$, i.e., $a_{n_t} = \mathrm{map}(\mathbf{g}_{n_t}) \in \mathscr{F}$.

Meanwhile, we assume that each transmitted symbol is independently taken from the same modulation constellation $\mathscr{F}$ and has the same average energy, i.e.,

$$E\{\mathbf{a}\mathbf{a}^H\} = E_b \mathbf{I}_{N_T}. \tag{151}$$

Finally, $\mathbf{w} = [w_1, w_2, \ldots, n_{N_R}]^T$ is the AWGN vector with covariance matrix determined by

$$\mathbf{K_w} = E\{\mathbf{w}\mathbf{w}^H\} = \sigma_w^2 \mathbf{I}_{N_R}. \tag{152}$$

$\mathbf{I}_{N_T}$ and $\mathbf{I}_{N_R}$ are the identity matrices.

4.3. FIR beamforming for GR with linear equalization

According to [75], the unbiased *SNR* for linear equalization with the optimum infinite impulse response equalizer filters at the GR back end is given by

$$SNR(\mathbf{g}) = \frac{\sigma_b^4}{\sigma_e^4} - \chi, \tag{153}$$

where σ_b^2 is given by (139) and the linear equalization error variance σ_e^2 will be defined below. We note that the assumption of infinite impulse response linear equalization filters at the GR back end is not a major restriction, since typically FIR linear equalization filters of length equal to $L_F = 4L_{eq}$ can approach closely the performance of infinite impulse response linear equalization filters. In (153) we consider the constant $\chi = 0$ for the case of zero forcing linear equalization and $\chi = 1$ for the case of MMSE linear equalization, respectively [74]. In (153) the beamforming filter vector

$$\mathbf{g} = \left[g_1(0)g_1(1)\cdots g_1(L_g-1)g_2(0)\cdots g_{N_T}(L_g-1)\right]^T \tag{154}$$

consists of the coefficients of all beamforming filters.

The GR linear equalization error variance defined based on results discussed in [76] is given by

$$\sigma_e^4 = 4\sigma_w^4 \int\limits_{-0.5}^{0.5} \frac{1}{\sum_{n_r=1}^{N_R} |H_{n_r}^{eq}(f)|^2 + \mu} df, \tag{155}$$

where $\mu = 0$ and $\mu = 4\sigma_w^4/\sigma_b^4$ are valid for the case of zero-forcing linear equalization and for the case of MMSE linear equalization, respectively. Furthermore, the frequency response $H_{n_r}^{eq}(f) = \mathcal{F}\{h_{n_r}^{eq}(k)\}$ of the equivalent channel can be defined in the following form

$$H_{n_r}^{eq}(f) = \mathbf{q}^H(f)\mathbf{H}_{n_r}\mathbf{g}, \tag{156}$$

where the subscript H means the Hermitian transpose,

$$\mathbf{q}(f) = \{1 \ \exp(j2\pi f) \cdots \exp[j2\pi f(L_{eq}-1)]\}^T, \tag{157}$$

$$\mathbf{H}_{n_r} = [\mathbf{H}_{1n_r} \mathbf{H}_{2n_r} \cdots \mathbf{H}_{N_T n_r}]^T \tag{158}$$

and $\mathbf{H}_{n_t n_r}$ is a $L_{eq} \times L_g$ column-circulant matrix with the vector $[h_{n_t n_r}(0) \ldots h_{n_t n_r}(L-1)\mathbf{0}_{L_g-1}^T]^T$ in the first column. Therefore, the GR SNR with the zero-forcing linear equalization and MMSE linear equalization can be presented in the following form:

$$SNR(\mathbf{g}) = \frac{\sigma_b^4}{4\sigma_w^4 \int\limits_{-0.5}^{0.5} \frac{1}{\mathbf{g}^H \mathbf{G}(f)\mathbf{g} + \zeta} df} - \chi \tag{159}$$

with the $N_T L_g \times N_T L_g$ matrix

$$\mathbf{G}(f) = \sum_{n_r=1}^{N_R} \mathbf{H}_{n_r}^H \mathbf{d}(f)\mathbf{d}^H(f)\mathbf{H}_{n_r}. \tag{160}$$

The optimum beamforming filter vector $\mathbf{g}_{opt}$ shall maximize $SNR(\mathbf{g})$ subject to power constraint $\mathbf{g}^H\mathbf{g} = 1$. Unfortunately, this optimization problem is not convex, i.e. the standard tools from convex optimization cannot be applied. Nevertheless, the Lagrangian of the optimization problem can be formulated in the following form:

$$L(\mathbf{g}) = SNR(\mathbf{g}) + \mu\mathbf{g}^H\mathbf{g}, \tag{161}$$

where μ denotes the Lagrange multiplier. The optimum vector $\mathbf{g}_{opt}$ has to satisfy the following equality

$$\frac{\partial L(\mathbf{g})}{\partial \mathbf{g}^*} = \mathbf{0}_{N_T L_g}, \tag{162}$$

which leads to the nonlinear eigenvalue problem, namely,

$$\left[\int_{-0.5}^{0.5} \frac{\mathbf{G}(f)}{[\mathbf{g}_{opt}^H \mathbf{G}(f)\mathbf{g}_{opt} + \zeta]^2} df \right] \mathbf{g}_{opt} = \tilde{\mu} \mathbf{g}_{opt}, \tag{163}$$

with the eigenvalue $\tilde{\mu}$. Unfortunately, (163) does not seem to have a closed-form solution.

Therefore, we use the following gradient algorithm for calculation of the optimum FIR beamforming filters at the GR, which recursively improves an initial beamforming filter vector $\mathbf{g}_0$. The main statements of the gradient algorithm are:

1. Let $i = 0$ and initialized the beamforming filter vector with a suitable $\mathbf{g}_0$ satisfying $\mathbf{g}_0^H \mathbf{g}_0 = 1$.

2. Update the beamforming filter vector

$$\tilde{\mathbf{g}}_{i+1} = \mathbf{g}_i + \delta \left[\int_{-0.5}^{0.5} \frac{\mathbf{G}(f)}{[\mathbf{g}_i^H \mathbf{G}(f)\mathbf{g}_i + \zeta]^2} df \right] \mathbf{g}_i, \tag{164}$$

where δ_i is a suitable adaptation step size.

3. Normalize the beamforming filter vector

$$\mathbf{g}_{i+1} = \frac{\tilde{\mathbf{g}}_{i+1}}{\sqrt{\tilde{\mathbf{g}}_{i+1}^H \tilde{\mathbf{g}}_{i+1}}}. \tag{165}$$

4. If $1 - |\mathbf{g}_{i+1}^H \mathbf{g}_i| < \varepsilon$, go to Step 5, otherwise increment $i \to i+1$ and go to Step 2.

5. $\mathbf{g}_{i+1}$ are the desired beamforming filter vector.

For the termination constant ε in Step 4 a suitably small value should be chosen, e.g. $\varepsilon = 10^{-4}$. Ideally the adaptation step size δ_i should be optimized to maximize the speed of convergence. Here, we follow [77] and choose δ_i proportional to λ_i^{-1}, where λ_i is the maximal eigenvalue of the matrix

$$\left[\int_{-0.5}^{0.5} \frac{\mathbf{G}(f)}{[\mathbf{g}_i^H \mathbf{G}(f)\mathbf{g}_i + \zeta]^2} df \right] \tag{166}$$

in iteration i. In particular, we found empirically that $\delta_i = 0.01\lambda_i^{-1}$ is a good choice.

Because of non-convexity of the underlying optimization problem, we cannot guarantee that the gradient algorithm converges to the global maximum. However, adopting the initialization procedure explained below, the solution found by this gradient algorithm seems to be close to optimum, i.e., if L_g is chosen sufficiently large the FIR beamforming filters obtained with the gradient algorithm approach and the performance of the optimal infinite impulse response beamforming filters at the GR was discussed in [52].

We found empirically that a convergence to the optimum or a close to optimum solution is achieved if the beamforming filter length is gradually increased. If the desired beamforming filter length is L_g, the gradient algorithm is executed L_g times. The beamforming filter vector is initialized with the normalized all-ones vector of size N_T for the first execution ($v=1$) of the gradient algorithm. For the v-th execution, $2 \leq v \leq L_g$, the first $(v-1)$ beamforming filters coefficients of each antenna are initialized with the optimum beamforming filter coefficients for that antenna found in the $(v-1)$-th execution of the gradient algorithm and the v-th coefficients are initialized with zero. In each execution step v, the algorithm requires typically less than 50 iterations to converge, i.e., the overall complexity of the algorithm are on the order of 50 L_g.

4.4. MMSE GR

4.4.1. Channel estimation

It was proved that for ML MIMO channel estimator the optimal pilot matrix minimizing the mean square estimation error is an orthogonal pilot matrix [71, 72]. Under the use of the pilot matrix, i.e.,

$$\mathbf{S}_p\mathbf{S}_p^H = E_P N_P \mathbf{I}_{N_T}, \tag{167}$$

where $N_P \geq N_T$ and E_P is the energy of each pilot symbol, the estimated channel matrix can be expressed as [71, 72] $\hat{\mathbf{H}} = \mathbf{H} + \Delta\mathbf{H}$, where

$$\Delta\mathbf{H} = \mathbf{w}\mathbf{S}_p^H (E_P N_P)^{-1} \tag{168}$$

is the channel estimation error matrix, which is correlated with the matrix $\mathbf{H}$ and with entries subjected to Gaussian distribution with zero mean and variance

$$\sigma_{\Delta h}^2 = \sigma_w^2 (E_P N_P)^{-1}, \tag{169}$$

which is determined independently of instantaneous channel realization. We can conclude that $\hat{\mathbf{H}}$ is a complex Gaussian matrix with zero mean and covariance matrix

$$Cov[\hat{\mathbf{H}}] = E\{\hat{\mathbf{H}}\hat{\mathbf{H}}^H\} = N_T(\mathbf{R_r} + \sigma_{\Delta h}^2\mathbf{I}_{N_R}). \tag{170}$$

Let $\mathbf{h}_m, \Delta\mathbf{h}_m$ and $\hat{\mathbf{h}}_m, (m = 1,2,\ldots,N_T)$ denote the m-th column of matrices $\mathbf{H}, \Delta\mathbf{H}$ and $\hat{\mathbf{H}}$, respectively. Then, by the important properties of complex Gaussian random vector [78] and with some manipulations, we obtain

$$E\{\Delta\mathbf{h}_m \mid \hat{\mathbf{h}}_m\} = \sigma_{\Delta h}^2\hat{\mathbf{h}}_m(\mathbf{R_r} + \sigma_{\Delta h}^2\mathbf{I}_{N_R})^{-1}; \tag{171}$$

$$Cov[\Delta\mathbf{h}_m\Delta\mathbf{h}_m^H \mid \hat{\mathbf{h}}_m] = \sigma_{\Delta h}^2\mathbf{I}_{N_R} - \frac{\sigma_{\Delta h}^4}{\mathbf{R_r} + \sigma_{\Delta h}^2\mathbf{I}_{N_R}}. \tag{172}$$

4.4.2. Computation of MMSE GR

Let $k_i \in \{1,2,\ldots,N_T\}$ be the index of i-th detected spatial data stream according to the maximal post-detection *SINR* ordering rule. Denote μ_{a_j} and $\sigma_{a_j}^2$ as the mean and variance of the signal a_j, respectively, which can be determined by *a posteriori* symbol probability estimation as in [70]. By performing the soft interference cancellation (SIC) [70] and considering channel estimation error, the corresponding interference-cancelled received signal vector $\tilde{\mathbf{s}}_{k_i}$ can be determined in the following form:

$$\tilde{\mathbf{s}}_{k_i} = \mathbf{Ha} - \sum_{j=k_1}^{k_{i-1}}\hat{\mathbf{h}}_j\mu_{a_j} + \mathbf{w}_{PF} = \sum_{j=k_i}^{k_{N_T}}(\hat{\mathbf{h}}_j - \Delta\mathbf{h}_j)a_j + \sum_{j=k_1}^{k_{i-1}}\hat{\mathbf{h}}_j(a_j - \mu_{a_j}) - \sum_{j=k_1}^{k_{i-1}}\Delta\mathbf{h}_ja_j + \mathbf{w}_{PF}, \tag{173}$$

where $\mathbf{w}_{PF}$ is the noise forming at the PF output of GR front end linear system.

Then, conditionally on $\hat{\mathbf{H}}$, the MMSE GR output is given as [3, 51]

$$\tilde{\mathbf{Y}}_i = \frac{E\{2a_{k_i}\tilde{\mathbf{s}}_{k_i}^H \mid \hat{\mathbf{H}}\} - E\{\tilde{\mathbf{s}}_{k_i}\tilde{\mathbf{s}}_{k_i}^H \mid \hat{\mathbf{H}}\} + E\{\mathbf{w}_{AF_i}\mathbf{w}_{AF_i}^H\}}{E\{\tilde{\mathbf{s}}_{k_i}\tilde{\mathbf{s}}_{k_i}^H \mid \hat{\mathbf{H}}\}}, \tag{174}$$

where $\mathbf{w}_{AF}$ is the reference zero mean Gaussian noise with *a priori* information **a "no" signal** and with the following covariance matrix in a general case [1, 3]

$$E\{\mathbf{w}_{PF}\mathbf{w}_{PF}^H\} = E\{\mathbf{w}_{AF}\mathbf{w}_{AF}^H\} = \sigma_w^2\mathbf{I}_{N_R}, \tag{175}$$

because the AF and PF of GR front end linear system do not change the statistical parameters of input process (Gaussian noise, for example). Thus, according to (173) and (175), we can write

$$E\{\tilde{\mathbf{s}}_{k_i}\tilde{\mathbf{s}}_{k_i}^H \mid \hat{\mathbf{H}}\} = \Big\{ \sum_{j=k_i}^{k_{N_T}} [\tilde{\mathbf{h}}_j\tilde{\mathbf{h}}_j^H - \tilde{\mathbf{h}}_j E\{\Delta\mathbf{h}_j^H \mid \hat{\mathbf{H}}\} - E\{\Delta\mathbf{h}_j \mid \hat{\mathbf{H}}\}\tilde{\mathbf{h}}_j^H] + \sum_{j=1}^{k_{N_T}} E\{\Delta\mathbf{h}_j\Delta\mathbf{h}_j^H \mid \hat{\mathbf{H}}\} \Big\} E_b$$
$$+ \sum_{j=k_1}^{k_{i-1}} [\hat{\mathbf{h}}_j\hat{\mathbf{h}}_j^H - \hat{\mathbf{h}}_j E\{\Delta\mathbf{h}_j^H \mid \hat{\mathbf{H}}\} - E\{\Delta\mathbf{h}_j \mid \hat{\mathbf{H}}\}\hat{\mathbf{h}}_j^H]\sigma_{a_j}^2 + \sigma_w^2\mathbf{I}_{N_R}. \tag{176}$$

Based on results discussed in the previous Section, it is evidently that $\Delta\mathbf{h}_j$ is only correlated with $\hat{\mathbf{h}}_j$. Then, we have

$$E\{\Delta\mathbf{h}_j\Delta\mathbf{h}_j^H \mid \hat{\mathbf{H}}\} = E\{\Delta\mathbf{h}_j\Delta\mathbf{h}_j^H \mid \hat{\mathbf{h}}_j\}. \tag{177}$$

From the basic relationship between the autocorrelation and covariance functions, we have

$$E\{\Delta\mathbf{h}_j\Delta\mathbf{h}_j^H \mid \hat{\mathbf{h}}_j\} = Cov\{\Delta\mathbf{h}_j\Delta\mathbf{h}_j^H \mid \hat{\mathbf{h}}_j\} + E\{\Delta\mathbf{h}_j \mid \hat{\mathbf{h}}_j\}E\{\Delta\mathbf{h}_j^H \mid \hat{\mathbf{h}}_j\}. \tag{178}$$

Substituting (171) and (172) into (178), we can write

$$E\{\Delta\mathbf{h}_j\Delta\mathbf{h}_j^H \mid \hat{\mathbf{h}}_j\} = \sigma_{\Delta h}^2\mathbf{I}_{N_R} - \sigma_{\Delta h}^4(\mathbf{R_r} + \sigma_{\Delta h}^2\mathbf{I}_{N_R})^{-1} + \sigma_{\Delta h}^4(\mathbf{R_r} + \sigma_{\Delta h}^2\mathbf{I}_{N_R})^{-1}\mathbf{h}_j\mathbf{h}_j^H(\mathbf{R_r} + \sigma_{\Delta h}^2\mathbf{I}_{N_R}). \tag{179}$$

Introduce the following notations

$$\mathbf{\Lambda} = (\mathbf{R_r} + \sigma_{\Delta h}^2\mathbf{I}_{N_R})^{-1}, \tag{180}$$

$$\mathbf{\Xi} = \mathbf{I}_{N_R} - \sigma_{\Delta h}^2\mathbf{\Lambda}, \tag{181}$$

$$\mathbf{R}_{aa} = diag\{\sigma_{a_{k_1}}^2, \sigma_{a_{k_2}}^2, \ldots, \sigma_{a_{k_{i-1}}}^2\}. \tag{182}$$

Substituting (171) and (179) into (176) and taking into consideration (180)–(182), we have

$$E\{\tilde{\mathbf{s}}_{k_i}\tilde{\mathbf{s}}_{k_i}^H\} = E_b\mathbf{\Xi}\hat{\mathbf{H}}_{k_i:k_{N_T}}\hat{\mathbf{H}}_{k_i:k_{N_T}}^H\mathbf{\Xi} + E_b\sigma_{\Delta h}^4\mathbf{\Lambda}\hat{\mathbf{H}}_{k_1:k_{i-1}}\hat{\mathbf{H}}_{k_1:k_{i-1}}^H\mathbf{\Lambda} + (\hat{\mathbf{H}}_{k_1:k_{i-1}}\mathbf{R}_{aa}\hat{\mathbf{H}}_{k_1:k_{i-1}}^H + N_T E_b\sigma_{\Delta h}^2)\mathbf{\Xi}$$
$$-\sigma_{\Delta h}^2\mathbf{\Lambda}\hat{\mathbf{H}}_{k_1:k_{i-1}}\mathbf{R}_{aa}\hat{\mathbf{H}}_{k_1:k_{i-1}}^H + \sigma_w^2\mathbf{I}_{N_R}, \tag{183}$$

where the notation $\mathbf{H}_{n:m}$ denotes the submatrix containing the n-th to m-th columns of the matrix $\mathbf{H}$.

Based on similar manipulations, we can write

$$E\{2a_{k_i}\tilde{\mathbf{s}}_{k_i}^H \mid \hat{\mathbf{H}}\} - E\{\tilde{\mathbf{s}}_{k_i}\tilde{\mathbf{s}}_{k_i}^H \mid \hat{\mathbf{H}}\} + E\{\mathbf{w}_{AF_i}\mathbf{w}_{AF_i}^H\} = E_b\hat{\mathbf{h}}_{k_i}^H\sigma_{\Delta h}^2(\mathbf{R_r} + \sigma_{\Delta h}^2\mathbf{I}_{N_R})^{-1} + (\mathbf{w}_{AF}\hat{\mathbf{h}}_{k_i}^H\mathbf{w}_{AF}^H - \mathbf{w}_{PF}\hat{\mathbf{h}}_{k_i}^H\mathbf{w}_{PF}^H)\mathbf{I}_{N_R}. \quad (184)$$

In the root mean-square sense, the second term in (184) representing the GR back end background noise tends to approach zero. By this reason, finally we can write

$$E\{2a_{k_i}\tilde{\mathbf{s}}_{k_i}^H \mid \hat{\mathbf{H}}\} - E\{\tilde{\mathbf{s}}_{k_i}\tilde{\mathbf{s}}_{k_i}^H \mid \hat{\mathbf{H}}\} + E\{\mathbf{w}_{AF_i}\mathbf{w}_{AF_i}^H\} = E_b\hat{\mathbf{h}}_{k_i}^H\sigma_{\Delta h}^2(\mathbf{R_r} + \sigma_{\Delta h}^2\mathbf{I}_{N_R})^{-1}. \quad (185)$$

Combining (183) and (185), we obtain the MMSE GR output $\widetilde{\mathbf{Y}}_i$, conditionally on $\hat{\mathbf{H}}$.

4.4.3. Computation of LLR

By applying $\widetilde{\mathbf{Y}}_i$ to $\tilde{\mathbf{s}}_{k_i}$, we have the process at the MMSE GR output [13,52,61] $\widetilde{\mathbf{Z}}_{k_i} = \widetilde{\mathbf{Y}}_i\tilde{\mathbf{s}}_{k_i}$. According to the Gaussian approximation of the MMSE GR back end process, we can write

$$\widetilde{\mathbf{Z}}_{k_i} \approx \tilde{\boldsymbol{\mu}}_{k_i}a_{k_i}^2 + \tilde{\boldsymbol{\eta}}_{k_i}, \quad (186)$$

where

$$\tilde{\boldsymbol{\mu}}_{k_i} = E\{\widetilde{\mathbf{Y}}_i(\hat{\mathbf{h}}_{k_i} - \Delta\mathbf{h}_{k_i}) \mid \mathbf{H}\} = \widetilde{\mathbf{Y}}_i\mathbf{\Xi}\hat{\mathbf{h}}_{k_i} \quad (187)$$

and $\tilde{\boldsymbol{\eta}}_{k_i} = \mathbf{w}_{AF_{ki}}^2 - \mathbf{w}_{PF_{ki}}^2$ is the background noise at the MMSE GR output with zero-mean and variance $\sigma_{\tilde{\eta}_{k_i}}^2 = 4\sigma_w^4$.

Therefore, the LLR value of the coded bit $\mathbf{g}_{k_i}^\lambda$ can be approximated as [68, 69]

$$\mathscr{L}(\mathbf{g}_{k_i}^\lambda) \approx \frac{1}{\sigma_{\tilde{\eta}_{k_i}}^2}\left(\min_{\alpha_i \in \mathscr{F}_\lambda^0}|\mathbf{Z}_i - \boldsymbol{\mu}_i\alpha_i|^2 - \min_{\alpha_i \in \mathscr{F}_\lambda^1}|\mathbf{Z}_i - \boldsymbol{\mu}_i\alpha_i|^2\right), \quad (188)$$

where $\mathscr{F}_\lambda^0$ and $\mathscr{F}_\lambda^1$ denote the modulation constellation symbols subset of $\mathscr{F}$ whose λ-th bit equals 0 and 1, respectively.

4.4.4. Remarks

When the channel estimation error is neglected, i.e., $\sigma_{\Delta h}^2 = 0$ in (180), (181) and (183), the MMSE GR output given by (174) reduces to that of the modified soft-output MMSE GR, in which only decision error propagation is considered, [13, 61]. On the other hand, if $\mathbf{R_r} = \mathbf{I}_{N_R}$ and no residual interference cancellation error is assumed the MMSE GR output given by (174) reduces to that of [50]. For the sake of simplicity, we call this detector as the conventional soft-output MMSE GR hereafter if this detector is applied in channel coded MIMO DS-CDMA wireless communication system. Meanwhile, if both decision error propagation and channel estimation error are neglected, the MMSE GR output given by (174) reduces to that of the conventional MMSE GR output of [51].

4.5. SER definition

We continue a discussion of SER formula derivation presented in (61)-(72), subsection 3.3.1. In the case of *M*-ary PSK system the exact expression for the SER takes the following form [79]

$$P_{SER} = \frac{1}{\pi} \int_0^{\pi - \frac{\pi}{M}} \exp\left\{ -\frac{\frac{E_b}{N_0} \sin^2 \frac{\pi}{M}}{\sin^2 \theta} \right\} d\theta. \tag{189}$$

Taking into account (61), (67), and (189), we can write the *SER* of QPSK system employed the GR in the following form:

$$P_{SER} = \frac{1}{\pi} \int_0^{\pi - \frac{\pi}{M}} \phi_{q_{QBHS/MRC}} \left(-\frac{1}{2 \sin^2 \theta} \right) d\theta. \tag{190}$$

There is a need to note that a direct comparison of QPSK and BPSK systems on the basis of average symbol-energy-to-noise-spectral-density ratio indicates that the QPSK is approximately 3 dB worse than the BPSK.

Another signaling scheme that allows multiple signals to be transmitted using quadrature carries is the QAM. In this case, the transmitted signal can be presented in the following form:

$$a_k(t) = \sqrt{\frac{2}{T_s}} \left[A_i \cos(2\pi f_c t) + B_i \sin(2\pi f_c t) \right], \quad 0 \leq t \leq T_s \tag{191}$$

where A_i and B_i take on the possible values $\pm p; \pm 3p, \ldots, \pm(\sqrt{M}-1)p$ with equal probability, where M is an integer power of 4; T_s is the sampling interval, and f_c is the carrier frequency. The parameter p can be related to the average symbol energy E_b as given by

$$p = \sqrt{\frac{3E_b}{2(M-1)}}.$$ (192)

Taking into consideration a definition of the *SER* derived in [80] for *M*-ary QAM system employed the GR, we obtain

$$P_{SER} = 1 - \frac{1}{M} \left\{ (\sqrt{M}-2)^2 \left[1 - 2Q\left(\sqrt{\frac{3\varphi_{q_{QBHS/MRC}}}{M-1}} \right) \right]^2 + 4(\sqrt{M}-2) \left[1 - 2Q\left(\sqrt{\frac{3\varphi_{q_{QBHS/MRC}}}{M-1}} \right) \right] \left[1 - Q\left(\sqrt{\frac{3\varphi_{q_{QBHS/MRC}}}{M-1}} \right) \right] \right.$$

$$\left. + 4 \left[1 - Q\left(\sqrt{\frac{3\varphi_{q_{QBHS/MRC}}}{M-1}} \right) \right]^2 \right\},$$ (193)

where $Q(x)$ is the Gaussian *Q*-function given by

$$Q(x) = \frac{1}{\sqrt{2\pi}} \int_x^\infty \exp(-0.5t^2)dt.$$ (194)

4.6. Simulation results

4.6.1. FIR beamforming and MIMO wireless communication system

For a definition of numerical results using simulation, we consider the typical urban channel [81] of the GSM/EDGE system as a practical example. As is usually done for GSM/EDGE, the transmit pulse shape is modeled as a linearized Gaussian minimum-shift keying pulse [82]. The GR input linear system filter is a square-root raised-cosine filter with roll-off factor 0.3. Furthermore, we assume $N_T = 3$ transmit and $N_R = 3$ receive antennas and a maximum channel length of $L = 5$. The correlation coefficient between all pairs of transmit antennas is $\rho = 0.5$.

Figure 9 shows the average $\overline{SNR}$ as a function of the *SNR* noted by E_b/N_0 for the GR with MMSE linear equalization in the cases of FIR (the curves 2 and 3) and infinite impulse response (the curve 1) beamforming filter, respectively, where E_b denotes the average received energy per symbol. The curve 5 corresponds to the case for infinite impulse

response beamforming filter for receiver discussed in [67]. The $\overline{SNR}$ was obtained by averaging the respective *SNR*s over 1000 independent realizations of the typical urban channel. For this purpose, in the case of FIR beamforming filter at the GR, the *SNR* given by (159) was used and the corresponding beamforming filters at the GR were calculated using the gradient algorithm discussed in Section 4.3. For infinite impulse response beamforming filter at the GR the result given in [52] was used.
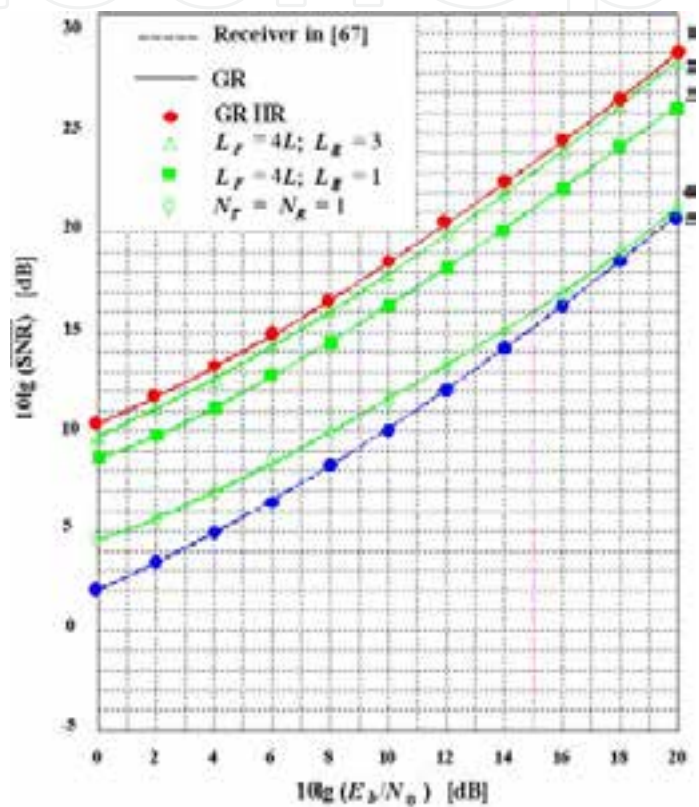
Figure 9. Average *SNR* of MMSE linear equalization at the GR for beamforming with FIR and infinite impulse response filters. The result for single antenna transmission is also indicated (the curve 4). IIR – infinite impulse response beamforming filter.

For comparison, we also show simulation results with FIR linear equalization filters at the GR of length $L_F = 4L$ for FIR beamforming filters at the GR with $L_g = 1$ (the curve 3) optimized for infinite impulse response linear equalization filters at the GR. These simulation results confirm that sufficiently long FIR linear equalization filters at the GR closely approach performance of infinite impulse response linear equalization filters at the GR, which are necessary for (178) to be valid. As expected, the beamforming with infinite impulse response beamforming filters at the GR constitutes a natural performance upper bound for the beamforming with FIR beamforming filters at the GR. However, interestingly, for the typical urban channel the FIR beamforming filter of length $L_g = 3$ (the curve 2) is

sufficient to closely approach the performance of the infinite impulse response beamforming at the GR (the curve 1).

We note that for high values of E_b/N_0 even an FIR beamforming filter at the GR of length $L_g = 1$ achieves a performance gain of more than 4.5 dB compared to single antenna transmission, i.e. $N_T = N_R = 1$ (the curve 4). Additional simulations not shown here for other GSM/EDGE channel profiles have shown that, in general, the FIR beamforming filter at the GR of length $L_g \leq 6$ is sufficient to closely approach the performance of the infinite impulse response beamforming at the GR. Thereby, the value of L_g required to approach the performance of the infinite impulse response beamforming at the GR seems to be smaller if the channel is less frequency selective.

4.6.2. Channel estimation and spatially correlation

We choose the 0.5 rate Low Density Parity Check (LDPC) code with a block length of 64800 bits, which is also adopted by DVB-S.2 standard [86]. QPSK modulation with Gray mapping is adopted in $N_T = N_R = 4$ MIMO system. Meanwhile, we set $\sigma_{\Delta h}^2 = 1$ $N_T = N_R$, and $E_P = E_b$. The channel is generated with coherence time of $N_P + N_D = 85$ MIMO vector symbol intervals, and then a LDPC codeword is transmitted via 100 channel coherent time intervals for QPSK modulation. For GR spatially correlated MIMO channel the GR array correlation matrix $\mathbf{R_r}$ with the following elements is adopted [68]

$$\begin{cases} \mathbf{R_r}(n,n) = 1, \mathbf{R_r}(m,n) = \mathbf{R_r^*}(m,n), m,n = 1,2,3,4; \\ \mathbf{R_r}(1,2) = \mathbf{R_r}(2,3) = \mathbf{R_r}(3,4) = 0.4290 + 0.7766j; \\ \mathbf{R_r}(1,3) = \mathbf{R_r}(2,4) = -0.3642 + 0.5490j; \\ \mathbf{R_r}(1,4) = -0.4527 - 0.0015j. \end{cases} \tag{195}$$

The performance comparison, in terms of *BER*, of the proposed soft-output MMSE GR, the modified soft-output MMSE GR [83], the conventional soft-output MMSE GR [84], and the conventional MMSE GR [85] is presented in Fig.10 for spatially independent MIMO channel and GR receiver spatially correlated MIMO channel. Also, a comparison with the soft-output MMSE V-BLAST detector discussed in [73] is made. The proposed MMSE GR outperforms all the existing schemes with considerable gain, especially for receiver correlation MIMO channel scenario. The underlying reason of this improvement is that the MMSE GR, by taking channel estimation error, decision error propagation and channel correlation into account, can output more reliable LLR to channel decoder. As channel estimation error is the dominant factor influencing the system performance under the lower *SNR* region, it can observed that the *BER* of the conventional soft-output MMSE GR [84] is slightly better than that of the modified soft-output MMSE GR in the case of spatially independent MIMO channel.
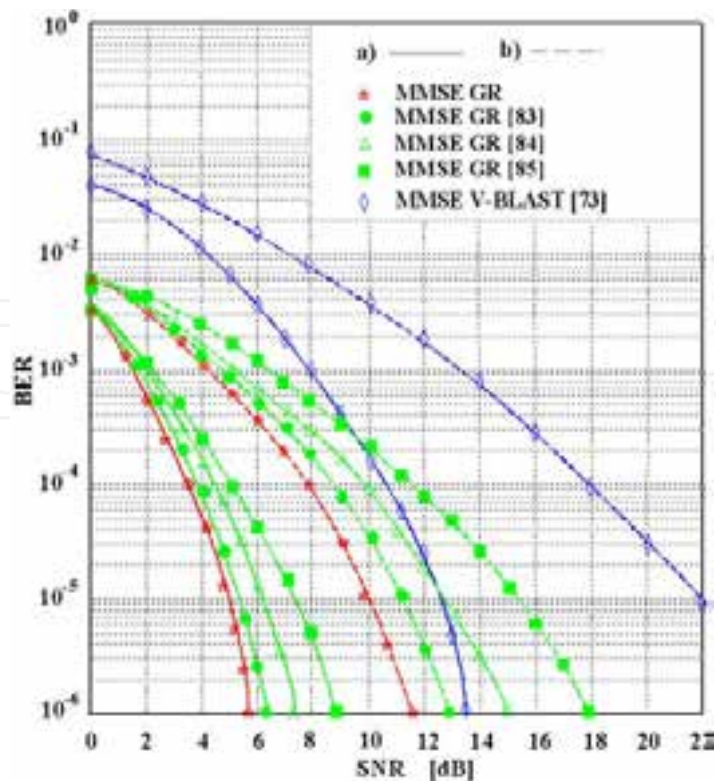
Figure 10. *BER* performance of different detectors under a) spatially independent MIMO channel and b) receiver spatially correlated MIMO channel.

4.7. Conclusions

In the present section, we have considered the FIR beamforming at the GR with perfect channel state information for single carrier transmission over frequency-selective fading channels with zero-forcing linear equalization and GR MMSE linear equalization. We employed a gradient algorithm for efficient recursive calculation of the FIR beamforming filters at the GR. Our results show that for typical GSM/EDGE channel profiles short FIR beamforming filters at the GR suffice to closely approach the performance of optimum infinite impulse response beamforming at the GR discussed in [52]. This is a significant result, since in practice, the quantized beamforming filter coefficients have to be fed back from the receiver to the transmitter, which makes short beamforming filters preferable.

The proposed MMSE GR outperforms all the existing schemes with considerable gain especially for receiver correlation MIMO channel scenario. The underlying reason of this improvement is that the MMSE GR, by taking channel estimation error, decision error propagation, and channel correlation into account, can output more reliable LLR to channel decoder. As channel estimation error is the dominant factor influencing the system performance under the lower *SNR* region, it can observed that the *BER* of the conventional soft-output MMSE GR [87] is slightly better than that of the modified soft-output MMSE GR in the case of spatially independent MIMO channel.

5. Signal processing with fading channels

5.1. Brief review

It is well known that the DS-CDMA transmission technique allows multiple users to share the same spectrum range simultaneously. Using DS-CDMA transmission technique in wireless communication systems, we can reach spectrum efficiency, high system capacity, robustness against interference, high quality of service (QoS) and so on [88,89]. In DS-CDMA wireless communication systems, the concatenating orthogonal Walsh-Hadamard (WH) channelization sequences and pseudonoise (PN) random scrambling sequences are used to generate the orthogonal spreading codes employed by multiple users for simultaneous signal transmission. There are multipaths in DS-CDMA wireless communication systems that destroy orthogonality between codes by introducing non-zero time delays and lead to interference among the transmitted signals in the downlink. One way to solve this problem is to use the scrambling sequences with the purpose to randomize signals transmitted by users and inhomogeneous behavior at nonzero time delays. One technique demonstrating how this problem can be solved is discussed in [90].

At the present time, the wideband DS-CDMA technique employed by wireless communication systems attracts a great attention of researchers, in particular, in mobile communication systems. An important feature of wideband DS-CDMA is an implementation of complex spreading sequences. The term "complex spreading" was generated from terminology used in constant to dual-channel spreading [91]. It is shown in [92-94] that the complex spreading can be realized either by a complex-valued sequence or by two binary sequences. As was shown in [92], the complex sequences can be 3 dB better than the binary Gold sequences [95] in the maximum periodic correlation parameters. Moreover, larger sets are available in complex sequences. Unfortunately, all these sequences are nonorthogonal and can be characterized as the complex-valued PN spreading sequences. Lam and Ozluturk investigated in [95] an application area of nonorthogonal complex sequences in DS-CDMA downlink wireless communication systems. As was defined in [95], the performance bounds were derived for the DS-CDMA wireless communication systems with complex signature sequences over the AWGN channels.

In this section, we investigate a generalized receiver (GR) constructed on the basis of GASP [1-3,6-8]. Using the GR in the DS-CDMA downlink wireless communication system, we would like to get answers on the following questions:

- Is it possible to maintain the orthogonality between users under GR implementation in the DS-CDMA downlink wireless communication system?

- Is it possible to reduce the effect of multipath fading and interference from other users under GR implementation in the DS -CDMA downlink wireless communication system?

- What are benefits under GR implementation in DS-CDMA downlink wireless communication system in comparison with other conventional receivers, for example, the Rake receiver?

To give answers on these questions we carry out our analysis using, for instance, the orthogonal 4-phase complex sequences in the DS-CDMA downlink wireless communication system. These sequences are generated by the unified complex Hadamard transform matrix discussed in [96], the correlation properties of which are studied in [97], where it is shown that the unified complex Hadamard transform sequences possess the better autocorrelation properties in comparison with the WH sequences, which are characterrized by very poor autocorrelation properties.

The use of orthogonal unified complex Hadamard transform sequences by the transmitter as channelization spreading codes scrambled by long PN sequences and further processing these sequences by the GR allows us to maintain the orthogonality between the users, and at the same time, to reduce the effect of multipath fading and interference from other users. A coherent GR [6], for example, can be used to combat the adverse effects of short-term multipath fading in mobile radio propagation environments. Owing to computational simplicity of the signal-to-interference-plus-noise ratio (SINR) in comparison with the probability of error, SINR is mostly used for evaluating and selecting code sequences among several candidates. Therefore, in this section, we investigate the SINR at the GR output when the unified complex Hadamard transform spreading sequences are generated by transmitter in the DS-CDMA downlink wireless communication system and compare this with the SINR at the GR output under transmission of WH real sequences. It is shown that the SINR at the GR output is independent of the phase offsets between different paths when the unified complex Hadamard transform spreading sequences are generated by the transmitter in the DS-CDMA downlink wireless communication system. The SINR at the GR output of the same system is a function of the squared cosine of path phase offsets under generation of WH real sequences by the transmitter. Because of this, as a direct result, the bit error rate (BER) performance of GR employing by the DS-CDMA downlink wireless communication system when the unified complex Hadamard transform spreading sequences are generated by the transmitter is better that that of the system with the WH sequences under Gaussian approximation. Also, we carry out a BER performance comparison of the DS-CDMA system employing the GR with the same system using then conventional receiver, for example, the Rake receiver [95]. Comparative analysis shows us a great superiority in the BER performance under GR employment in the DS-CDMA downlink wireless communication system over the use of the Rake receiver.

This section is organized as follows. At first, we present some basic definitions of the unified complex Hadamard transform sequences. Additionally, we study the DS-CDMA downlink wireless communication system model under the GR employment when the unified complex Hadamard transform spreading sequences are generated and propagated in a multipath fading channel. Further, we investigate the SINR performance at the GR output

when the unified complex Hadamard transform spreading sequences are generated and compare this with the SINR of the same system using the WH sequences. Computer simulation and comparison with the Rake receiver are also presented. Some concluding remarks are given.

5.2. Unified complex Hadamard transform sequences

The considered DS-CDMA downlink wireless communication system uses the orthogonal unified complex Hadamard transform spreading sequences. These so-called orthogonal unified complex Hadamard transform sequences are easy to generate. Larger sets of complex sequences are also available. They are categorized into two groups: the half-spectrum property orthogonal unified complex Hadamard transform spreading sequences and the non-half-spectrum property orthogonal unified complex Hadamard transform spreading sequences. Consider briefly how these sequences can be generated and note the main definitions and remarks discussed in [96, 97].

A unified complex Hadamard transform matrix **A** of order $N = 2^n$ is a square matrix with elements ± 1 and $\pm j$, and is constructed by [96,97]

$$A_n = \overset{n}{\underset{i=1}{\otimes}} A_1 = A_1 \otimes A_{n-1} = \underbrace{A_1 \otimes \cdots \otimes A_1}_{n \text{ times}}, \tag{196}$$

where $\otimes$ denotes the Kronecker product, and A_1 is defined as

$$A_1 = \begin{bmatrix} a_1 & a_1 a_3 \\ a_2 & -a_2 a_3 \end{bmatrix} \tag{197}$$

with

$$a_1, a_2, a_3 \in \{1, -1, j, -j\} \quad \text{and} \quad j = \sqrt{-1}. \tag{198}$$

There are 64 different matrices for A_1 satisfying (197) with elements ± 1 and $\pm j$,

$$A_1 A_1^* = A_1^* A_1 = 2I_2 \tag{199}$$

and

$$\left| \det (A_1) \right|^2 = 2^2, \tag{200}$$

where $*$ indicates the complex conjugate. Hence, the unified complex Hadamard transform matrix is orthogonal. Furthermore, the unified complex Hadamard transform matrices contain a WH transform matrix as a special case, with

$$a_1 = a_2 = a_3 = 1 \tag{201}$$

in the matrix A_1.

The unified complex Hadamard transform matrices have two categories of 32 basic matrices, depending on whether a_3 in (197) is imaginary or not [97]. If a_3 is imaginary, the matrix group is called the half-spectrum property unified complex Hadamard transform. Otherwise, the group is called the non-half-spectrum property unified complex Hadamard transform. The unified complex Hadamard transform spreading sequence $c_k, k = 1, \ldots, N$ is defined by the k-th row of the unified complex Hadamard transform matrix. It has been shown in [97] that the non-half-spectrum property unified complex Hadamard transform sequences have very similarly poor autocorrelation properties as WH sequences, and some of the half-spectrum property unified complex Hadamard transform sequences exhibit a reasonable compromise between the autocorrelation and cross-correlation functions. In this section, we just consider the half-spectrum property unified complex Hadamard transform sequences, i.e., $a_3 = j$ or $-j$.

5.3. System model

In this section, we think that to assess accurately the effects of multipath fading and interference components from other users on the performance of DS-CDMA downlink wireless communication system it is enough to consider a single-cell environment system model. In particular, we analyze a complex baseband-equivalent model with the binary phase-shift keying (BPSK) data and complex signature sequences over a multipath fading channel for the DS-CDMA downlink wireless communication system. The baseband representation of the total signal transmitted on the downlink can be presented in the following form:

$$a(t) = \sum_{k=0}^{K-1} a_k(t) = \sum_{k=0}^{K-1} \sqrt{P_{a_k}} b_k(t) c_k(t), \tag{202}$$

where K is the number of users;

$$a_k(t) = \sqrt{P_{a_k}} b_k(t) c_k(t) \tag{203}$$

is the transmitted signal of the k-th user; P_{a_k} is the power of the k-th transmitted signal;

$$b_k(t) = \sum_{n=-\infty}^{\infty} b_k^{(n)} p_T(t - nT) \tag{204}$$

is the data signal of the k-th user;

$$b_k^{(n)} \in \{-1, +1\} \tag{205}$$

denotes the n-th data bit value of the k-th user; the function $p_T(t)$ is the rectangular pulse of symbol duration T; $c_k(t)$ is the complex spreading signal defined by

$$c_k(t) = \sum_{m=-\infty}^{\infty} c_k^{(m)} \phi(t - mT_c); \tag{206}$$

and $c_k^{(m)}$ denotes the m-th complex chip value of the k-th user. The function $\varphi(t)$ is a chip waveform that is time-limited to $[0, T_c)$ with

$$\int_0^{T_c} \phi^2(t) dt = T_c, \tag{207}$$

including the rectangular pulse of duration T_c, and T_c is called the chip duration. Throughout this section, we assume that

$$T = NT_c. \tag{208}$$

Power control is assumed to be perfect, and we suppose that the transmitted signal power P_{a_k} is assumed to be known. We also assume

$$c_k^{(m)} = d^{(m)} a_k^{(m)}, \tag{209}$$

where

$$d = \{d^{(m)}\} \quad \text{with} \quad d^{(m)} \in \{+1, -1\} \tag{210}$$

is the random scrambling code commonly used by all users, and

$$a^{(k)} = \{a_k^{(m)}\} \tag{211}$$

is the user-specific orthogonal unified complex Hadamard transform spreading sequence with period N. Thus,

$$c^{(k)} = \{c_k^{(m)}\} \tag{212}$$

is the random sequence with

$$E\{c_k^{(m)}(c_{k'}^{(n)})^*\} = 0, \quad m \neq n \tag{213}$$

for all k and k', where $E\{\cdot\}$ denotes the mathematical expectation.

The final results of our analysis in this section are applicable to the DS-CDMA downlink wireless communication systems that use long PN scrambling sequences such as m-sequences and Gold sequences [95]. This is because the periods of these long scrambling codes are much larger than that of the spreading factor N, and have correlation properties similar to those of the random scrambling sequences.

For instance, at the base station transmitter in mobile communication system, the signals of all K users are symbol synchronously added before passing through a frequency-selective multipath-fading channel. The complex baseband-equivalent impulse response of the multipath channel can be presented in the following form:

$$h(t) = \sum_{l=0}^{L-1} \alpha_l \exp(j\theta_l)\delta(t - \tau_l), \tag{214}$$

where L is the number of resolvable propagation paths, and $\alpha_l \exp(j\theta_l)$ and τ_l are the complex fading factor and propagation delay of the l-th path, respectively. Note, α_l may be Rayleigh-, Rician-, or Nakagami-distributed, depending on a specific channel model. All random variables in (214) are assumed to be independent for l. The channel parameters, such as α_l, θ_l, and τ_l are here assumed to be known in the dispreading and demodulation process, although in practice, the impulse response of the channel is typically estimated using the pilot symbol or pilot channel.

Moreover, we assume that the multipaths at the GR input are resolvable and chip-synchronized, i.e., they are spaced, at least one chip duration apart in time and the relative delays are multiples of the chip duration. Without loss of generality, the resolved paths are assumed to be numbered such that

$$0 \leq \tau_0 < \tau_1 < \cdots < \tau_{L-1} < T. \tag{215}$$

Hence, the baseband complex representation of the signal at the GR input (the input of GR linear system) of any user is given by

$$x(t) = \sum_{k=0}^{K-1} \sum_{l=0}^{L-1} \sqrt{P_{a_k}} \, \alpha_l \exp(j\theta_l) b_k(t - \tau_l) c_k(t - \tau_l) + w(t), \tag{216}$$

where $w(t)$ is the complex background AWGN with zero mean and one-sided power spectral density N_0.
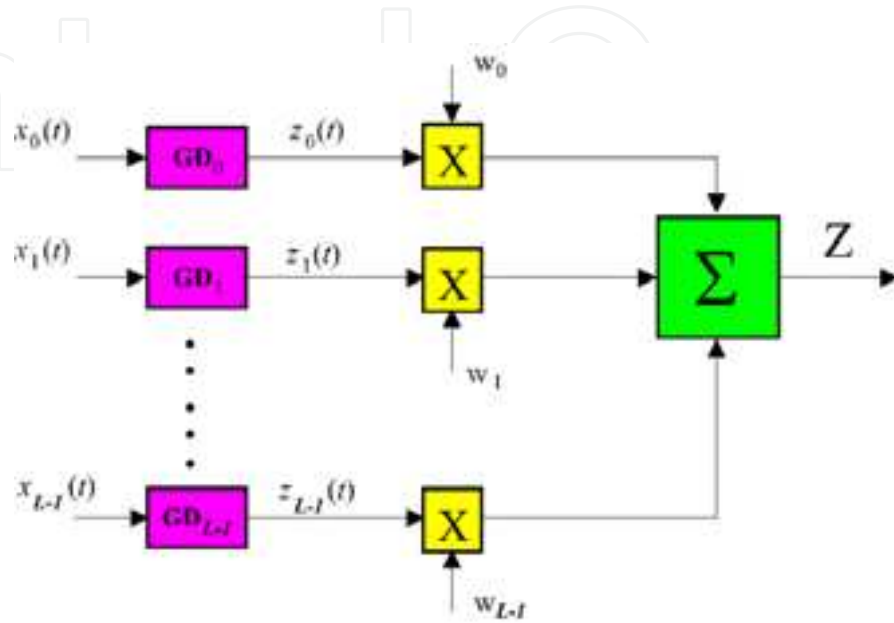
Figure 11. GR structure with $L-1$ fingers.

In order to mitigate the multipath fading effect, the GR with coherent demodulation is implemented. The GR structure is presented in Fig.11, where the number of fingers is equal to the number of resolvable paths.

Since the symbols $b_k^{(n)}$ are i.i.d. from one symbol duration to another and from one user to another, without loss of generality, we focus our attention on the GR output of the user 0 for the zero-th transmitted symbol. The complex GR output of the i-th finger of user 0 in accordance with the GASP in noise [1–3,6–9,11] is

$$z_i = \mathcal{R}e \left\{ \int_{\tau_i}^{T+\tau_i} 2x(t) \sqrt{P_{a_0}^*} \, c_0^*(t - \tau_i) \exp(-j\theta_i) dt - \int_{\tau_i}^{T+\tau_i} x(t) x^*(t - \tau_i) dt + \int_{\tau_i}^{T+\tau_i} \eta(t) \eta(t - \tau_i) dt \right\}, \tag{217}$$

where $\sqrt{P_{a_0}^*} \, c_0^*(t - \tau_i) \exp(-j\theta_i)$ is the model of transmitted signal for user 0, i.e., the reference signal generated by the GR, [3,6]; τ_i is the delay factor that can be neglected for simplicity of analysis; $\eta(t)$ is the noise forming at the GR AF output given by (4).

The main functioning condition under employment of GR in DS-CDMA wireless communication systems discussed in detail in Section 2.1 takes the following form

$$P_{a_k} = P_{a_k}^*, \qquad (218)$$

where P_{a_k} is the power of information signal and $P_{a_k}^*$ is the power of model signal (the reference signal). In practice, we can perform this matching implementing, for example, tracking systems. These statements and possible ways to solve this problem and how we can implement all this in practice are discussed in detail in [1–3,6–9,11]. Thus, the following process, in a general case, is formed at the GR output for k-th user according to implementation of GASP in DS-CDMA wireless communication systems.

The case 1: a "yes" signal in the input process –

$$
\begin{aligned}
Z = \mathfrak{Re} & \left\{ \int_{\tau_i}^{T+\tau_i} \sum_{l=0}^{L-1} a_k(t)\alpha_l \exp(j\theta_l) a_k^*(t-\tau_i) dt - \int_{\tau_i}^{T+\tau_i} \sum_{l=0}^{L-1} \xi_k(t)\alpha_l \exp(j\theta_l) \xi_k^*(t-\tau_i) dt + \int_{\tau_i}^{T+\tau_i} \sum_{l=0}^{L-1} \eta_k(t)\alpha_l \exp(j\theta_l) \eta_k^*(t-\tau_i) dt \right\} \\
= \mathfrak{Re} & \left\{ \int_{\tau_i}^{T+\tau_i} \sum_{l=0}^{L-1} \left[\sqrt{P_{a_k}} \sqrt{P_{a_k}^*} b_k(t)\alpha_l \exp(j\theta_l) b_k^*(t-\tau_i) c_k(t) c_k^*(t-\tau_i) - \xi_k(t)\alpha_l \exp(j\theta_l) \xi_k^*(t-\tau_i) + \eta_k(t)\alpha_l \exp(j\theta_l) \eta_k^*(t-\tau_i) \right] dt \right\}
\end{aligned} \qquad (219)
$$

The case 2: a "no" signal in the input process –

$$
Z = \mathfrak{Re} \left\{ \int_{\tau_i}^{T+\tau_i} \sum_{l=0}^{L-1} \eta_k(t)\alpha_l \exp(j\theta_l) \eta_k^*(t-\tau_i) dt - \int_{\tau_i}^{T+\tau_i} \sum_{l=0}^{L-1} \xi_k(t)\alpha_l \exp(j\theta_l) \xi_k^*(t-\tau_i) dt \right\} = \Delta_i, \qquad (220)
$$

where Δ_i is the background noise forming at the GR output. Finally, the GR combiner output that produces a decision statistic is

$$Z = \sum_{i=0}^{L-1} w_i z_i, \qquad (221)$$

where the selection of the combining weights w_i's determines the specific diversity-combining technique.

5.4. Performance analysis

5.4.1. SINR at GR output

In this section, we investigate SINR by considering the GR shown in Fig. 11. It follows from (217)-(221) that the i-th GR finger output for user 0 can be presented in the following form

$$z_i = TP_{a_0} \alpha_i b_0^{(0)} + I_{MUI}^{(i)} + I_{MP}^{(i)} + \Delta_i(t), \qquad (222)$$

where the first term is the signal component; the second term is the multiple-user interference component determined by

$$I_{MUI}^{(i)} = \Re e \left\{ \sum_{k=1}^{K-1} P_{a_k} \alpha_i b_k^{(0)} \int_{\tau_i}^{T+\tau_i} c_k(t-\tau_i) c_0^*(t-\tau_i) dt \right\} \tag{223}$$

the third term is the multipath interference component given by

$$I_{MP}^{(i)} = \Re e \left\{ \sum_{k=0}^{K-1} \sum_{l=0, l\neq i}^{L-1} P_{a_k} \alpha_l \exp\left[j(\theta_l - \theta_i) \right] \int_{\tau_i}^{T+\tau_i} b_k(t-\tau_i) c_k(t-\tau_i) c_0^*(t-\tau_i) dt \right\}; \tag{224}$$

and the fourth term $\Delta_i(t)$ is the background noise at the GR output given for a general case by (7).

We can see that the multiple-user interference component $I_{MUI}^{(i)}$ and the multipath interference component $I_{MP}^{(i)}$ are due to the interference from the i-th path of other users' signals and from the remaining $L-1$ paths from all users' signals, respectively. The background noise $\Delta_i(t)$ at the GR output is the i.i.d. random process obeying the asymptotic Gaussian distribution with zero mean and variance of $4T\sigma_w^4$ [1–3,6–9,11].

Define a periodic correlation function $R_{k,m}$ by

$$R_c^{(k,m)}(q) = \begin{cases} \sum_{p=0}^{N-1-q} c_k^{(p)} \left(c_m^{(p+q)} \right)^*, & 0 \le q \le N-1 \\ \sum_{p=0}^{N-1+q} c_k^{(p-q)} \left(c_m^{(p)} \right)^*, & 1-N \le q < 0 \\ 0, & |q| \ge N. \end{cases} \tag{225}$$

Then, let

$$\tau_l - \tau_i = q_l T_c. \tag{226}$$

With the assumption of chip synchronization, it can be obtained that q_l is an integer and the multiple-user interference and multipath interference components can be presented in the following form:

$$I_{MUI}^{(i)} = \Re\left\{T_c \sum_{k=1}^{K-1} P_{a_k} \alpha_i b_k^{(0)} R_c^{(k,0)}(0)\right\}, \tag{227}$$

$$I_{MP}^{(i)} = \Re\left\{T_c \sum_{l=0}^{i-1}\sum_{k=0}^{K-1} P_{a_k} \alpha_l \exp\left[j(\theta_l - \theta_i)\right]R_{k0} + T_c \sum_{l=i+1}^{L-1}\sum_{k=0}^{K-1} P_{a_k} \alpha_l \exp\left[j(\theta_l - \theta_i)\right]\hat{R}_{k0}\right\}, \tag{228}$$

where

$$R_{k0} = b_k^{(0)} R_c^{(k,0)}(q_l) + b_k^{(1)} R_c^{(k,0)}(N + q_l), \tag{229}$$

$$\hat{R}_{k0} = b_k^{(-1)} R_c^{(k,0)}(q_l - N) + b_k^{(0)} R_c^{(k,0)}(q_l). \tag{230}$$

In the following, we are going to compare the SINR at the GR output in the DS-CDMA downlink wireless communication system implementing the unified complex Hadamard transform spreading codes with that at the GR output in the DS-CDMA downlink wireless communication system using the WH spreading sequences. Note, that under employment of the orthogonal spreading codes in DS-CDMA downlink wireless communication system, such as the WH real spreading codes and the orthogonal unified complex Hadamard transform spreading codes considered in this section, we must take into consideration that

$$R_c^{(k,0)}(0) = 0, \quad k \neq 0. \tag{231}$$

Consequently, the multiple-user interference component is equal to zero, i.e.,

$$I_{MUI}^{(i)} = 0. \tag{232}$$

When the WH spreading codes are used in the DS-CDMA downlink wireless communication system employing the GR, we can obtain that the multipath interference component takes the following form:

$$I_{MP}^{(i)} = T_c \sum_{l=0}^{i-1}\sum_{k=0}^{K-1} P_{a_k} \alpha_l \cos(\theta_l - \theta_i) R_{k0} + T_c \sum_{l=i+1}^{L-1}\sum_{k=0}^{K-1} P_{a_k} \alpha_l \cos(\theta_l - \theta_i)\hat{R}_{k0}. \tag{233}$$

Owing to the mutually independent random variables $b_k^{(n)}$ for $0 \leq k \leq K-1$, the multipath interference component $I_{MP}^{(i)}$ has zero mean. With regard of (213), it can be easily shown via straightforward computation that, for the WH spreading sequences we are able to obtain

$$E\{R_{k0}^2\} = E\{\hat{R}_{k0}^2\} = N. \tag{234}$$

Therefore, the variance of the multipath interference component $I_{MP}^{(i)}$ is denoted by $\sigma^2_{I_{MP}^W}$ and can be determined in the following form:

$$\sigma^2_{I_{MP}^W} = NT_c^2 \sum_{l=0,l\neq i}^{L-1} \alpha_l^2 \cos^2\left(\theta_l - \theta_i\right) \sum_{k=0}^{K-1} P_{a_k}^2. \tag{235}$$

Hence, the SINR at the GR i-th finger output for the WH spreading codes is determined in the following form:

$$SINR_{WH}^{(i)} = \frac{E_{a_0} \alpha_i^2}{\sqrt{\dfrac{1}{N} \displaystyle\sum_{l=0,l\neq i}^{L-1} \alpha_l^2 \cos^2\left(\theta_l - \theta_i\right) \displaystyle\sum_{k=0}^{K-1} E_{a_k}^2 + 4\sigma_w^4}}, \tag{236}$$

where

$$E_{a_k} = P_{a_k} T, \quad k = 0, 1, \ldots, K-1 \tag{237}$$

is the energy per data symbol of the m-th user and the variance σ_w^2 is given by (23).

Similarly, when the unified complex Hadamard transform spreading codes are employed by the DS-CDMA downlink wireless communication system using the GR, we can obtain that the multipath interference component $I_{MP}^{(i)}$ takes the following form:

$$
\begin{aligned}
I_{MP}^{(i)} = {} & T_c \sum_{l=0}^{i-1} \sum_{k=0}^{K-1} P_{a_k} \alpha_l \cos(\theta_l - \theta_i) \mathcal{R}e\{R_{k0}\} + T_c \sum_{l=i+1}^{L-1} \sum_{k=0}^{K-1} P_{a_k} \alpha_l \cos(\theta_l - \theta_i) \mathcal{R}e\{\hat{R}_{k0}\} \\
& + T_c \sum_{l=0}^{i-1} \sum_{k=0}^{K-1} P_{a_k} \alpha_l \sin(\theta_l - \theta_i) \mathrm{Im}\{R_{k0}\} + T_c \sum_{l=i+1}^{L-1} \sum_{k=0}^{K-1} P_{a_k} \alpha_l \sin(\theta_l - \theta_i) \mathrm{Im}\{R_{k0}\}.
\end{aligned}
\tag{238}
$$

Note that the multipath interference component $I_{MP}^{(i)}$ has zero mean. If the half-spectrum property unified complex Hadamard transform spreading sequences are employed by the DS-CDMA downlink wireless communication system using the GR, it can be easily shown from (213) via straightforward computation that

$$E\left\{ \left[\mathcal{R}e(R_{k0})\right]^2 \right\} = E\left\{ \left[\mathrm{Im}(R_{k0})\right]^2 \right\} = \frac{N}{2}, \tag{239}$$

$$E\left\{ \left[\mathcal{R}e(\hat{R}_{k0})\right]^2 \right\} = E\left\{ \left[\mathrm{Im}(\hat{R}_{k0})\right]^2 \right\} = \frac{N}{2}. \tag{240}$$

Hence, the variance of the multipath interference component $I_{MP}^{(i)}$ is denoted by $\sigma_{I_{MP}^H}^2$ and can be determined in the following form:

$$\sigma_{I_{MP}^H}^2 = \frac{N}{2} T_c^2 \sum_{l=0, l\neq i}^{L-1} \alpha_l^2 \sum_{k=0}^{K-1} P_{a_k}^2. \tag{241}$$

Therefore, the SINR at the GR i-th finger output for the half-spectrum property unified complex Hadamard transform spreading sequences employed by the DS-CDMA downlink wireless communication system using the GR is determined by

$$SINR_H^{(i)} = \frac{E_{a_0} \alpha_i^2}{\sqrt{\dfrac{1}{2N} \sum_{l=0, l\neq i}^{L-1} \alpha_l^2 \sum_{k=0}^{K-1} E_{a_k}^2 + 4\sigma_w^4}}. \tag{242}$$

5.4.2. GR finger weights

There is a need to note that the interference plus the thermal noise power seen by different fingers of the GR employed by DS-CDMA downlink wireless communication systems is different. Assume that the multipath interference signals are uncorrelated from one finger to another. In this case, the optimal weight in terms of the maximizing SINR at the GR output is dependent on the multipath interference. This optimal weight is called the modified maximal ratio combining (MMRC). There is a need to note that for the traditional maximal ratio combining (MRC) the weights are chosen in the following manner

$$w_i = \alpha_i. \tag{243}$$

Here, if the MMRC is employed as the combiner, the combining weights for DS-CDMA downlink wireless communication system using the WH codes and DS-CDMA downlink wireless communication system with the unified complex Hadamard transform spreading sequences under employment of the GR are different. This is a direct consequence of the difference in the SINR values at the GR finger output of the two systems.

For the WH spreading sequences used by the DS-CDMA downlink wireless communication system employing the GR, MMRC weights take the following form:

$$w_i^{WH} = \sqrt{\frac{P_{a_0} \alpha_i^2}{\dfrac{1}{N} \sum_{l=0, l\neq i}^{L-1} \alpha_l^2 \cos^2\left(\theta_l - \theta_i\right) \sum_{k=0}^{K-1} E_{a_k}^2 + 4\sigma_w^4}}. \tag{244}$$

For the unified complex Hadamard transform spreading sequences used by the DS-CDMA downlink wireless communication system employing the GR, MMRC weights have the following form:

$$w_i^H = \sqrt{\frac{P_{a_0} \alpha_i^2}{\frac{1}{2N} \sum_{l=0, l \neq i}^{L-1} \alpha_l^2 \sum_{k=0}^{K-1} E_{a_k}^2 + 4\sigma_w^4}}. \tag{245}$$

After the MMRC scheme, the SINR at the GR output is equal to the sum of all fingers' SINRs, as in (236) or (242). The use of the unified complex Hadamard transform spreading sequences in DS-CDMA downlink wireless communication system employing the GR ensures that the SINR at the GR output is independent of the phase offsets between different paths. The use of the WH real sequences in DS-CDMA downlink wireless communication systems employing the GR causes the SINR at the GR output to be related to the squared cosine of the phase offsets between paths, as seen by comparing (236) and (242). Even though the average SINR per finger at the GR output in the DS-CDMA downlink wireless communication system under employment of the WH codes is the same as that at the GR output in the DS-CDMA downlink wireless communication system under the use of the unified complex Hadamard transform spreading sequences, owing to

$$E\{\cos^2(\theta_l - \theta_i)\} = 0.5, \tag{246}$$

the SINR distribution over the random variable $\cos^2(\theta_l - \theta_i)$ can cause degradation in BER performance under some conditions. This is analogous to the case of a transmission over flat Rayleigh fading channels: even when the Rayleigh gain has a mean of 1, the performance is far worse than in an AWGN channel.

Now, we compare the BER performance of DS-CDMA downlink wireless communication system employing the GR under the use of the unified complex Hadamard transform spreading sequences with that of DS-CDMA downlink wireless communication system employing the GR under the use of the WH real sequences. To analyze the performance of spreading sequences and the diversity-combining schemes considered, we adopt a Gaussian approximation approach based on the central limit theorem [99]. The Gaussian approximation is known not only to give accurate estimations of the probability of error in the region of practical interest, but also to offer insights into the effects of various sequence and system parameters and interference sources on the performance of the GR [1–3]. For simplicity, here we only consider the single finger GR case, i.e., the GR has only one demodulating finger, and the finger is locked onto an arbitrary path, say, the *i*-th multipath component. Under the Gaussian approximation, for the WH spreading sequences a straightforward derivation based on the decision process indicates that the conditional symbol error probability (SEP) for a given

$$\theta = (\theta_0, \theta_1, \ldots, \theta_{L-1}) \qquad (247)$$

takes the following form

$$SEP_i^{WH}(\theta) = \Phi\left(\sqrt{SINR_{WH}^{(i)}}\right), \qquad (248)$$

where $SINR_{WH}^{(i)}$ is as in (236), and

$$\Phi(x) = \frac{1}{\sqrt{2\pi}} \int_x^\infty \exp\left(-\frac{y^2}{2}\right) dy \qquad (249)$$

is the error integral.

Averaging (248) with respect to the associated random variables, the average probability of error may be determined in the following form:

$$SEP_i^{WH_{av}} = E_\theta \left\{ SEP_i^{WH}(\theta) \right\} \qquad (250)$$

The averaging may most efficiently be carried out via the Monte Carlo or MatLab techniques.

Under employment of the unified complex Hadamard transform spreading sequences in the DS-CDMA downlink wireless communication system using the GR, the Gaussian approximation leads us to the following form of the conditional SEP:

$$SEP_i^H = \Phi\left(\sqrt{SINR_H^{(i)}}\right), \qquad (251)$$

where $SINR_H^{(i)}$ is as in (242). At this point, we should compare (250) and (251). For this purpose, we use a procedure proposed in [99]. If any function $f(x)$ is the convex function and X is the random variable, then Jensen's inequality

$$E\{f(X)\} \geq f(E\{X\}) \qquad (252)$$

is satisfied. To apply Jensen's inequality, first define

$$X = \cos^2(\theta_l - \theta_i). \qquad (253)$$

Then since θ_i, $i = 0, 1, 2, \ldots, L-1$ are uniformly distributed within the limits of the interval $[0, 2\pi)$, straightforward calculations give us the following result

$$E\{X\} = 0.5. \tag{254}$$

Moreover, the function $f(x)$ here has the following form:

$$f(x) = \Phi\left(\sqrt{\frac{1}{a+bx}}\right), \tag{255}$$

where $a > 0$ and $b \geq 0$. Calculating the second derivative of the function $f(x)$ with respect to x, we found that $f(x)$ is a convex function if the following condition is satisfied

$$a + bx \leq \frac{1}{3} \tag{256}$$

is satisfied.

A sufficient condition

$$E_{a_0} \geq \frac{3}{\alpha_i^2} \sqrt{\frac{1}{N} \sum_{l=0, l \neq i}^{L-1} \alpha_l^2 \sum_{k=0}^{K-1} E_{a_k}^2 + 4\sigma_w^4} \tag{257}$$

satisfies the inequality (256) and allows applications of Jensen's inequality successively to each component in θ by using (248) and (250). Then we obtain

$$SEP_i^{WH_{av}} \geq \Phi\left(\sqrt{SINR_{WH}^{(i,low)}}\right), \tag{258}$$

where

$$SINR_{WH}^{(i,low)} = \frac{E_{a_0} \alpha_i^2}{\sqrt{\dfrac{1}{2N} \sum_{l=0, l \neq i}^{L-1} \alpha_l^2 \sum_{k=0}^{K-1} E_{a_k}^2 + 4\sigma_w^4}}. \tag{259}$$

Comparing the results of (258) and (259) for the WH spreading sequences employed by the DS-CDMA downlink wireless communication system under the use of the GR and the result of (251) for the unified complex Hadamard transform spreading sequences employed by the DS-CDMA downlink wireless communication system under the GR use, we found that

$$SINR_{WH}^{(i,low)} = SINR_H^{(i)}. \tag{260}$$

Thus, (251) is a lower bound on the SEP when the WH spreading sequences are used in the DS-CDMA downlink wireless communication system employing the GR if the condition (257) is satisfied. This result implies that the DS-CDMA downlink wireless communication system employing the GR with the unified complex Hadamard transform spreading sequences is more resistant to MAI in comparison with the WH spreading sequences used by the DS-CDMA downlink wireless communication system employing the GR in the case where the only finger is selected in the GR. For more fingers and various combining schemes, although simple closed-form bounds for the SEP of the DS-CDMA downlink wireless communication system employing the GR with the WH spreading sequences are difficult to obtain, we believe that the same conclusion can be made under some similar conditions obtained by using Jensen's inequality and some intensive calculations. This conclusion can be verified under discussion of numerical simulations made in the next section. Furthermore, in view of (58) and (64)–(67), we observe that the DS-CDMA downlink wireless communication system employing the GR with the unified complex Hadamard transform spreading sequences can achieve high reliable performance at not only high SNR E_b/N_0, as in the case of the Rake receiver, but at low SNR, too.

5.5. Simulation results

In this section, we compare the BER performance of the DS-CDMA downlink wireless communication system employing the GR for the cases when the WH spreading sequences and the unified complex Hadamard transform spreading sequences are used under different combining schemes for finger weights such as the traditional equal gain combining (EGC), MRC, and MMRC. Also we present the comparative analysis of BER performance under employment of the GR and Rake receiver by the DS-CDMA downlink wireless communication system. Simulations are performed over the Rayleigh, Ricean, and AWGN channels, respectively.

The spreading sequences of length $N = 64$ are considered, and powers are chosen as

$$P_{a_0} = P_{a_1} = \cdots = P_{a_{K-1}} = 1. \tag{261}$$

Unless stated otherwise, the default system under consideration contains $K = 10$ active users, and the number of paths $L = 4$ in Rayleigh fading multipath channel with

$$E\{\alpha_l^2\} = 1, \ l = 0, \ 1, \ \ldots, \ L-1, \tag{262}$$

and uses the MMRC technique for the GR. In accordance with Section 5.2, we choose

$$\mu_1 = 1, \ \mu_2 = -j, \ \text{and} \ \mu_3 = j \tag{263}$$

to construct a set of the half-spectrum property unified complex Hadamard transform spreading sequences. Note that a different sequence assigned to the user-of-interest results in different BER; the BER in the following examples is an average over the sequence subset.

5.5.1. Effect of GR finger weights

Figure 12 presents different combining techniques in the GR, namely, the traditional EGC, MRC, and MMRC. Additionally, a comparison of the GR with the Rake receiver is made. From presented simulation results it is evident that the GR with MMRC technique has a great superiority over EGC and MRC techniques, especially in the high SNR region. This phenomenon can be explained by the GR finger weights in (244) and (245), where the effect of interference is taken into consideration under MMRC technique, but it is not considered under the traditional EGC and MRC techniques. Additionally, Fig.12 demonstrates a great superiority under employment of the GR by the DS-CDMA downlink wireless communication system with the unified complex Hadamard transform spreading sequences and WH spreading sequences over the implementation of the Rake receiver in the DS-CDMA downlink wireless communication system under the same conditions.
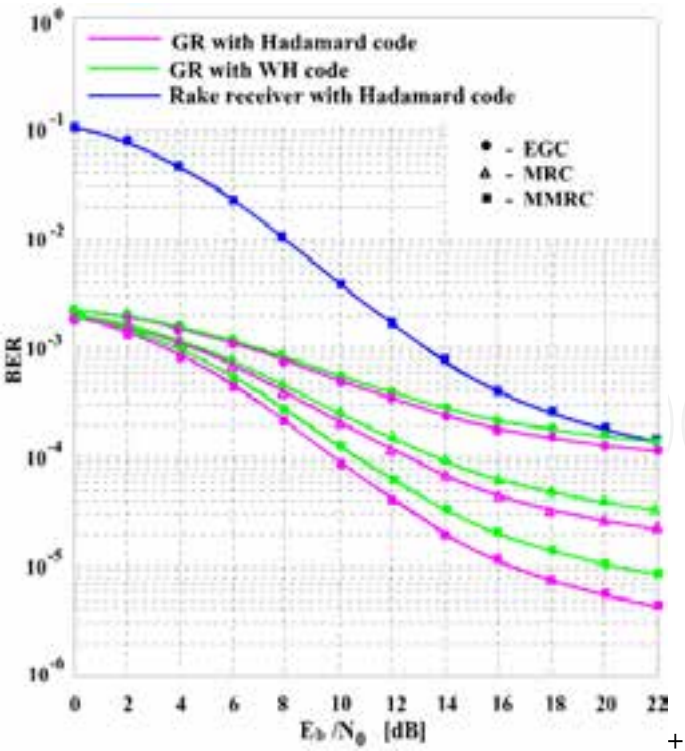
Figure 12. BER performance as a function of SNR E_b/N_0 with different combining techniques in GR over Rayleigh fading channel $(K = 10, L = 4)$.

5.5.2. Effect of different fading channels

Figure 13 shows the BER performance of the DS-CDMA downlink wireless communication system employing the GR with the unified complex Hadamard transform spreading sequences and WH spreading sequences over different channels, including the AWGN channel, Rayleigh fading channel, and Ricean fading channel with the factor $F = 5$. It can be seen that in all the channels under consideration, the DS-CDMA downlink wireless communication system employing the GR with the unified complex Hadamard transform spreading sequences has the better BER performance, especially in the high SNR region. Also, we can see a great superiority under employment of the GR in the DS-CDMA downlink wireless communication system with the unified complex Hadamard transform spreading sequences and WH spreading sequences over the implementation of the Rake receiver in the DS-CDMA downlink wireless communication system under the same conditions.

5.5.3. Effect of MAI

To show the effect of MAI, Fig.14 depicts the BER performance of the DS-CDMA downlink wireless communication system employing the GR with the unified complex Hadamard transform spreading sequences and WH spreading sequences as a function of the number of active users *K*. The BER performance of the DS-CDMA downlink wireless communication system employing the GR with the unified complex Hadamard transform spreading sequences is better than that of the DS-CDMA downlink wireless communication system employing the GR with the WH spreading sequences at the high SNR and all the chosen values of *K*. Although the advantage brought by using the unified complex Hadamard transform spreading sequences in the DS-CDMA downlink wireless communication system employing the GR fades gradually with the increase of MAI. For example, under the large number of users and small SNR, the BER performance of the DS-CDMA downlink wireless communication system employing the GR with the unified complex Hadamard transform spreading sequences is comparable to that of the DS-CDMA downlink wireless communication system employing the GR with the WH spreading sequences in the low SNR region. Also, for all cases, a great superiority of the GR implementation in the DS-CDMA downlink wireless communication system with the unified complex Hadamard transform spreading sequences and WH spreading sequences in comparison with employment of the Rake receiver in the same system is evident. These results in simulations have verified our theoretical analysis.
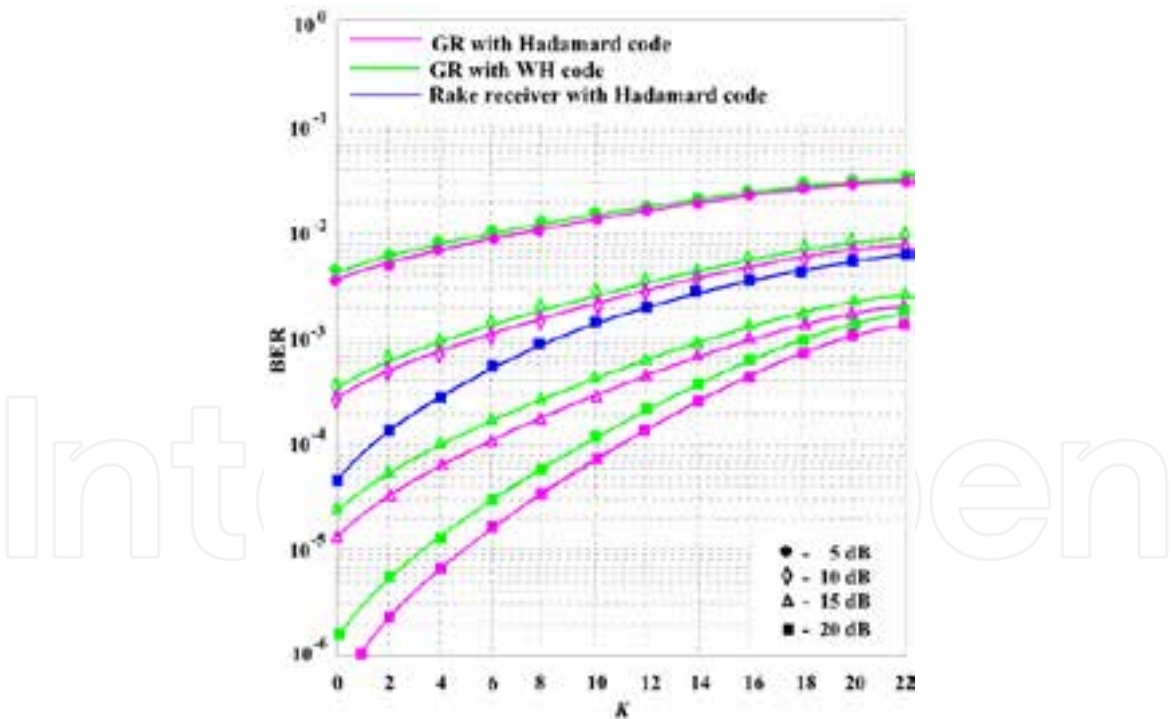
5.6. Conclusions

In this section, we investigate a possibility to employ both the orthogonal unified complex Hadamard transform spreading sequences and the WH real spreading sequences in the DS-CDMA downlink wireless communication system using the GR constructed based on the GASP and carry out a comparative analysis. The SINR at the GR output in the DS-CDMA
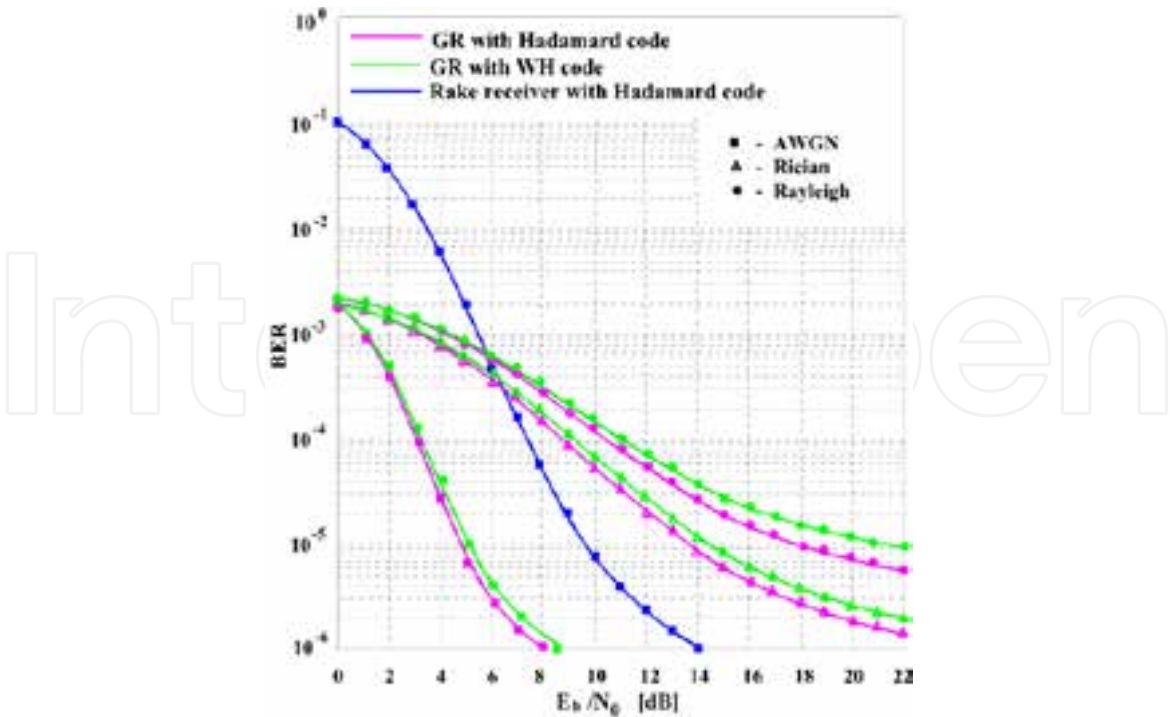
Figure 13. BER performance as a function of SNR E_b/N_0 in different channels $(K = 10, L = 4)$, MMRC.

Figure 14. BER performance as a function of the number of users K. Rayleigh fading channel, MMRC, $L = 4$.

downlink wireless communication system with the unified complex Hadamard transform spreading sequences is independent of the phase offsets between different paths. The SINR at the GR output in the DS-CDMA downlink wireless communication system with the WH

real spreading sequences is a function of the squared cosine of path phase offsets. By this reason, the employment of the orthogonal unified complex Hadamard transform spreading sequences in the DS-CDMA downlink wireless communication system using the GR provides the better BER performance with respect to the DS-CDMA downlink wireless communication system using the GR with the WH real spreading sequences, especially, at high SNRs. Evaluation of the BER performance demonstrating the benefits of employment of the unified complex Hadamard transform spreading sequences and MMRC weights in the GR employed by the DS-CDMA downlink wireless communication system has been carried out over simulation. Comparative analysis of employment of the GR and Rake receiver in the DS-CDMA downlink wireless communication system with the orthogonal unified complex Hadamard transform spreading sequences and the WH real spreading sequences has been performed over simulation. Comparison showed a great superiority in favor of the GR.

Author details

Vyacheslav Tuzlukov

Department of Communications and Information Technologies, School of Electronics Engineering, College of IT Engineering, Kyungpook National University, Daegu, South Korea

References

[1]   Tuzlukov V. A new approach to signal detection theory. *Digital Signal Processing*, 1998; 8 (3) pp. 166 –184.

[2]   Tuzlukov V. *Signal Processing in Noise*: *A New Methodology*, Minsk: IEC, 1998.

[3]   Tuzlukov V. *Signal Detection Theory*, New York: Springer-Verlag, 2001.

[4]   Shbat M.S., Tuzlukov V. Spectrum sensing under correlated antenna array using generalized detector in cognitive radio systems. *International Journal of Antennas and Propagation*, 2013, Vol. 2013, Article ID 853746, 8 pages, 2013. doi:10.1155/2013/853746.

[5]   Shbat M.S., Tuzlukov V. Evaluation of detection performance under employment of the generalized detector in radar sensor systems. *Radioengineering*. 2014; 23 (1) pp. 50–65.

[6]   Tuzlukov V. *Signal Processing Noise*, Boca Raton, London, New York, Washington D.C.: CRC Press, Taylor & Francis Group, 2002.

[7]   Tuzlukov V. *Signal and Image Processing in Navigational Systems*. Boca Raton, London, New York, Washington D.C.: CRC Press, Taylor & Francis Group, 2005

[8]   Tuzlukov V. *Signal Processing in Radar Systems*, Boca Raton, London, New York, Washington D.C.: CRC Press, Taylor & Francis Group, 2012

[9]   Tuzlukov V. Generalized Approach to Signal Processing in Wireless Communications: The Main Aspects and Some Examples. Chapter 11 in *Wireless Communications and Networks: Recent Advances*, Editor: Eksim Ali, INTECH, Chroatia, 2012, pp.305– 338.

[10] Tuzlukov V. – Editor. *Communication Systems: New Research.* NOVA Science Publishers, Inc., New York, USA, 2013, 423 pp.

[11] Tuzlukov V. Wireless Communications: Generalized Approach to Signal Processing., Chapter 6 in *Communication Systems: New Research.* Editor: Vyacheslav Tuzlukov. NOVA Science Publishers, Inc., New York, USA, 2013, pp. 175–268.

[12] Tuzlukov V. Optimal combining, partial cancellation, and channel estimation and correlation in DS-CDMA systems employing the generalized detector. *WSEAS Transactions on Communications*, 2009; 8 (7) pp. 718–733.

[13] Tuzlukov V. Multiuser generalized detector for uniformly quantized synchronous CDMA signals in AWGN channels. *Telecom munications Review*. 2010; 20 (5) pp. 836–848.

[14] Tuzlukov V. Signal processing by generalized detector in DS-CDMA wireless communication systems with frequency-selective channels," *Circuits, Systems and Signal Processing*. 2011; 30 (6) pp. 1197–1230.

[15] Tuzlukov V. Signal processing by generalized receiver in DS-CDMA wireless communication systems with optimal combining and partial cancellation. *EURASIP Journal on Advances in Signal Processing*. 2011, Vol. 2011, Article ID 913189, 15 pages, doi:10.1155/2011/913189; 2011.

[16] Tuzlukov V. DS-CDMA downlink systems with fading channel employing the generalized receiver. *Digital Signal Processing*, 2011; 21 (6) pp. 725–733.

[17] Tuzlukov V. Design of optimal waveforms in MIMO radar systems based on the generalized approach to signal processing," *WSEAS Transactions on Communications*. 2012; 11 (12) pp. 448–462.

[18] Tuzlukov V. Implementation of generalized detector in MIMO radar systems. *WSEAS Transactions on Communications*, 2013;12 (3) pp. 107–120.

[19] Tuzlukov V. Bit error probability of quadriphase DS– CDMA wireless communication systems based on generalized approach to signal processing. *Telecommunications Review*. 2013; 23 (4) pp. 501–515.

[20] Tuzlukov V. Error probability performance of quadriphase DS-CDMA wireless communication systems based on generalized approach to signal processing. *WSEAS Transactions on Communications*. 2014; 13 (2) pp. 116–129.

[21] Shbat M.S., Tuzlukov V. Definition of adaptive detection threshold under employment of the generalized detector in radar sensor systems," *IET Signal Processing*. 2014; 8 (6) pp.622–632.

[22] Maximov M. Joint correlation of fluctuative noise at the outputs of frequency filters. *Radio Engineering and Telecommunications*.1956; 35 (9) pp. 28–38.

[23] Chernyak Y. Joint correlation of noise voltage at the outputs of amplifiers with non-overlapping responses. *Radio Physics and Electronics*. 1960; 28 (4) pp. 551–561.

[24] Shbat M.S. Performance analysis of signal detection by GD in radar sensor and cognitive radio systems," *Kyungpook National University, PhD Thesis*, December 2013.

[25] Taboga M. *Lectures on Probability Theory and Mathematical Statistics*. 2nd Ed. Amazon Create Space. 2012.

[26] Gradshteyn I., Ryzhik I. *Table of Integrals, Series, and Products*, 7th Ed. Academic Press: Amsterdam, Boston, London, New York, Oxford, Paris, San Diego, San Francisco, Singapore, Sydney, Tokyo, 2007.

[27] Shbat M.S, Tuzlukov V. Noise power estimation under generalized detector employment in automotive detection and tracking systems," in *Proceedings of the 9th IET Data Fusion and Target Tracking Conf. (DF&TT'12)*, doi: 10.1049/cp.2012.0416, Lon- don, UK, 2012.

[28] Alouini M.S., Abdi A., Kaveh M. Sum of gamma variates and performance of wireless communications systems over Nakagami-fading channels. *IEEE Transactions on Vehicular Technology*. 2001; 50 (6) pp.1471 - 1480.

[29] Win M.Z., Winters J.H. Analysis of Hybrid Selection/Maximal Ratio Combining in Rayleigh Fading. *IEEE Transactions on Communications*. 1999; 47 (12) pp.1773–1776.

[30] Win M.Z., Winters J.H. Virtual Branch Analysis of Symbol Error Probability for Hybrid Selection/Maximal-Ratio Combining in Rayleigh Fading. *IEEE Transactions on Communications*. 2001; 49 (11) pp.1926–1934.

[31] Kong N., Milstein L.B. Average SNR of a Generalized Diversity Selection Combining Scheme. *IEEE Communications Letters*. 1999; 3 (3) pp.57–59.

[32] Alouini M.S., Simon M.K. Performance of Coherent Receivers with Hybrid SC/MRC over Nakagami Fading Channels," *IEEE Transactions on Vehicular Technology*. 1999; 48 (4) pp.1155–1164.

[33] Alouini M.S., Simon M.K. A MGF-Based on Performance Analysis of Generalized Selection Combining over Rayleigh Fading Channels," *IEEE Transactions on Communications*. 2000; 48 (3) pp.401–415.

[34] Malik R.K., Win M.Z. Analysis of Hybrid Selection/Maximal-Ratio Combining in Correlated Nakagami Fading," *IEEE Transactions on Communications*. 2002; 50 (8) pp.1372–1383.

[35] Annamalai A., Tellambura C. A New Approach to Performance Evaluation of Generalized Selection Diversity Receivers in Wireless Channels," in Proceedings *IEEE Vehicular Technology Conference*, Vol. 4, October 2001, pp. 2309–2313.

[36] Proakis, J.G. *Digital Communications*, 4th ed. New York: McGraw-Hill, 2001.

[37] Mengali U., Andrea A.N.D. *Synchronization Techniques for Digital Receivers*, New York: Plenum, 1997.

[38] Tong L., Perreau S. Multichannel Blind Identification: From Subspace to Maximal Likelihood Methods. *Proceedings IEEE*. 1998; 86 (10) pp.1951–1968.

[39] Tugnait J.K, Tong L., Ding Z. Single-User Channel Estimation and Equalization. *IEEE Signal Processing Magazine*. 2000; 17 (3) pp.17–28.

[40] Abed-Meraim K., Qaiu W., Hua Y. Blind System Identification. *Proceedings IEEE*. 1997; 85 (8) pp.1310–1322.

[41] Alouini M.S., Goldsmith A.J. A Unified Approach for Calculating Error Rates of Linearly Modulated Signals over Generalized Fading Channels. *IEEE Transactions on Communications*. 1999; 47 (9) pp.1324–1334.

[42] Tuzlukov V., Yoon W.S., Kim Y.D. Wireless Sensor Networks Based on the Generalized Approach to Signal Processing with Fading Channels and Receive Antenna Array. *WSEAS Transactions on Circuits and Systems*. 2004; 10 (3) pp. 2149–2155.

[43] Divsalar D., Simon M.K., Raphaeli D. Improved Parallel Interference Cancellation for CDMA.. *IEEE Transactions on Communications*. 1998; 46 (2) pp.258–268.

[44] Renucci P.G., Woerner B.C. Optimization of Soft Interference Cancellation for DS-CDMA. *Electronics Letters*. 1998; 34 (4), pp.731–733.

[45] Guo D Linear Parallel Interference Cancellation in CDMA, Master Degree Dissertation in Engineering. *National University of Singapore*, 1998.

[46] Hsieh Y.-T., Wu W.-R. Optimal Two-Stage Decoupled Partial PIC Receivers for Multiuser Detection. *IEEE Transactions on Wireless Communications*. 2005; 4 (1) pp.112-127.

[47] Ghotobi M., Soleymani M.R. Multiuser Detection of DS-CDMA Signals Using Partial Parallel Interference Cancellation in Satellite Communications. *IEEE Journal on Selective Areas in Communications.* 2004; 22 (4) pp.584-593.

[48] Wu K.-W., Wang C.-L. Soft-Input Soft-Output Partial Parallel Interference Cancellation for DS-CDMA Systems. in *Proceed- ings IEEE International Conference on Communications (ICC'01)*, Helsinki, Finland, June 2001, pp.1172–1176.

[49] Papoulis A., Pillai S.U. *Probability, Random Variables and Stochastic Processes*, 4th ed, New York: McGraw-Hill, 2002.

[50] Xue G., Weng, J.F., Lee-Ngoc T., Tahar S An Analytic Model for Performance Evaluation of Parallel Interference Cancellers in CDMA Systems. *IEEE Communications Letters.* 2000; 4 (6) pp.84–186.

[51] Kim J.H., Tuzlukov V., Yoon W.-Y., Kim Y.D. Generalized Detector under Non-orthogonal Multipulse Modulation in Remote Sensing Systems. *WSEAS Transactions on Signal Processing.* 2005; 2 (1) pp.203–208.

[52] Tuzlukov V., Yoon W.S., Kim Y.D. Adaptive Beam-Former Generalized Detector in Wireless Sensor Networks. in *Proceedings of the IASTED International Conference on Parallel and Distributed Computing and Networks (PDCN 2004)*, February 17-19, Innsbruck, Austria, 2004, pp.195–200.

[53] Kim J.H., Tuzlukov V., Yoon W.-Y., Kim Y.D. Macrodiversity in Wireless Sensor Networks Based on the Generalized Approach to Signal Processing. *WSEAS Transactions on Communications.* 2005; 8 (4) pp.648–653.

[54] Craig J.W. A New, Simple and Exact Result for Calculating the Probability of Error for Two-Dimensional Signal Constellations. in *Proceedings IEEE MILCOM'91 Conference*, November15-18, Boston, MA, USA, 1991, pp. 25.5.1–25.5.5.

[55] Ziemer R.E., Tranter W.H. *Principles of Communications: Systems, Modulation, and Noise.* 6th Ed. New York, NY: John Wiley & Sons, Inc., 2010.

[56] Renucci P.G., Woerner B.D. Optimization of Soft Interference Cancellation for DS-CDMA. *Electron. Letters.* 1998; 34 (4) pp. 731–733.

[57] Morrow Jr. R.K., Lehnert J.S. Bit-to-Bit Error Dependence in Slotted DS/SSMA Packer Systems with Random Signature Sequences. *IEEE Transactions on Communications.* 1989; 37 (10) pp.1052–1061.

[58] Liberti Jr. J.C., Rappaport T.S. *Smart Antennas for Wireless Communications: IS-95 and Third Generation CDMA Applications.* Upper Saddle River, NJ: Prentice Hall, 1999.

[59] Brown III D.R., Johnson Jr. C.R SINR, Power Efficiency, and Theoretical System Capacity of Parallel Interference Cancellation *Journal of Communications and Networks.* 2001; 3 (9) pp.228–237.

[60] Manohar S., Tikiya V., Annavajjala R., Chockalingam A. BER-Optimal Linear Parallel Interference Cancellation for Multicarrier DS-CDMA in Rayleigh Fading. *IEEE Transactions on Communications*. 2007; 55 (6) pp.1253–1265.

[61] Tuzlukov V. Selection of Partial Cancellation Factors in DS-CDMA Systems Employing the Generalized Detector," in *Proceed ings 12th WSEAS International Conference on Communications: New Aspects of Communications*, July 23-25, Heraklion Crete, Greece, 2008, pp.129–134.

[62] Dighe P., Mallik R., Jamuar S. Analysis of Transmit-Receive Diversity in Rayleigh Fading. *IEEE Transactions on Communications*. 2003; 51(4) pp.694–703.

[63] Jongren G., Skoglund M., Ottersten B. Combining Beamforming and Orthogonal Space-Time Block Coding, *IEEE Transactions on Information Theory*. 2002; 48(3) pp.611–627.

[64] Love D., Heath R., Strohmer T. Grassmannian Beamforming for Multiple-Input Multiple-Output Wireless Systems, *IEEE Transactions on Information Theory*. 2003; 49(10) pp.2735–2747.

[65] Mukkavilli K., Sabharwal A., Erkip E., Aazhang B. Beamforming with Finite Rate Feedback in Multiple Antenna Systems. *IEEE Transactions on Information Theory*. 2003; 49(10) pp.2562–2579.

[66] Choi J., Heath R. Interpolation Based Transmit Beamforming for MIMO-OFDM with Limited Feedback. *IEEE Transactions on Signal Processing*. 2005; 53(11) pp.4125–4135.

[67] Palomar D.P., Lagunas M.A. Joint Transmit-Receive Space-Time Equalization in Spatially Correlated MIMO Channels: a Beamforming Approach. *IEEE Journal on Selected Areas in Communications*. 2003; 21 pp.730–743.

[68] Lee H., Lee B., Lee I. Iterative Detection and Decoding with an Improved V-BLAST for MIMO-OFDM Systems, *IEEE Journal on Selected Areas in Communications*. 2006; 24(3) pp.504 –513.

[69] Lee H., Lee I. New Approach for Error Compensation in Coded V-BLAST OFDM Systems. *IEEE Transactions on Communications*. 2007; 55(2) pp.345–355.

[70] Wang J., Wen O.Y., Li S. Capacity and Performance of MIMO BICM System with Soft-Output MMSE Soft Interference Cancellation. in *Proceedings CCNC 2008*, 2008, January 10-12, Las Vegas, Nevada, USA, pp.100–104.

[71] Marzetta T.L. BLAST Training: Estimating Channel Characteristics for High-Capacity Space-Time Wireless, in *Proceedings 37th Annual Allerton Conference on Communications, Control, and Computing.* 1999 pp.958–966.

[72] Taricco G., Biglieri E. Space-Time Decoding with Imperfect Channel Estimation. *IEEE Transactions on Wireless Communications*. 2005; 4(4) pp.1874–1888.

[73] Lee K., Chun J. Symbol Detection in V-BLAST Architectures under Channel Estimation Error. *IEEE Transactions on Wireless Communications*. 2007; 6(2) pp.593–597.

[74] Clark M.V., Greenstein L.J., Kennedy W.K., Shafi M. Optimum Linear Diversity Receivers for Mobile Communications, *IEEE Transactions on Vehicular Technology.* 1994; 43(2) pp. 47–56.

[75] Cioffi J.M., Dudevoir G.P., Eyuboglu M.V., Forney Jr. G.D. MMSE Decision-Feedback Equalizers and Coding - Part I: Equalization results. *IEEE Transactions on Communications*. 1995; 43(10) pp.2582–2594.

[76] Ghotobi M., Soleymani M.R. Multiuser Detection of DS-CDMA Signals Using Partial Parallel Interference Cancellation in Satellite Communications. *IEEE Journal on Selected Areas in Communications*. 2004; 22(4) pp. 584–593.

[77] T. K. Moon and W. C. Stirling, *Mathematical Methods and Algorithms for Signal Processing.* New York, Prentice Hall, 2000.

[78] Kay S.M., *Fundamentals of Statistical Signal Processing: Estimation Theory*. Englewood Cliffs, NJ: Prentice -Hall, 1993.

[79] Craig J.W. A New, Simple and Exact Result for Calculating the Probability of Error for Two-Dimensional Signal Constellations, in *Proceedings IEEE International Conference on Military Communications, Milcom'91*, November 4-7, 1991, McLean, Virgi- nia, USA, Vol. 2, pp.571–575, 1991.

[80] Ziemer R.E., Tranter W.H. *Principles of Communications: Systems, Modulation, and Noise.* 6th Ed. John Wiley & Sons, Inc., New York, 2010.

[81] GSM recommendation 05.05: Propagation conditions, Version 5.3.0, release 1996.

[82] Mukkavilli K., Sabharwal A., Erkip E., Aazhang B. Beamforming with Finite Rate Feedback in Multiple Antenna Systems, *IEEE Transactions on Information Theory*. 2003; 49(10) pp.2562–2579.

[83] Tuzlukov V. Multiuser Generalized Detector for Uniformly Quantized Synchronous CDMA Signals in Wireless Sensor Networks with Additive white Gaussian Noise Channels, in *Proceedings International Conference on Control, Automation, and Systems (ICCAS 2008)*, October 14-17, 2008, Seoul, Korea, pp.1526–1531.

[84] Tuzlukov V. Selection of Partial Cancellation Factors in DS-CDMA Systems Employing the Generalized Detector, in *Proceedings 12th WSEAS International Conference on Communications: New Aspects of Communications*, July 23-25, 2008, Heraklion, Crete, GREECE, 2008, pp.129–134.

[85] Kim J.H, Tuzlukov V., Yoon W.S, Kim Y.D. Performance Analysis under Multiple Antennas in Wireless Sensor Networks Based on the Generalized Approach to Signal Processing. *WSEAS Transactions on Communications*, 2005; 4 (7) pp.391–395.

[86] ETSI EN302 307 V1.1.1 (2004-06), Digital Video Broadcasting (DVB); Second Generation Framing Structure, Channel Coding and Modulation Systems for Broadcasting, Interactive Services, News Gathering and Other Broad-Band Satellite Applications.

[87] Tuzlukov V., Yoon W.S., Kim Y.D. MMSE Multiuser Generalized Detector for Non-orthogonal Multipulse Modulation in Wireless Sensor Networks, in *Proceedings 9th World Multi-Conference on Systemics, Cybernetics and Informatics (WMSCI 2005)*, July 10-13, 2005, Orlando, Florida, USA, 2005.

[88] Lee J.S., Miller L.E. *CDMA Systems Engineering Handbook.* Boston, MA: Artech House, 1998.

[89] Pickholtz R.L., Milstein L.B., Schiling D.L. Spread Spectrum for Mobile Communications, *IEEE Transactions on Vehicular Technology*. 1991; 40 (2) pp.313–322.

[90] Fong M. H., Bhargava V.K., Wang Q. Concatenated Orthogonal/PN Spreading Sequences and Their Application to Cellular DS- CDMA systems with Integrated Traffic. *IEEE Journal on Selected Areas in Communications*. 1996; 14(3) pp.547–558.

[91] Peterson R.L., Ziemer R.E, Borth D.E. *Introduction to Spread-Spectrum Communication.* Englewood Cliffs, NJ: Prentice-Hall, 1995.

[92] Boztas S., Hammons R., Kumar P.V. 4-Phase Sequences with Near-Optimum Correlation Properties, *IEEE Transactions on In- formation Theory*. 1992; 38(3) pp.1101–1113.

[93] Chu D.C. Polyphase Codes with Good Periodic Correlation Properties. I*EEE Transactions on Information Theory*. 1972;18 (3) pp.531–532.

[94] Frank R.L., Zadoff S.A. Phase Shift Pulse Codes with Good Periodic Correlation Properties. *IEEE Transactions on Information Theory.* 1962; 8 (2) pp.381–382.

[95] Lam A.W., Ozluturk F.M. Performance Bounds for DS/SSMA Communications with Complex Signature Sequences. *IEEE Transactions on Communications.* 1992; 40 (10) pp.1607–1614.

[96] Rahardja S., Falkowski B.J. Family of Unified Complex Hadamard Transforms. *IEEE Transactions on Circuits and Systems– II: Analog and Digital Signal processing.* 1999; 46 (8) pp.1094–1100.

[97] Rahardja S., Ser W., Lin Z. UCHT-Based Complex Sequences for Asynchronous CDMA Systems. I*EEE Transactions on Communications.* 2003; 51 (5) pp.618–626.

[98] Proakis J.G. *Digital Communications.* 4th Ed. New York: McGraw-Hill, 2001.

[99] Borovkov A.A. *Probability Theory.* Amsterdam, The Netherlands: Gordon and Breach, 1998.